CRANFIELD UNIVERSITY

KATARZYNA ODOLCZYK

COATINGS FOR THE PREVENTION OF MARINE FOULING

School of Aerospace, Transport and Manufacturing

PhD
Academic Year: 2012- 2016

Supervisor: Dr. Qi Zhang
October 2016

CRANFIELD UNIVERSITY

School of Areospace, Transport and Manufacturing

PhD

Academic Year 2012- 2016

KATARZYNA ODOLCZYK

COATINGS FOR THE PREVENTION OF MATINE FOULING

Supervisor: Dr Qi Zhang
October 2016

This thesis is submitted in partial fulfilment of the requirements for the degree of Doctor of Philosophy

ABSTRACT

Microorganisms attachment to the surfaces located in the marine water has become a significant problem. Historically, the antifouling properties of the coatings were achieved by using biocides, which had a negative consequence to the marine environment. Currently, alternative environmental friendly methods are required. This thesis aimed to investigate and produce the antifouling coatings that can be used as potential candidates in the marine industry. In this study, a range of novel polymer nanocomposite coatings was fabricated via the method of solvent and tested based on the strategy of microbial adhesion. The composition of the coatings mainly contains polidimethylsiloxane (PDMS) and different nanomaterials. The coatings applied on glass substrate were characterised using X-ray spectroscopy (XRD), scanning electron microscopy (SEM), contact angle measurements, inductively coupled plasma mass spectroscopy (ICP-MS) and atomic force microscopy (AFM).

In biofouling assays, attachment of bacteria *B. Subtilis* and three marine microalgae (*Skeletonema sp., Amphora sp., D. Salina*) was investigated in laboratory scale. The obtained results suggested that small amount of nanoparticles in the polymer matrix can improve the antifouling settlement behaviour of the coatings. All microalgae attached more on PDMS/SiO_2 and control surfaces (glass and PDMS) compared to the coatings containing multiwall carbon nanotubes (MWCNT) and sodium bismuth titanate (NBT).

The influence of contact time, surface roughness and surface wettability was also studied. The microbial attachment varied significantly with respect to contact time and surface properties. There was no obvious evidence showing that the wetting properties and the roughness of the coatings have an effect on growth.

Finally, the physico-chemical properties of all tested microorganisms and coatings were investigated in order to examine the thermodynamic model for cell adhesion prediction. The work of attachment and its components were

quantified based on contact angle measurements and calculated surface energy along with OWRK (Owens, Wendt, Rabel and Kaelble) approach. The results showed that the thermodynamic modeling did not predict microbial adhesion. However, it revealed that there is a possible link between work of attachment and the actual microbial adhesion if some coatings are tested separately.

Keywords:

algae, antifouling coatings, bacteria, biofouling, nanocomposites, PDMS

ACKNOWLEDGEMENTS

First of all, I wish to express my gratitude to my supervisor, Dr Qi Zhang who gave me the opportunity to conduct this research. Thank for continuous support and guidance during this study. I would also like to thank Dr Raffaella Villa and Prof Robert Dorey for their interest in, invaluable suggestions and sharing of knowledge.

Many thanks for all staff from Surface Engineering and Nanotechnology Institute at Cranfield University who created a perfect workplace for me. Thank to Andrew Stallard who was very helpful. I appreciate his commitment and assistance during my research. To Dr Christopher Shaw and Dr Glenn Leighton for contribution and advice towards the study.

I would also like to thank to Richard Onarinde School of Energy, Environment and Agrifood (SEEA), Cranfield University, for the collaboration during this project.

Very special thanks to Ewa, for her continuous support and introduction to the Cranfield University. I wish to thank all my friends and colleagues, especially Kasia, Rebecca, Dominika and Adam.

This project would have not been possible without the presence of my family. I would like to thank for love and support. They have always believed in me and encouraged to work. I would like to express my sincere gratitude to my partner for his continuous trust and consolation in self-doubt moments.

TABLE OF CONTENTS

LIST OF FIGURES

LIST OF TABLES

LIST OF EQUATIONS

LIST OF ABBREVIATIONS

AHL	Acylated homoserinelactones
AF	Antifouling
AFM	Atomic force microscopy
CA	Contact angle
EPS	Extracellular polymeric substance
FR	Fouling-release
FRC	Fouling-release coatings
ICP-MS	Inductively coupled plasma mass spectroscopy
l	Liquid medium
m	Microorganism
NP	Nanoparticles
PDMS	Polydimethylsiloxane
PDMS/NP	Polydimethylsiloxane nanocomposites
QS	Quorum sensing
Ra	Roughness
s	Substrate
SEM	Scanning electron microscope
SPC	Self polishing coating
TBT	Tributyltin
TBT-SPC	Tributyltin self polishing coating
TEM	Transmission electron microscopy
W	Work of attachment
XRD	X-ray diffraction
γ_{ml}	microorganism-liquid interfacial free energy
γ_{sl}	substratum-liquid interfacial free energy
γ_{ms}	microorganism liquid interfacial free energy

1 Introduction

1.1 Project Background

Marine biofouling is a worldwide problem, defined as unwanted accumulation and growth of seawater organisms on all surfaces exposed to the marine environment with negative consequences. The organisms responsible for fouling include microorganisms, plants and animals.

The problems associated with biofouling are well known and understood. Marine fouling has detrimental effects on the objects in the sea. It incurs environmental problems causing spread of unwanted species around the world, reduction of product quality, additional costs of operation and is also directly related to the corrosion of marine structures (Schultz et al., 2011; Tribou and Swain, 2010).

To find the effective method of controlling marine biofouling, it is important to understand the influence of physico-chemical properties (such as wettability, topography, surface energy and elasticity) of fouled organisms and surfaces immersed in water (Ederth et al., 2008).

Various methods have been used to solve this problem and the most effective have been antifouling paints based on the biocides as tributyltin (TBT) and copper (Thomas and Brooks, 2010), which slow the growth of organisms that attach to the hull and can affect a vessel's performance and durability. These paints have been banned by the International Convention on the Control of Harmful Anti-fouling Systems on Ships of the International Marine Organization due to its serious toxic effects on marine life (such as the collapse of a French shellfish fishery), which has accelerated the research to seek for alternative antifouling systems (Evans, 1999). Currently, research is still ongoing to find environmentally friendly methods against marine fouling (Yebra et al.,2004; Chambers et al., 2006; Genzer and Efimenko, 2006). From an ecological point of view, the most promising possibility against biofouling is controlling the wettability of the coatings and exploiting the paints creating low surface energies (Beigbeder et al., 2008; Cho et al. 2011). The compounds, which

possess such properties, belong to a class of water-insoluble silicone matrix elastomers. However, the silicone coatings do not prevent the settling of marine organisms but prevent them from adhering the surface due to the non-stick properties. They are effective only in the case of high-speed vessels in motion as high shear forces on the surface are required for detachment of fouling species. At the moment there is not enough information about the required speed, which is needed to remove fouling organisms. However, it is known, that these coatings, even at very high speeds, are not able to prevent slime fouling. The main drawback of the silicone-based coatings is poor strength and adhesion to the substrate. Consequently, they are prone to damage, also have limited use in practice. They are used, mainly by focusing on a small number of areas where ships can reach high speeds. Although the use of silicone coatings is increasing, still need to be improved. Coating modification on the nano-scale can disrupt the initial settlement of spores in the early stages of the fouling process. Also, it is believed that this will change resistance for damages and corrosion.

1.2 Aim and Objectives

The main aim of this research is to develop novel polymer nanocomposite coatings, which would prevent the possible marine fouling.

To achieve the goal, the following objectives need to be completed:

1) To select less toxic coating materials

2) To develop a novel antifouling coating

3) To characterise and optimise the properties of the coating

4) To evaluate performance of the coating on different types of microorganisms

5) To investigate influence of surface properties on microorganisms attachment

6) To investigate the thermodynamic approach as a prediction of microorganisms adhesion

1.3 Structure of Thesis

This PhD thesis is divided into nine chapters outlined in Table 1-1. The introduction (Chapter 1) is followed by a detailed literature review (Chapter 2) and description of the experimental procedures along with the analytical methods used in this study (Chapter 3). Nanoparticle synthesis and characterisation are presented in Chapter 4. Chapter 5 presents the coating preparation methods and characterisation, where each section describes a different PDMS/NP coating. The antifouling properties of the coatings and the influence of surface properties on microorganism attachment are presented in the next two chapters (Chapters 6 & 7). The investigation of microbial attachment prediction is presented in Chapter 8. Chapter 9, conclusions and future work, summarises the key results and suggests recommendations for future investigations on the development of novel antifouling coatings. The appendixes contain relevant experimental data.

Table 1-1 Thesis structure

Chapter	Title	Objective addressed
1	Introduction	-
2	Literature Review	-
3	Characterisation Techniques	-
4	Methodology of Nanopowders	1
5	Synthesis and Characterisation of Antifouling Coatings	2, 3
6	Bacteria Adhesion Assay	4, 5
7	Algae Adhesion Assay	4, 5
8	Thermodynamic Analysis of Microbial Attachment to PDMS/NP Coatings	6
9	Conclusions and Recommendations for Future Work	-

2 Literature Review

2.1 Biofouling

Biofouling is defined as the accumulation and growth of undesirable plants and animal organisms on structures submerged in water (Zobell and Allen, 1934). The marine fouling is probably the most recognised form of biofouling as it is a significant worldwide problem which has detrimental effects on the man-made objects in the sea water. Issues include increased costs of operation, reduce speed and quality of product work, corrosion of marine structures and environment problems.

The problem of biofouling on the shipping industry affecting all its elements submerged in the marine water. Such elements include for example the ship hull, heat transfers and coolers. This reduces the efficiency of work, causing a higher frictional resistance, lowering speed and manoeuvrability (Brady Jr and Singler, 2000). For example, an increase in frictional drag decreases the speed vessels in excess of 10%. It was estimated that fouled ship burns 40% more fuel (AMBIO 2010), thereby increasing the time of drydocking, resulting in major costs (Burns et al., 1946), approximate between 180 and 260 $ million per annum to the US Navy fleets (Callow and Callow 2011). The impact of biofouling also can be found in offshore structures, screens, heat exchangers, piping systems causing the overall decline in power plants (AMBIO 2010).

2.1.1 Mechanism of Biofouling

The colonisation of unwanted organisms is unavoidable for almost any man-made structure submerged in the marine environment (Rittschof, 2000). The process of marine biofouling is relatively well understood and generally considered to involve four steps as illustrated in Figure 2-1 (Candries, 2000).

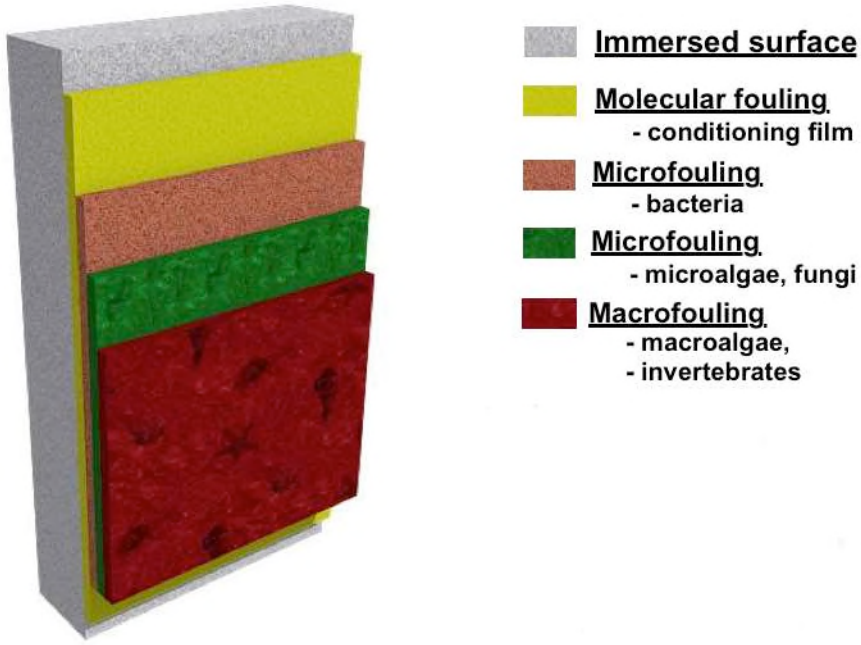

Figure 2-1 Stages of marine biofouling mechanism

When a new surface is immersed in water, it is rapidly covered by molecules and organic matter such as polysaccharides and proteins, creating a thin 'conditioning film' (Loeb and Neihof, 1975; Compere et al. 2001; Callow and Callow, 2002). This is the first phase of marine fouling and is called molecular fouling. This stage creates a foundation for the next step; it begins within seconds of submersion in seawater and is fully established within a few hours.

During the second stage, floating bacteria and unicellular organisms develop on the 'conditioning film'. This layer is a primary colonisation of microfouling stage (Abarzua and Jakubowski, 1995) and involves the sticky exudates (extracellular polymeric substances, EPS), which are secreted by the attached bacteria (Callow et al., 2002). The EPS connect settled cells to each other as well as to the surface. The connection of cells and EPS is called a 'biofilm'. It is thought that the biofilm provides a good surface for colonisation of flora and fauna species.

The transition of a biofilm into an increasingly complex assemblage of multicellular species is considered as part of microfouling stage (secondary colonisation). These are likely to include fungi, algae spores and protozoa. This is due to the presence of adhesive exudates and increased roughness of the surface due to the microorganism colonies formed at stage two.

In the final stage of biofouling, a surface exhibits settlement and growth of macrofouling organisms. The major representatives of marine fouling macroorganisms are larvae of barnacles, mussels, macroalgae and tubeworms.

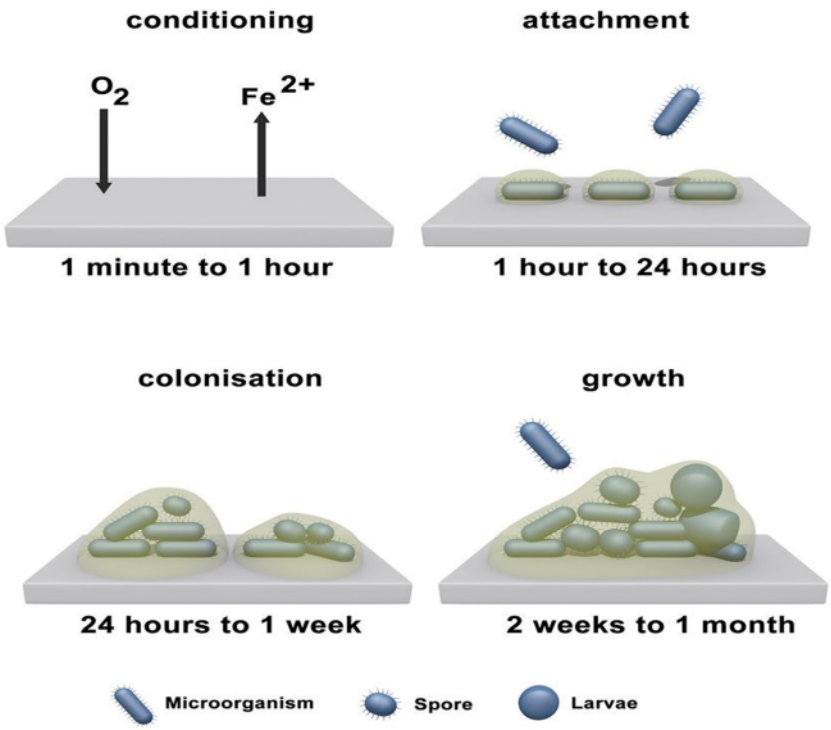

Figure 2-2 The time scale required for the formation of each of the critical steps of biofouling: conditioning film, attachment, colonisation and growth.

It is understood that the initial steps of biofouling are formed within a few minutes while large marine organisms settle within one month (Figure 2-2).

Bacteria seem to occur after approximately 1 h to 2 h on material immersed in the marine environment. Diatoms appear within days, followed by secondary colonisation after a week and tertiary colonisers in 2 weeks to 1 month (Abarzua and Jakubowski, 1995; Chambers et al., 2006). While this process can be considered as completed, at this stage, it needs to be remembered that biofouling is an ongoing process and will continue as long as the surface is in contact with sea water.

2.1.2 Conditioning Film

It takes only a few seconds when the conditioning film is starting to create at a material immersed in water. Percival et al. 2000 investigated that a thin layer with a thickness between 30 – 80 nm can be fully created after 15 min after surface immersion. The presence of the conditioning film alters the physico-chemical properties of the surface such as wettability, surface energy, roughness and surface charge (Dexter 1979; Baier 1980; Bakker et al. 2004), what make the substrate more attractive to microorganisms (Edwards 1983; Garg et al. 2009,). This is caused by adsorption of chemical compounds such as proteins, polysaccharides, humic materials or glycoproteins (Loeb and Neihof, 1975; Baier 1980; Christensen, 1999; Compere et al., 2001). However, it is important to mention that the presence of conditioning film may tend to inhibit rather than promote adhesion of some bacteria species (Percival et al., 2011).

2.1.3 Biofilm Process

Bacteria and organic matters are microorganisms encountered in the marine environment, which in contact with a solid substrate form the initial biofilm (Marhaeni et al., 2009). This is a major factor affecting later stages of biofouling. The biofilm may be caused by both, physic-chemical properties of the colonised material and properties of the microorganisms included in the biofilm. The common development of biofilm can be divided into different stages:

attachment, maturation of biofilm and biofilm dispersion, as illustrated in Figure 2-3.

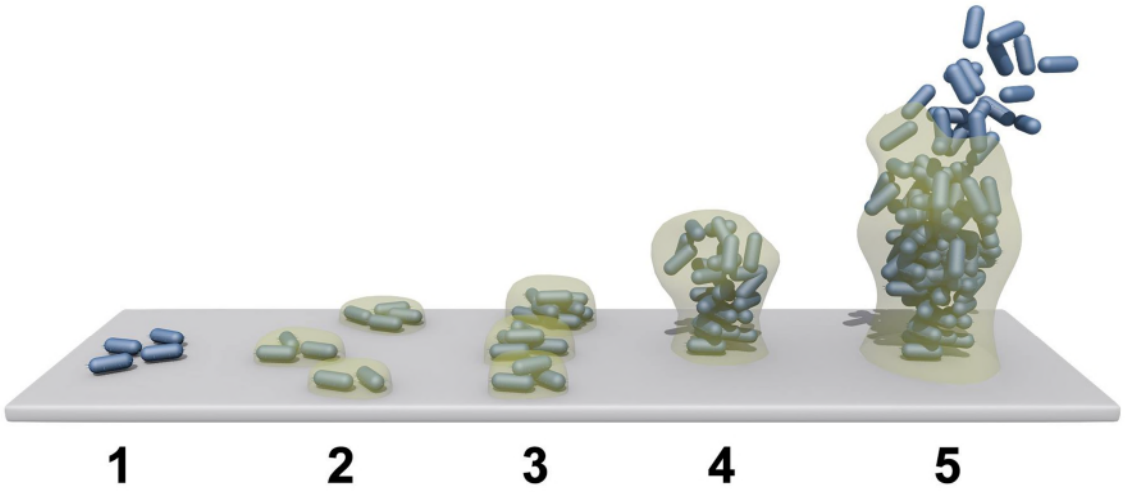

Figure 2-3 Steps of biofilm formation: 1) adsorption, 2) adhesion, 3) microcolony formation, 4) biofilm maturation, 5) dispersion.

The bacterial settlement involving two steps sequence: adsorption and adhesion (Abarzua and Jakubowski, 1995). Adsorption can be regarded as a temporary attraction, which holds the bacteria when approaching the material (Abarzua and Jakubowski, 1995). This is the reversible phase because the cells can be easily removed from the surface using physical and chemical agents. The bacterial adsorption is mainly caused by the presence of the van der Waals forces, hydrodynamic forces, gravity and Brownian motion (Walt et al., 1985). The second step of attachment is a permanent and irreversible connection. It occurs when the bacterial cells are in the distance less than 1.5 nm from the solid surface (Busscher and Weerkamp, 1987) and involve the extracellular polymeric substance (EPS). EPS is a mainly consisted of water, polysaccharides and proteins, and their function is to glue the cells to one another and a surface. According to Costerton (1999), the microbial biofilm is composed of 75 - 90 % EPS and only 10 - 25 % cells. The bacterial adhesion is followed by microcolony formation and biofilm maturation. During this phase,

the proliferation of microorganisms and their gradual differentiation through the changes in the activity of some genes takes place. This leads to the last resort of biofilm maturation and changes some characteristics of an organism such as morphology (Lopez et al., 2010), metabolism and biochemical properties (Bryers, 2008). All these changes make the bacteria cells forming part of biofilm possess different characteristics than free cells (Lopez et al., 2010). The transport of cells from a mature biofilm to an environment is generally achieved in last stage of biofilm formation. The biofilm reaches a maximum thickness and gradually stops to maintain form. The reason for detachment of cells can be exhaustion of nutrients or problems with their transfer within the biofilm. Cells dispersed in sea water, starting the process of searching new solid surfaces for re-colonisation (Liu and Tay, 2001).

2.1.4 Micro- and Macro- fouling

Marine biofouling generally can be roughly divided into microbiofouling and macrobiofouling (Callow and Callow, 2002; Epstein, 1983). Both categories have negative effects on materials submarged in water, leading to the corrosion. Macrobiofouling is usually conditioned by a microbiofouling, which occurred before. This stages of the biofouling development are called ‘successional’ (Rittschof, 2000; Yebra et al., 2004; Chambers et al., 2006) in the sense that the order of events is a subsidiary of one another. It can be assumed that prevention of microfouling could have the positive impact on macrofouling inhibition. There is evidence in the literature that the presence of bacterial biofilm affects the better growth of larvae (Hugget et al., 2006). However, this is subjected to constant research as there are conflicting opinions on whether this mechanism is real in all cases (Little, 1984).

2.1.5 Quorum sensing

As described before, the new materials after immersion in water are rapidly covered with bacteria and other microorganisms. There is great interest how

organisms can sense surfaces. It turns out that bacteria cells, as higher organisms (animals, humans), also have their own communication system, called Quorum sensing (QS) (Rutherford and Bassler, 2012). This is a phenomenon of bacteria communication, which involves the formation and separation of the signal molecules, used during the biofilm formation. For the first time, the Quorum sensing concept was introduced a relatively long time ago. In 1979, Nealson and Hasting studying popular marine bacteria species (*Vibro fischeri* and *Vibro harveyi*) have noticed that they have the ability to emit light only when they are living in organisms. The authors demonstrated that bacteria in the high density are also able to emit light and produce chemical signals (autoinducers) whose concentration depends on a number of bacteria. It was concluded that in this way bacteria species can send a signals about the limit proliferation.

Widespread use of the phenomenon of communication between bacteria in microbiology has been experienced and understood recently. Studies have shown that bacteria can send signals for both within one and many species. Bacteria are able to analyse the chemical nature of signals which allows for better processes control, such as bioluminescence, virulence, bacterial conjugation and biofilm formation (Jaworski et al., 2005). It turns out that the way of communication between bacteria cells is not necessarily the same for different species. It is different in the case of gram-positive bacteria and gram-negative bacteria because they have developed different transfer schemes particle signal. In the case of gram-positive bacteria, features of autoinducers form oligo-peptides, in the gram-negative bacteria are acylated homoserinelactones (AHL).

2.2 Surface Properties Affecting Fouling Growth

The process of biofouling depends on many environmental factors. Varying physical and chemical factors could cause conditions that make the man-made structures more attractive to marine organisms and affect the rate of formation complexity of marine fouling. Significant biological influences are the type of

organisms, their growth rate and metabolic activity. Surface properties variables may include wettability, charge, surface energy and topography. Marine environmental factors are pH, temperature, flow velocity and electrolyte type (Bott and Pinheiro, 1977; Melo and Bott, 1997). In this section, the influence of some main variables affecting biofouling will be summarised.

The influence of water temperature on microbial fouling is well known and documented (Van Loosdrecht et al., 1990; Yebra et al., 2004; Giaouries et al., 2005). As the temperature of the sea water can change in the range from -2 ºC to 28 ºC, even locally can reach 35 ºC (Yebra et al., 2004), it is important to understand the effect of it on the microorganisms adhesion. It was proven, that the water temperature is one of the main parameters that affects biofouling. It has a significant impact on the changes taking place on the surface of cells (Giaouries et al., 2005), by changing their charge and hydrophobicity that could affect cell attachment (Van Loosdrecht et al., 1990). The increase in the number of microorganisms fouled on solid surfaces submerged in marine water can be expected under high temperatures. This is valid only until biofilm reaches a maximum value. Experiments carried out in seawater in Sweden (Novak, 1982) showed that the biofilm reached its maximum rate at temperature 35 ºC – 37 ºC. Bott and Pinheiro (1977) also indicated that cell attachment increased at 35 ºC. However, Pompermayer and Gaylarde (2000) during the test on various bacteria species noticed that some bacteria adhere better under high temperature, while the others prefer lower temperature. The changes in pH value, a presence of metals, nutrients, oxygen could also affect in marine fouling (Melo and Bott, 1997). It was found that small changes in pH of water affect the growth speed of bacteria (Cullimore et al., 1978; Garrett et al., 2008). For the pH value of 7, iron bacteria grow faster than for pH 9 (Pinheiro et al., 1988). However the optimum pH for biofilm production depends on the individual marine species (Garrett et al., 2008).

The wettability of a solid surface is very important physical property, which affects the attachment of fouling organisms. It is generally thought that surface wettability has a great influence on the initial attachment and strength of adhesion of marine microorganisms (Magin et al., 2010).

A number of studies have shown that some marine organisms preferring to attach on hydrophobic surfaces (Callow et al., 2002; Aldred et al., 2006; Li et al., 2010). Finlay et al. (2002) investigated the adhesion of the common microalgae (*Enteromorpha sp.* and *Amphora spp*.) on the glass slide and self-assembled monolayers (SAMs) terminated with methyl (CH_3) or hydroxyl (OH) group. Results showed that attachment of tested spores to surfaces increases with increasing value of the contact angle. However, the adhesion strength of *Enteromorpha* spores was higher on the hydrophilic surfaces. Rosenhahn et al. (2010) obtained similar results after examination of the effect of surface wettability on the adhesion of *Ulva* zoospores. After 1 h of incubation, there were more diatoms attached the hydrophobic surface (-CH_3 SAM) than to hydrophilic one (glass, -OH SAM). However, the *Ulva* zoospores were weakly attached to the hydrophobic SAM and the percentage of removed cells was larger.

Overall, it can be assumed that hydrophobic surfaces such as fluorinated polymers, siloxanes and ω-substituted alkanethiolates are effective as fouling release (Callow et al., 2000; Yebra et al., 2004; Krishnan et al., 2006; Beigbeder et al. 2008). However, surfaces with hydrophilic nature (such as PEG, polyethylene glycol) possess properties, which help in the preventing of microorganisms attachment (Krishnan et al. 2006; Finlay et al. 2008).

The influence of surface roughness on the adhesion of marine organisms is one of the properties deeply studied by many researches. Studies on coatings abraded by sandpaper with different grid size showed that biofilms colonisation increased with a surface roughness (Verran et al., 1991; Barton et al., 2007). However, still is not clear what kind of changes in the topography could cause

biofouling. Surface roughness can be divided into nano-, micro- and macro roughness. It was observed that changes in the surface topography on the macro scale are relatively unimportant in biofouling. However, micro roughness plays an important role in marine fouling and it is one of the most studied properties of the solid surface. Callow et al. (2002) investigated the attachment of *Enteromorpha* zoospores to polydimethylsiloxane coatings modified on micro scale. The microtopographic changes were based on 5 µm deep valleys with ridges and valley floors varying between 5 – 20 µm. In the results, the authors observed a significantly higher number of cells attached to the substrate valleys and against pillars compared to smooth PDMS coating. The greater number of spores was observed when the features were 5 µm deep, which was in the similar range of size of the attached spore (Figure 2-4).

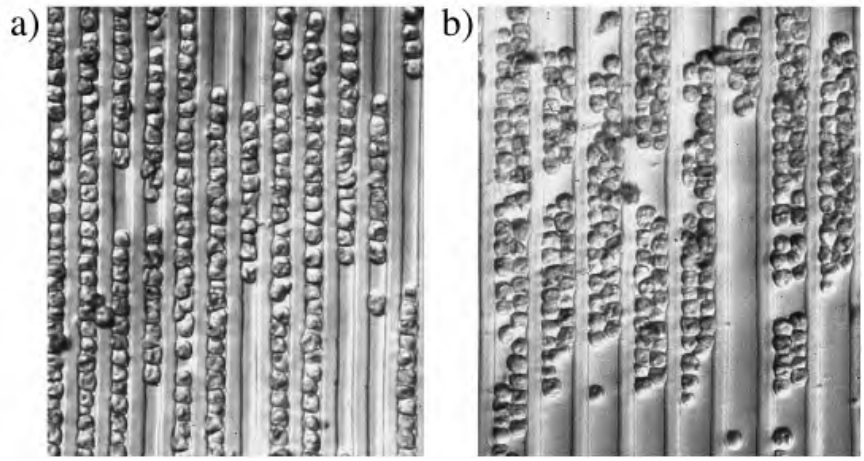

Figure 2-4 Micrographs of spores settled on PDMS coating with a) 5 µm and b) 10 µm wide valleys (Callow et al. 2002)

Understanding the role of micropatterning could be explained by the work on adhesion (Nurioglu et al., 2015). The relation between cell adhesion and surface area can be explained using model presented in Figure 2-5. Callow et al. (2002) concluded that cell settled into the valley need less energy to attach, which is caused by contact points between cell and substratum. However,

during the attachment of cell to smooth surface only one contact point exist, which results in increase of energy extend on the total system (Callow et al. 2002).

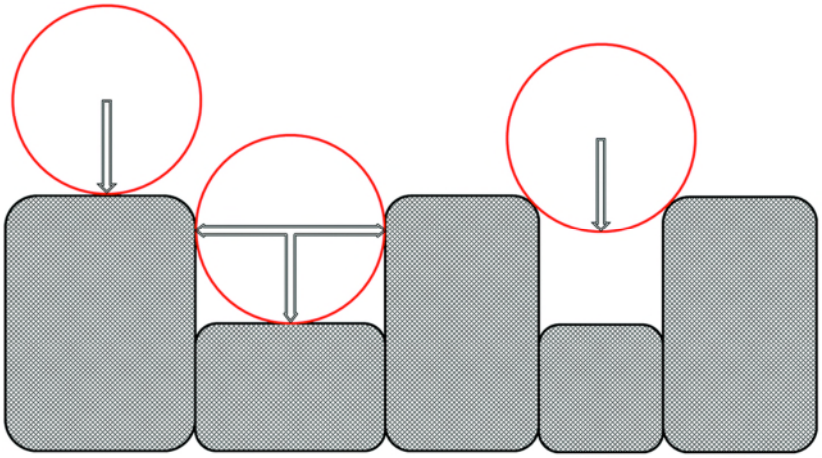

Figure 2-5 Diagrammatic representing of the cell adhesion to different surface features (Nurioglu et al., 2015)

In addition to this study it can be concluded that micro roughness is one of the main parameters affecting marine biofouling. However, it is great interest on topography changes on nano scale. Mitik-Dineva et al. (2008) suggested that bacteria adhere better to the surfaces with roughness on nanoscale. This could be caused by different EPS quantities produced by bacteria, but more research needs to be done.

2.3 Antifouling Strategies

The problem of biofouling on surfaces submerged in sea water is still a major issue and many laboratories around the world are looking for an effective way of limiting fouling of marine organisms (AMBIO, 2010). Figure 2-6 shows the most common methods to prevent fouling**.** Alternate techniques using electrical

current and high voltage, result in the corrosion of steel and the formation of lesion cathodes. There are also methods of using ammonia, hydrogen peroxide and bromine compounds. Ozonation of surfaces has also been studied and patented. However, all these methods have not come into general use.

In this section, the historical methods against marine fouling are described. This is followed by a description of the most common methods to prevent adhesion of marine organisms.

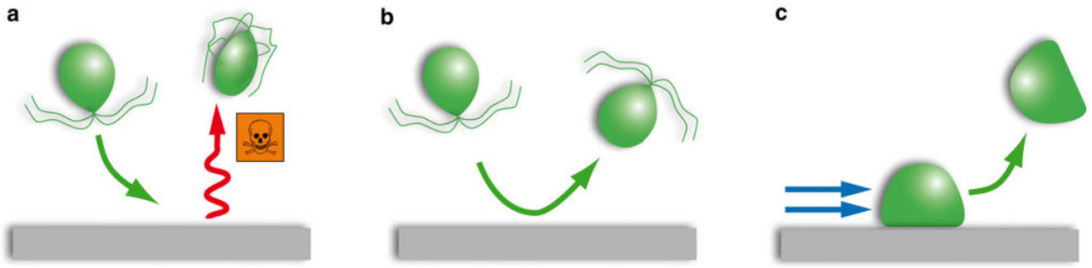

Figure 2-6 Three types of approaches against biofouling: a) toxic antifouling paint, b) fouling inhibition, c) foul-release coating (Rosenhahn and Sendra, 2012)

2.3.1 Historical Perspective

The problem of biofouling has existed since humans started sailing the oceans and some signs of fouling control methods have been recognised for more than 2000 years ago. At long before any effective methods were available and the ships were wooden, to protect them various preparations were used Including tar, wax, resin and animal fur (Yebra et al., 2004). However, it cannot unequivocally say that these treatments were used in particular to reduce the fouling organisms, because equally well for their original application could have been sealed ships. A first antifouling approach can be considered to be scraping the bottom and sides of ships. In this way, the fouled marine organisms were removed in the 1st century.

In the 18th century, introduced the copper plating which was supposed to protect bottom of the ship against biofouling. Initially, the main idea of this technique was to protect surfaces immersed in sea water against snails. However, it was observed that copper works equally well on the fouling of other organisms, for this reason, it became a great success and was widely used. It was noticed very quickly that the copper in contact with the iron components of ships leads to corrosion. The introduction of iron ships resulted in new search for more effective methods, which did not have adverse effects on materials structure.

The 19th century was the century of antifouling paints. Introduced paints were initially based on the biocides. However, the crucial period in the prevention of fouling turned out to be 20 century. After World War II, the new synthetic petroleum based resins were introduced. This brought substantial changes in the AF industry improving mechanical characteristics and antifouling efficiency. During this time, organotin compounds were used as resin-based soluble matrix paint. When the positive effects of the tin application was noted, the performance was improved even further and tributyltin was involved an ingredient of AF paints, this let to the creation of a new type of paint called tributyltin self-polishing copolymer paints (TBT-SPC). But increasing health and safety concern led to legislation, which caused these paints to be banned due to its serious toxic effects on marine life. This has accelerated the research to seek for alternative antifouling systems. These actions have led to accelerating the research to seek for alternative antifouling systems.

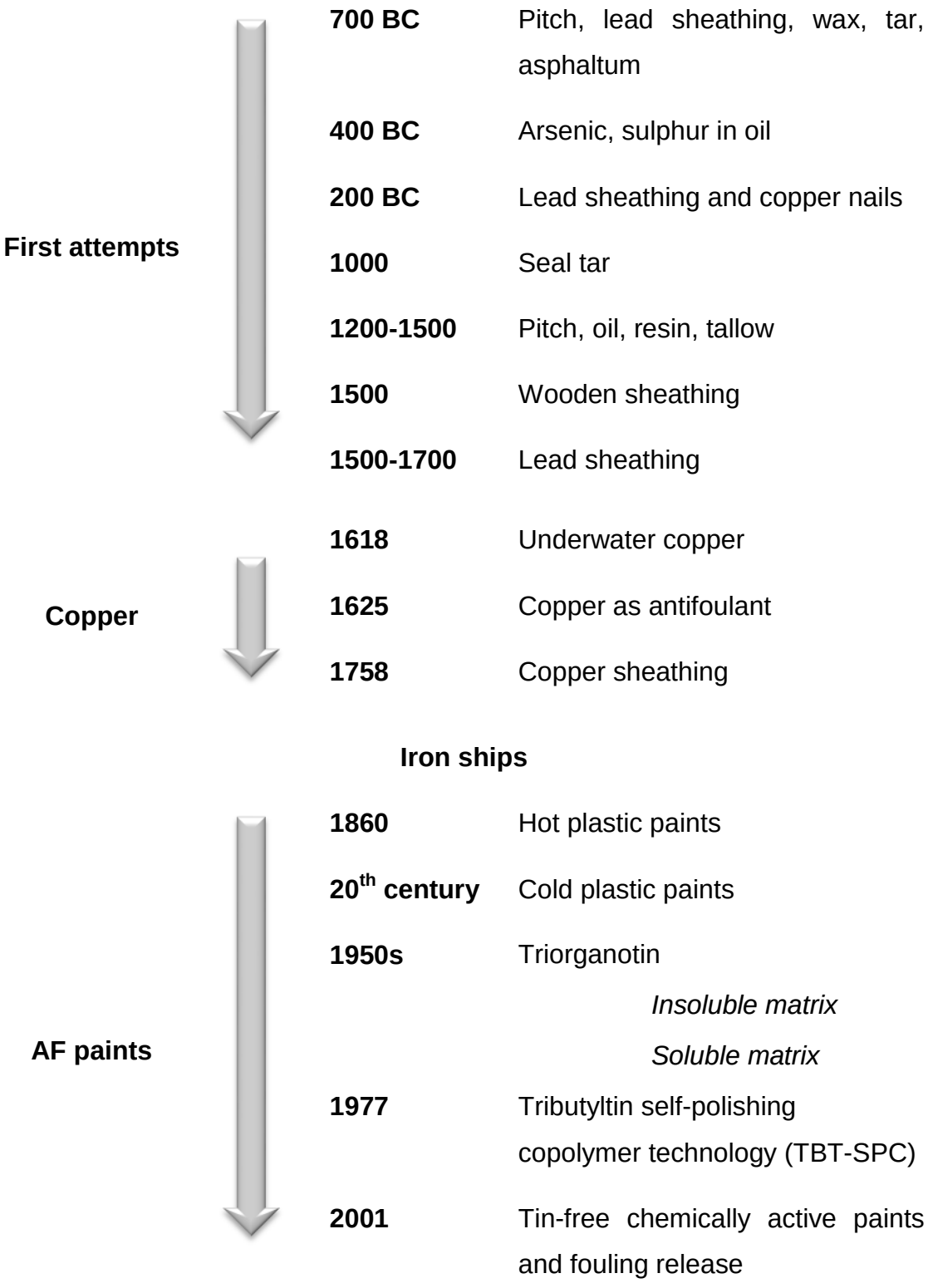

Figure 2-7 Timeline of the development of antifouling methods (based on Hellio and Yebra)

2.3.2 Current and Future Antifouling Methods

2.3.2.1 Self-polishing Copolymers Antifouling Paints

Antifouling paints have long been considered to be the most promising method to prevent biofouling. The most effective were those which, in a precise manner, release biocides into the sea water. The best biocidal properties are exhibited by paint based on a tributyltin self-polishing copolymer (TBT-SPC). The mechanism of action for these paints is the release of TBT compounds from the coating and inhibition of the organism's attachment. These paints containing TBT compounds rapidly revolutionized the fouling industry. It has been shown that these paints are very durable and can guarantee a fouling free surface for up to 5 years (Candries, 2000). The effective life is related with the thickness of layer applied on the surface.

The coatings based on TBT proved to be the most effective in preventing the biofouling. However, this technology is also considered to release the most toxic substance after introduction into the marine environment. There is evidence that its use in antifouling paints exerted harmful effects on non-target organisms (Gao et al., 2010). It has been shown that this compound causes deformations, bisexuality and extinction of some marine organisms. The effects of TBT were observed in organisms such as the Dog whelk, (*Nucella lapillus)*. It results in the development of male characteristics in the female genitalia, which leads to a reduction in fertility (Evans, 1999). The release of TBT from the antifouling paints is attributed to the decline in the oyster population and reproductive disorders in snails. A significant increase of biomagnification (Hoch, 2001) in the food chain of some animals (Blue sharks, Bottlenose dolphins, Bluefin tunas) has also been noted.

Due to the environmental concerns, the International Maritime Organization (Yebra et al., 2004) has prohibited the use of TBT compounds since 2001. Since 2008, there has been a total ban on the use of organotin coatings and the constructions covered by toxic TBT paints were secured to prevent tin leaching (IMO, 2001).

The introduction of prohibition led to the search for alternatives that could be used without adverse environmental effects. As a replacement for tin, other types of metals (zinc, copper) started to be used in SPC paints. The use hydrolysis and erosion in SPC coatings are becoming more common.

2.3.2.2 Foul Release Systems

The issues discovered with antifouling paints based on biocides have led to a search for alternative antifouling systems. From an ecological point of view, the most promising possibilities to control biofouling are non-stick and foul-release (FR) technology (Swain, 1999). The compounds, which possess such properties belong to a class of water-insoluble matrix silicone elastomers. The foul-release coatings (FRCs) based on silicone were originally reported in 1975 (Candries, 2000).

The characteristic features of FRCs are their hydrophobicity and low surface free energy. Thanks to such properties, the ability of marine organisms to form a strong interfacial bond with the solid surface decreases.

The most common FRCs are those include fluorinated polymers, ω-substituted alkanethiolates and polydimethylsiloxane (PDMS) (Callow et al., 2000; Ista et al., 2004; Beigbeder et al., 2008). The PDMS has a flexible linear backbone, which consists of connected alternating silicon and oxygen atoms. The majority of silicon atoms are substituted with two methyl groups ($-CH_3$) resulting in a low critical surface tension of 20-24 mJ/m^2 (Brady, 1999). In addition the PDMS foul-release coating has an extremely low elastic modulus ~1 MPa (Brady, 1999) and have microroughness. It has been shown that these unique properties can help remove the marine organisms from the surface. Introducing different substituents to methyl to the backbone can have a significant impact on the properties of PDMS. For example, introducing larger alkyl groups improves the lubricating properties of silicones. In addition, substitutes increase the hydrophobicity of the surface so that fouling organisms have difficulty adhering to the surfaces or are removed more readily by the action of seawater.

However, the silicone-based coatings show poor strength and adhesion to the substrate, which is the main drawback as they are prone to damage so too have limited use in practice. They are used, mainly by focusing on a small number of areas where ships can reach high speeds.

The FRC appear to be a promising alternative to toxic coatings. The coatings do not prevent the settling of marine organisms but prevent them from adhering the surface due to the non-stick properties. The texture and smoothness of the coatings at the molecular level makes the organisms are easy to move on the surface, if the object immersed in the water, moves beyond a certain speed.

However, they are effective only in the case of high-speed vessels in motion as high shear forces on the surface are required for detachment of fouling species. At the moment there is not enough information about the required speed, which is needed to remove fouling organisms. According to some literature, in order to the proper work of fouling-release properties of coatings, the ships have to reach 10-20 knots (Yebra et al., 2004). It is known, that this depends on the type of fouled organisms and the coatings even at very high speeds, are not able to prevent slime fouling (Candries, 2000).

2.3.2.3 Biomimetic Design of Antifouling Materials

There are many examples in the natural environment, where animals or plants use antifouling approach (Brady Jr. and Singler, 2000; Strand and Jocobsen, 2005). One of the most interesting methods of dealing with biofouling suggested by some authors (Sullivan and Regan, 2011) is the so-called biomimetic design. This method draws on the antifouling strategies used by marine organisms.

The biomimetics has been the subject of intense interest in recent years due to a large number of flora and fauna species possessed antifouling properties. It has been observed that the skin of whales has a self-cleaning property. The surface of skin consists nanostructured pores, and each of it is filled with gel. This special gel is rinsed with the attached organisms, preventing their adhesion.

The first prominent example of a successful transfer of biological surface structures is shark skin. This technology mimics the topographic characteristics of shark skin which is covered with small tentacles bent against each other. Imitation of shark skin was previously modified at the nano scale. It prevents the escape of toxic substances into the environment and provides a gentle protection against fouling organisms (Ball, 1999; Kesel and Liedert, 2007).

Observations carried out on the live organisms led to the hypothesis that surface changes made on the nanoscale could be effective on man-made structures.

2.3.2.4 Antifouling Coatings Based on Nanotechnology

Due to the fact that PDMS fouling-release coating is one of the most effective methods, different routes to improving its performance have been considered. Significant attention has been focused on changing the topography on a nano scale. This was achieved by the introduction of multi walled carbon nanotubes (MWCNT) to the silicone backbone. The result of topography modification is to disrupt the settlement of spores in the early stages of fouling process. This has a large impact on bioadhesion and biofouling. Presence of less than 0.1 wt% (Beigbeder et al., 2011) of MWCNT can change the settlement behavior of some species of algae. It has been shown that some spores prefer to settle in between the pillars on the surfaces with modified topography (Callow et al., 2002). This causes that nanotubes are investigated as promising materials for the reinforcement of silicone elastomers.

3 Characterisation Techniques

In order to gain a clearer understanding of the behaviour of materials in a seawater environment, it is important to know their chemical and physical properties. In this chapter a brief overview of the characterisation methods used during the analysis of chosen powders and final coatings, is described. Table 3-1 provides an overview and application of techniques used in this thesis.

Table 3-1 Overview of characterisation techniques

Technique	Tested material	Information
X-Ray Diffraction	Surface, powder	Chemical composition and structure
Scanning Electron Microscopy	Surface, powder	Particles and surface morphological characterisation
Transmission Electron Microscopy	Powder	Particles characterisation
Atomic Force Microscopy	Surface	Surface topography and roughness
ICP-MS Spectroscopy	Surface, powder	Chemical composition
Tensiometer	Surface	Contact angle and surface energy measurement

3.1 X-Ray Diffraction

X-ray diffraction analysis (XRD) is widely used to providing the possibility of determining chemical composition and phase structure of the sample. The XRD analysis of tested samples was carried out by a Siemens D5005 X-ray diffractometer, with a Cu Kα source. Prior to measurement, powders were placed in a metal mould attached to a glass slide; final coatings were tested without further treatment. The measurements were operated in an angular range of 2Θ=10-90º with a scan range of 0.05º per second. The results were evaluated using XRD Evaluation software and normalised in order to improve the clarity.

3.2 Scanning Electron Microscopy

Scanning electron microscopy (SEM) is a method used to observe the materials from the nano to the micro scale. SEM allows for observation at high resolution, which provides a more accurate monitoring of the microstructure. Tested samples must be electrically conductive to give a more accurate image contrast and to prevent changing. In the case of non-conductive samples, the thin layers of conductive film are used. In the current study, a scanning electron microscope (SEM, SFEG FEI XL30) was used to investigate the particle shape, size and the microstructural changes of the synthesised coatings. To prepare powders for SEM characterisation, a small amount of powder was placed on the top of conductive carbon tape. The tested powders and coatings were coated with a thin conductive layer of carbon for producing high-resolution images.

3.3 Transmission Electron Microscopy

Transmission electron microscopy (TEM) is another technique for the analysis and observation of objects at a very high magnification. For the investigation of very small particles, characterisation was performed on a Philips CM20

Scanning TEM. For TEM analysis, nanoparticles were dispersed in water and then placed on a carbon coated copper grid.

3.4 Atomic Force Microscopy

Atomic force microscopy (AFM) is used for enlarged contrast and resolution. A Dimension 3000 with a NanoScope IIIa controller was used to obtain very high quality images and 3D image reconstruction. The surface of samples was scanned over a 30μm x 30μm area, to provide quantitative information about the surface roughness and topography. The result of the measurements was a parameter describing the average range roughness- Ra.

3.5 ICP-MS Spectroscopy

ICP-MS spectroscopy is an analytical technique used for the detection mainly of metals in solutions with very low concentrations. The main principle of mass spectroscopy is a determination of ions by ionisation in the plasma (Jenner et al., 1990). A X-series II ICP-MS with NWR 213 esi laser ablation system was used to establish the presence of metals dispersed in water. Before analyse, coated glass slides were placed separately in the petri dish containing 10 ml of distilled water for 30 days, at room temperature. After the incubation time, samples were removed and water was examined by ICP-MS, in order to investigate whether the metal nanoparticles presented in coatings could penetrate to the water.

3.6 Contact Angle and Surface Energy

Contact angle measurement is a simple method for the analysis of the interaction between a liquid and a solid sample, which allows to evaluation of the wetting properties of the material (Chan, 1994). The contact angle (Figure

3-1) is defined as the angle formed by a liquid droplet at the three-phase boundary (gas-liquid-solid). The balance at contact of gas-liquid-solid phase is associated with a surface energy and is described by the Young's equation (Young, 1805; Busscher et al., 1984):

$$\gamma_{SG} = \gamma_{LG} \cdot cos\theta + \gamma_{SL} \quad \textbf{(3-1)}$$

where θ is contact angle and γ is interface surface energy:

- γ_{SG}, solid/vapour surface free energy
- γ_{LG}, liquid/vapour surface free energy
- γ_{SL}, solid/liquid surface free energy

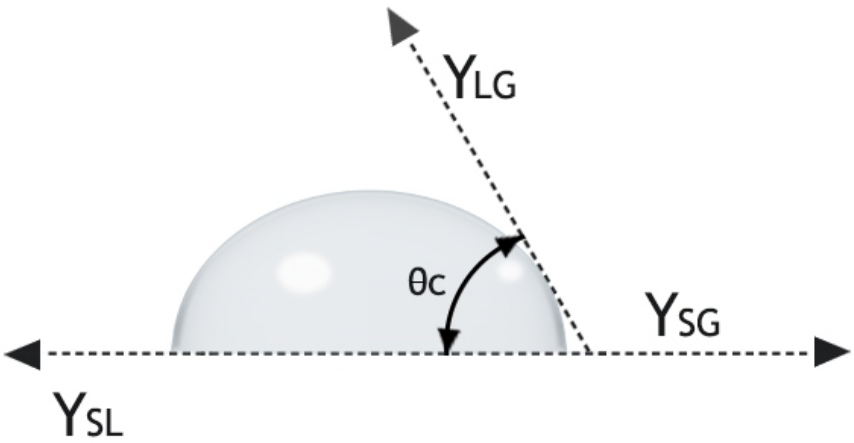

Figure 3-1 Contact angle formation on a solid surface

Depending on the size of an angle formed by a liquid drop, the surface can be classified as water-wettable or not water-wettable, as shown in the Figure 3-2. It is assumed that the solid surfaces which are characterised by contact angles θ<90º are considered to be hydrophilic, while those which exhibit contact angles θ>90º are hydrophobic. The wetting is complete when the contact angle is 0º.

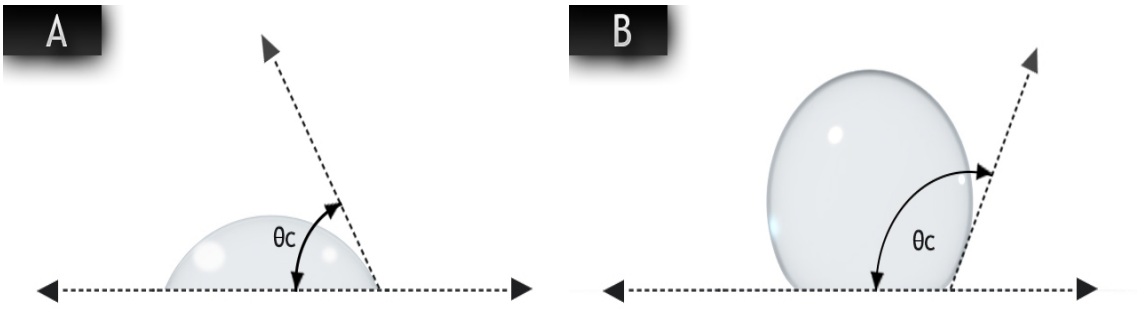

Figure 3-2 Liquid spreading over a solid surface and its relationship to contact angle

In the current study, the contact angle was measured by the sessile drop technique (Biegbeder, et al. 2008), in order to discern the hydrophobic and hydrophilic character of surface. The deionised water, diiodomethane (Sigma Aldrich) and ethylene glycol (Sigma Aldrich) were used as a reference liquid drop. The contact angle measurements were taken for all polymer nanocomposite coatings and substrates, using a Biolin Scientific Theta Lite Attension Tensiometer. Before measurements were taken, all samples were cleaned with deionised water, soap and isopropanol, and then dried by N_2. Each sample was examined on five different areas and contact angle was calculated as an average of the left- and right-angle of liquid drop, using OneAttension software. In order to calculate surface free energy, an Owens-Wendt (OWRK) method was applied. The surface tension components of the tested liquids are given in Table 3-2.

Table 3-2 Surface tension components of water, diiodomethane and ethylene glycol (Lange, 1967)

Surface tension [mN/m]	γ_{tot}	γ_d	γ_p
Water (DI)	72.8	21.8	51
Diiodomethane (DM)	50.8	50.8	0
Ethylene glycol (EG)	48	29	19

4 Methodology of Producing Nanopowders

This chapter describes the nanopowders used for the preparation of nanocomposite coatings. The first section is focused on the hydrothermal synthesis and characterisation of bismuth sodium titanate ($Na_{0.5}Bi_{0.5}TiO_3$), NBT. The second section of this chapter is concerned with characterisation of the commercial nanopowders used in this study.

4.1 Synthesis and Characterisation of NBT Nanopowder

4.1.1 Hydrothermal Technique

The hydrothermal method is a wet-chemical technique for the fabrication of different materials and chemical compounds. The word "hydrothermal" is of geological origin and for the first time was used by Sir Roderick Murchison who described the action of water at high temperature and pressure, causing the formation of rocks and minerals in the earth's crust (Byrappa & Yoshimura, 2001). The hydrothermal process is a method that uses water at high temperature (>100 ºC) and high pressure (>1 atm) (Setinc, et al., 2011; Rabenau, 1985) to disperse substances, which are largely insoluble under normal conditions. Synthesis under hydrothermal conditions is carried out in a closed autoclave (Figure 4-1), which can hold high temperatures and pressures for long duration time.

The hydrothermal technique is characterised by low energy consumption, which is beneficial in ecology and economics. This method is distinct from other wet-chemical methods due to the ability to control the growth and shape of the produced powder.

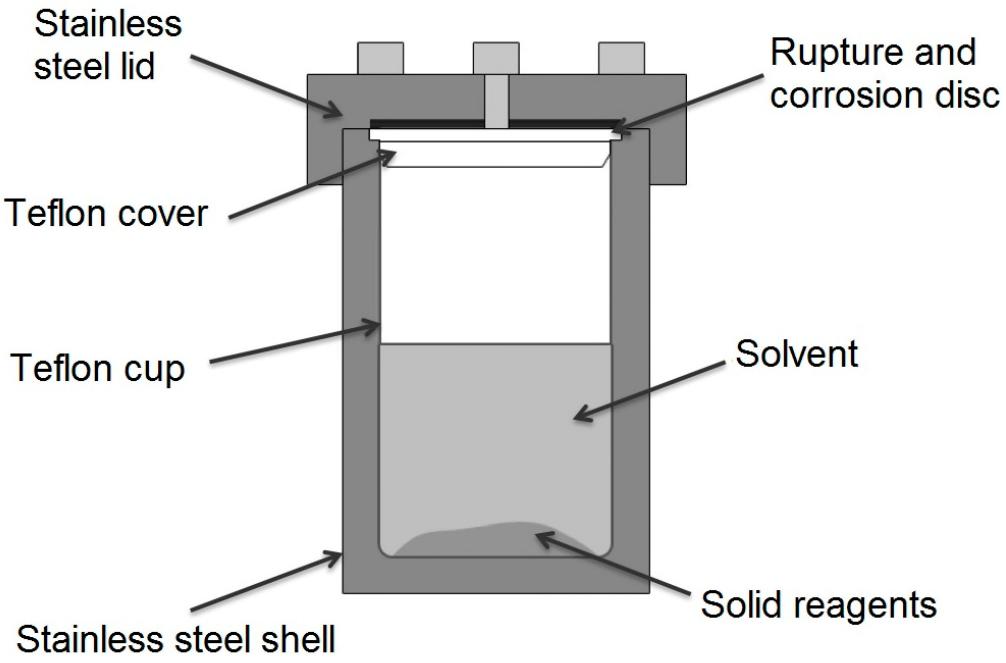

Figure 4-1 Teflon-lined, stainless steel autoclave

4.1.2 Synthesis of NBT Nanopowder

The hydrothermal method, described by Setinc et al. (2011), was chosen and modified to produce $Bi_{0.5}Na_{0.5}TiO_3$ (NBT) nanoparticles in this thesis. A schematic diagram for the overall nanopowder synthesis is shown in Figure 4-2. Sodium hydroxide (NaOH), bismuth (III) nitrate pentahydrate ($Bi(NO_3)_3$ $5H_2O$) and anatase (TiO_2) were provided by Sigma Aldrich and used as starting components. The standard hydrothermal synthesis of NBT nanopowder can be divided into two stages. The first stage is the preparation of a solution, which contains the chemical compounds to assist a chemical reaction. In this order, 1.45 g of $Bi(NO3)_3$ $5H_2O$ and 0.5 g of TiO_2 were added to 10 ml of distilled water. NaOH solution (12 M of NaOH dissolved in 20 ml of distilled water) was then added and constantly stirred for 30 minutes to form a yellowish mixture. The prepared solution was placed in a stainless steel, Teflon-lined autoclave with a filling capacity of 25%, where the hydrothermal process (second stage)

begins. Afterwards, the resulting product was ball milled and washed several times with distilled water, until a solution of pH=7 was obtained. The powder was dried in an oven at 90 ºC overnight for further characterisation.

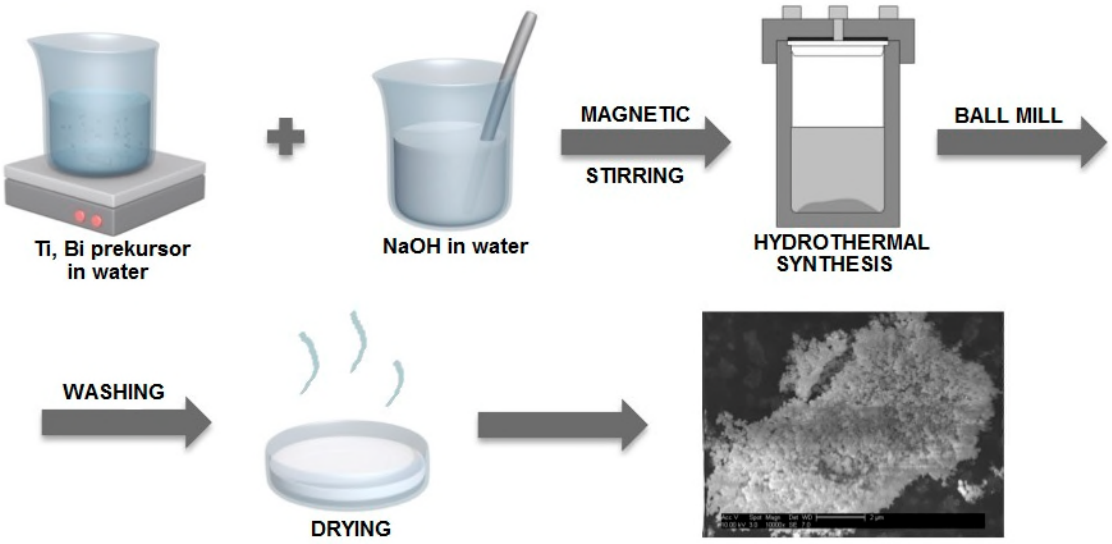

Figure 4-2 A Schematic diagram for NBT nanopowder preparation steps

4.1.3 Effect of Temperature

The prepared powders were analysed by X-ray diffraction (XRD) to determine the phase composition. XRD analysis was performed for each of the powder samples produced under different conditions. To study the influences of the reaction temperature, hydrothermal syntheses were carried out at temperatures of 120 ºC and 200 ºC for 24 h under a 8M NaOH solution. As seen from Figure 4-3, the crystalline phase of NBT starts to be visible at 120 ºC and the strongest peaks are associated with the presence of $Bi_{0.5}Na_{0.5}TiO_3$ (JCPDF no. 46-0001). However, the corresponding peaks are very low, which indicates that powders synthesised at this temperature are amorphous and show poor crystallisation.

Under the influence of high temperature, 200 ºC, the diffraction peaks intensity increase and a single-phase is more visible.

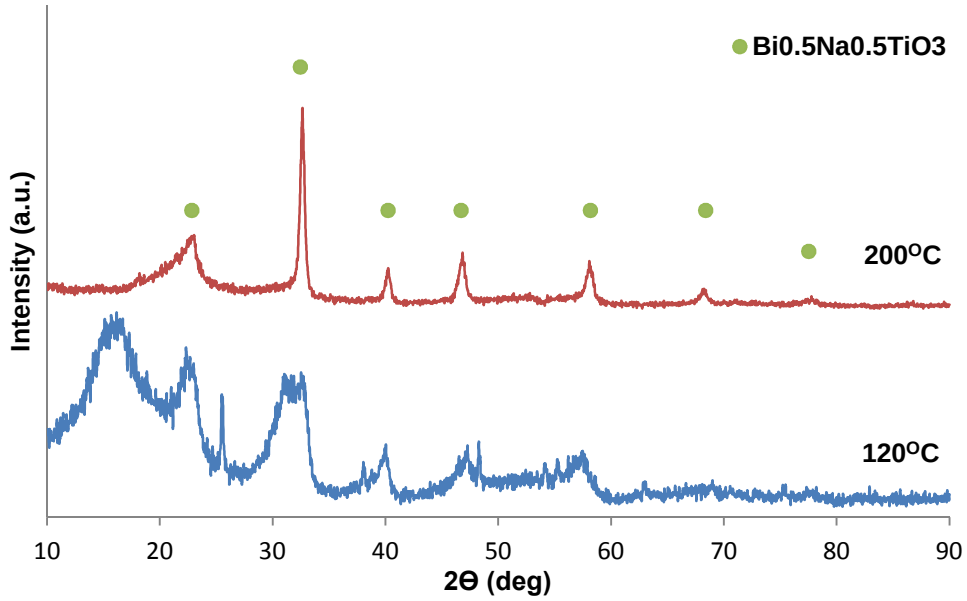

Figure 4-3 X-ray diffraction patterns obtained at different temperature

4.1.4 Effect of NaOH Concentration

During hydrothermal synthesis, NaOH was used not only as Na^+ source but also offers the alkalinity that was needed for NBT formation. To check the relationship between NaOH concentration and the NBT crystal growth, different ratios of NaOH were tested. Figure 4-4 shows the XRD diffraction patterns of the powders synthesised at 200 ºC for 24h under NaOH concentrations of 2 M, 8 M and 12 M, respectively. As can be seen, the formation of the NBT phase starts to emerge at a NaOH concentration of 2 M. There is also evidence of other peaks, which are assigned to TiO_2 phase (JCPDS no. 04-0477). This indicates that the powder is not fully synthesised. Similar observations were also reported by Setric et al. (2011), but the difference is that TiO_2 phase is not so clearly defined and a few diffraction peaks of Bi-rich phases can also be

observed. At a 8 M alkali concentration, the corresponding diffraction peaks are clearer and stronger, but a pure phase of NBT powder was obtained with an NaOH concentration of 12 M. This demonstrates that to synthesise NBT powder, high alkalinity is needed, which confirming the observations summarised in literature (Jiang et al. 2011; Ma et al. 2013).

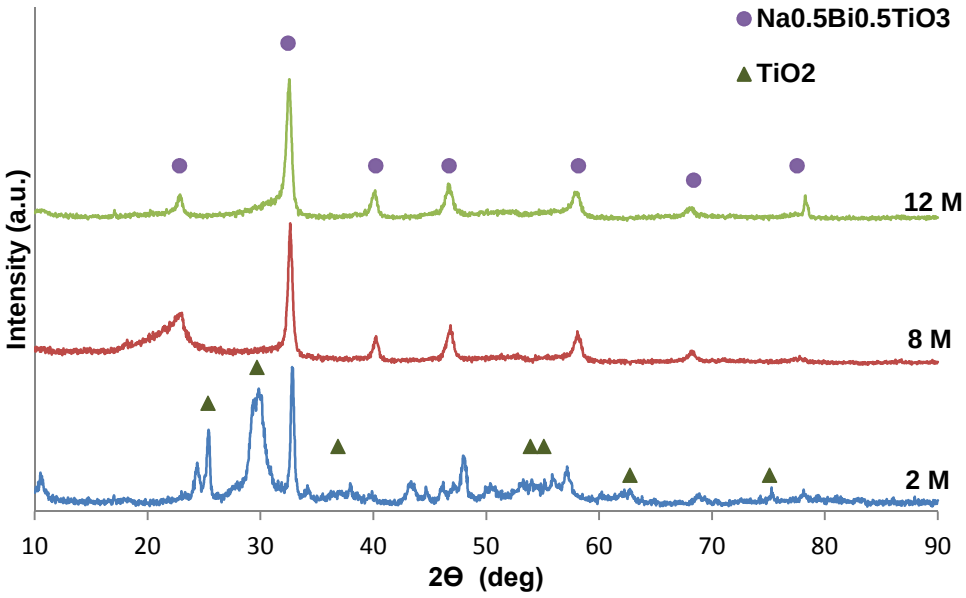

Figure 4-4 X-ray diffraction patterns obtained at different NaOH concentration

The morphology of synthesised particles, with different NaOH concentration was characterised by SEM. As can be observed in Figure 4-5, the alkali concentration plays an important role in NBT nanoparticle formation. As visualised on Figure 4-5 A, the material is strongly agglomerated at low concentrations of sodium hydroxide (2 M). The agglomerates formed very large aggregates and the individual NBT particles are not visible. This result is due to the fact that the Ti precursor was not reacted completely, as it was demonstrated during XRD analysis (Figure 4-4). The higher NaOH concentration of 8 M (Figure 4-5 B) resulted in formation of large spherical,

nanoparticle aggregates of about 200 nm diameters. Figure 4-5 C shows an SEM micrograph of NBT powder synthesised under an NaOH concentration of 12 M. Spherical particles in the diameter range of 5-15 nm can be observed.

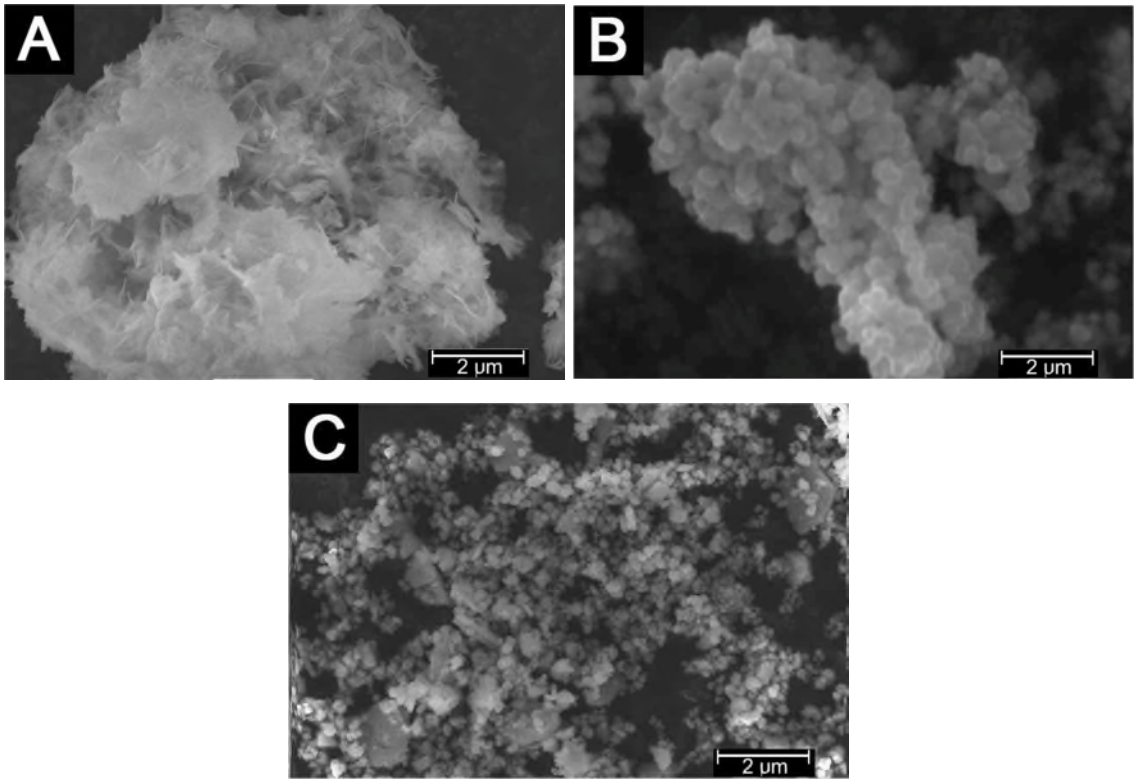

Figure 4-5 SEM images of nanoparticles obtained at different NaOH concentration A) 2 M, B) 8 M, C) 12 M

4.1.5 Effect of Reaction Time

The influence of reaction time was also investigated. The synthesis processes were carried out at 200 ºC under NaOH concentration 12 M for 12 h and 24 h, respectively. The XRD patterns, presented in Figure 4-6, show that powders obtained at both temperatures are the same NBT phase. However, the powder synthesised for 12 h contains impurities. The intensity of the peaks increases

and the crystallites grow larger with increasing reaction temperature. Pure phase and well-crystallised NBT crystals were achieved after 24 h.

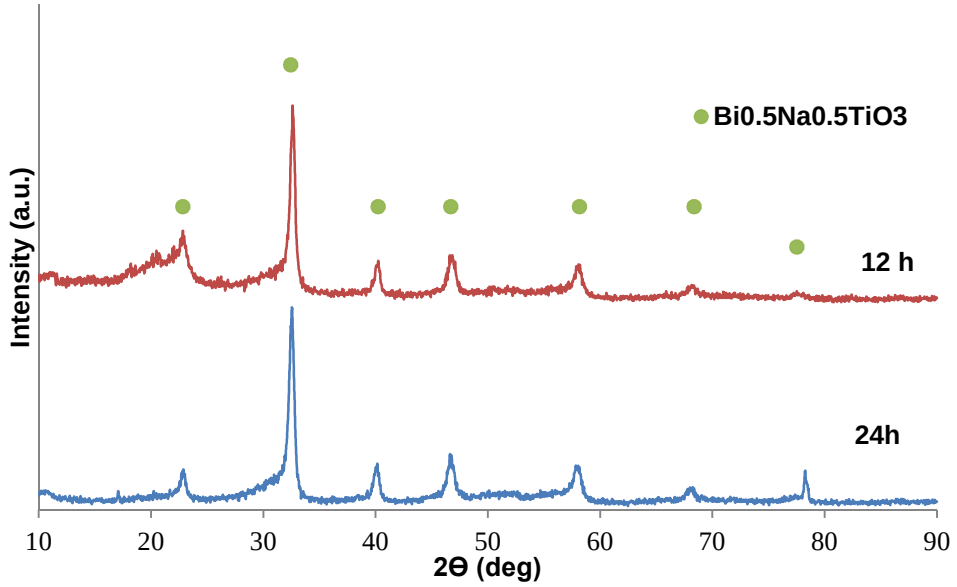

Figure 4-6 X-ray diffraction patterns obtained at different reaction time

4.2 Commercial Powders Characterisation

4.2.1 Nanopowders

The selection of the most appropriate materials for research was based on the biochemistry, availability, toxicity and cost. The properties of selected nanopowders are presented in Table 4-2.

The silicon dioxide (SiO_2), zinc oxide (ZnO) and titanium dioxide (TiO_2) were purchased from Sigma Aldrich and used without pretreatment. The nanotubes used in this study are L-MWCNT 1020 (commercial MWCNT), produced by Shenzhen Nanotech Port Co. Ltd. The properties declared by producer are listed in Table 4-1.

Table 4-1 Characterisation of commercial powders (Sigma Aldrich and Shenzhen Nanotech Port Co. Ltd datasheet)

Name	Formula	Particle size	Purity (%)
Silicon dioxide	SiO_2	12 nm	99.8
Titanium dioxide	TiO_2	21 nm	99.5
Zinc oxide	ZnO	<100 nm	90
Multi walled carbon nanotube	MWCNT	10-20 nm	95

Table 4-2 List of properties for selected nanopowders

Formula	Properties
SiO_2	inexpensive, corrosion resistance, high hardness, resistant to weathering, stability, low toxicity
TiO_2	low cost, very durable, large chemical and corrosion resistance
ZnO	anticorrosive, retain flexibility of material, improve adherence of paint, low cost
MWCNT	very durable, improve mechanical properties, tensile strength

4.2.2 Characterisation

The nanomaterials used in this study were examined by two different techniques. The SEM and TEM micrographs were used to obtain information regarding the size and morphology of particles. The X-ray diffraction tests were carried out in order to investigate the purity of the powders.

As shown in Figure 4-7, XRD patterns of selected nanopowders matched with the standards perfectly and the strongest peaks are associated with presence of SiO_2 (JCPDS no. 43-0596), TiO_2 (JCPDS no. 04-0477), ZnO (JCPDS no. 36-1451) and C (JCPDS no. 26-1076), respectively. There was no indication of impurities demonstrating a high purity of materials. Microscopic images of the samples (Figure 4-7) show a different size and shape of particles. It was proven that all powders were in the range 10-70 nm.

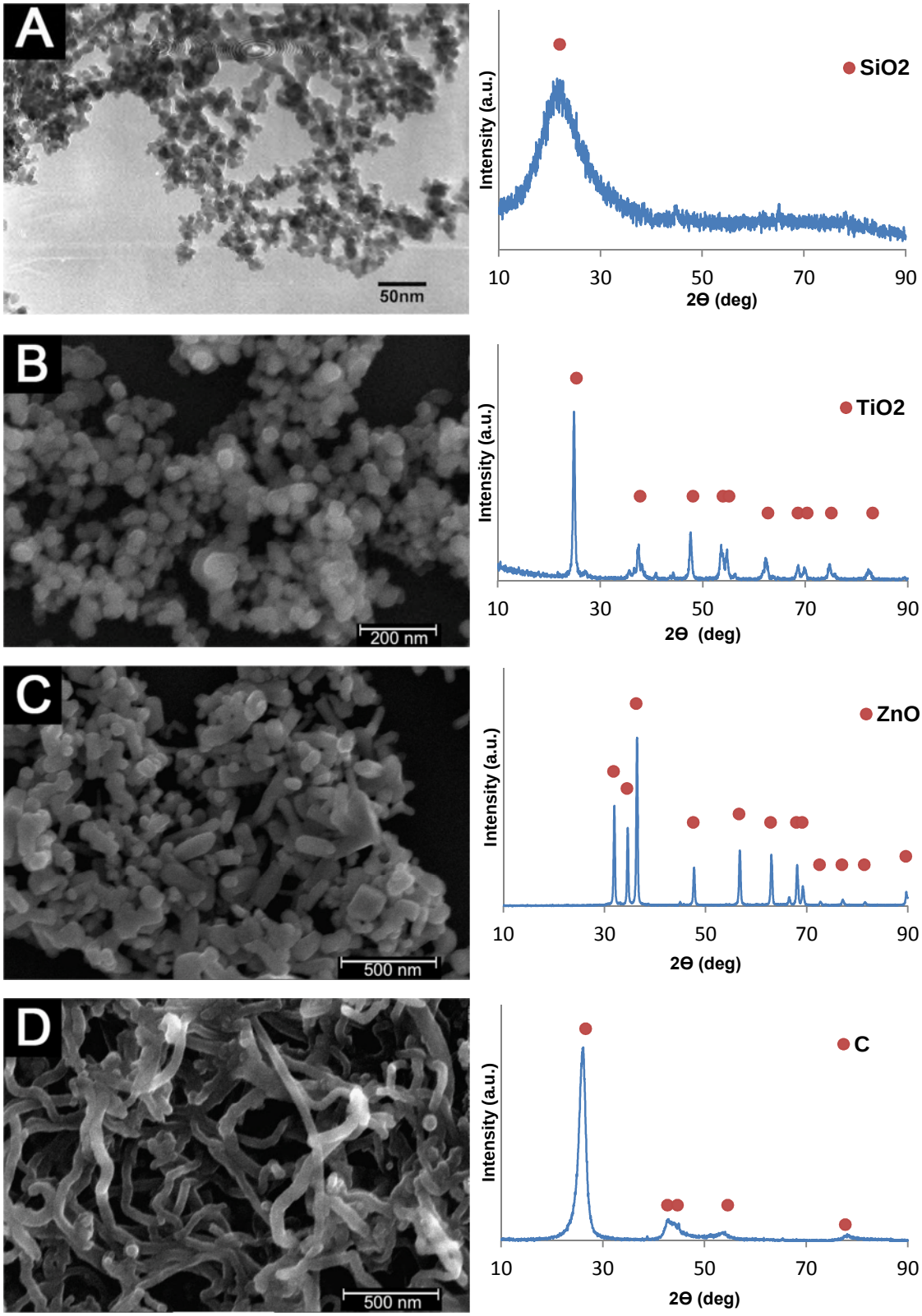

Figure 4-7 X-ray diffraction patterns, SEM and TEM microstructure of nanoparticles: A) SiO_2, B) TiO_2, C) ZnO, D) MWCNT

4.3 Conclusion

This chapter provides an overview of the NBT synthesis and characterisation of powders used in this study. In summary, NBT nanopowder was successfully prepared by a hydrothermal method. The characterisation results suggested that purity and particle composition of NBT are significantly dependent upon three factors: alkali concentration, reaction time and temperature. It was shown that morphology could be controlled by changing the concentration of the NaOH solution. Spherical NBT nanoparticles with diameters of 5-15 nm were obtained at 200 ºC for 24h under 12 M NaOH concentrations.

The morphology results of all chosen powders were described, which allowed the determination of the shape and size of particles. The results of chemical compositions confirmed purity of the powders. The application of these particles and their role in the antifouling coatings will be described in the next sections.

5 Synthesis and Characterisation of Antifouling Coatings

In this chapter the polymer nanocomposite coatings based on PDMS and the selected nanopowders were investigated as antifouling films. The first part of this chapter describes the synthesis of polymer nanocomposites and the preparation of coatings. The second part describes the impact of nanoparticles on the surface structure and morphology, followed by properties of the coatings.

5.1 Introduction to PDMS

The issues existed in antifouling paints based on biocides have led to a search for alternative antifouling systems. From an ecological point of view, the most promising possibilities to control biofouling employ foul-release (FR) technology (Swain, 1999; Brady Jr., 1999). The compounds, which possess such properties, belong to a class of water-insoluble silicone polymers (silicones). The appropriate structural form of the silicone is the silicone backbone, a repeating group of -Si-O- attached with various organic groups. Depending on the type of functional groups and the geometric characteristics of the molecule silicones can be liquids, gums, rubbers and elastomers. One of the most common silicone polymers is non-toxic and commercially available polydimethylsiloxane (PDMS). PDMS coating is very flexible, it has low critical surface tension of 20-24 mJ/m^2 and has an extremely low elastic modulus ~1 MPa (Brady Jr., 1999), what results in better antifouling properties. Introducing different substituents to methyl to the backbone of PDMS could change the physico-chemical properties of the coating. In addition, substitutes can help to prevent fouling by marine organisms.

5.2 Polymer Nanocomposites

Polymer nanocomposites (PNCs) are two-phase materials having polymer and nanoscale particles embedded in the polymer matrix. PNCs are prepared in order to impart better properties to material (mechanical, biological, optical). The beneficial properties of polymer nanocomposites can be obtained with a small amount of nanoparticles, but the size of particles is important and it is believed that they should not exceed 100 nm (Goins and Philips, 2011).

Polymer nanocomposites can be synthesised by the following methods:

- direct mixing
- mixing in solution
- in-situ polymerisation

The direct mixing method involves mechanical mixing of nanoscale particles with the polymer. This method is quite difficult due to the high viscosity of certain polymers. For this purpose, surfactants are often used to change the chemical properties of the polymer. The second method utilises a solvent, which is evaporated at the last stage. The nanoparticles are dispersed in polymer solution (polymer + solvent). To increase the intensity of mixing and the correct spread of particles in polymer solution, ultrasounds are often used. In the in-situ polymerisation method, nanoparticles are obtained during the synthesis of nanocomposite or they are mixed with monomer, followed by reaction of polymerisation.

5.3 Synthesis of PDMS Nanocomposites

The polymer incorporated in this research, polydimethysiloxane (PDMS) was purchased and then modified at the nano scale to obtain a new antifouling coating composite material. The most widely used and easily accessible Sylgard 184 was selected for this work (Dow Corning). The formulation came in two parts: a silicone elastomer base containing vinyl chain ends -PDMS (Part A) and a curing agent having SiH-terminated-PDMS and the Pt-catalyst (Part B).

Both compounds were manually stirred at a weight ratio of 10:1 in order to obtain PDMS polymer. Pure polymer was used as reference material.

The nanocomposites were prepared using nanopowders (NP) described in Chapter 4. In order to obtain a good dispersion of the nanoparticles in the polymer, ethanol (EtOH, Sigma Aldrich) and toluene (Sigma Aldrich) were used as organic solvents. Commercially available chemicals were used as received without further purification. In the present study, 9 types of nanocomposie coatings were tested. The nanopowders were used in two different weight ratios (PDMS:NP 20:1 and 10:1) and the actual combination of mixtures used in PDMS nanocomposites synthesis is presented in Table 5-1.

Table 5-1 The actual combinations of mixtures used in synthesis of polymer nanocomposites

Sample	Nanopowder	PDMS	Solvent
PDMS	-	3.3 g	-
PDMS/SiO_2 20:1	0.165 g SiO_2	3.3 g	2 ml toluene
PDMS/TiO_2 20:1	0.165 g TiO_2	3.3 g	1.5 ml ethanol
PDMS/TiO_2 10:1	0.33 g TiO_2	3.3 g	2.5 ml ethanol
PDMS/ZnO 20:1	0.165 g ZnO	3.3 g	1.5 ml ethanol
PDMS/ZnO 10:1	0.33 g ZnO	3.3 g	2.5 ml ethanol
PDMS/MWCNT 20:1	0.165 g MWCNT	3.3 g	2 ml toluene
PDMS/MWCNT 10:1	0.33 g MWCNT	3.3 g	2 ml toluene
PDMS/NBT 20:1	0.33 g NBT	6.6 g	-
PDMS/NBT 10:1	0.66 g NBT	6.6 g	-

5.3.1 PDMS/ZnO and PDMS/TiO_2 Nanocomposites

To manufacture nanocomposites based on ZnO and TiO_2, the following steps were followed: powders were separately dissolved in ethanol and sonicated for 15 min. The mixture was then combined with previously prepared PDMS. To make sure that particles were spread correctly in the polymer an ultrasonic bath was used for 1 h.

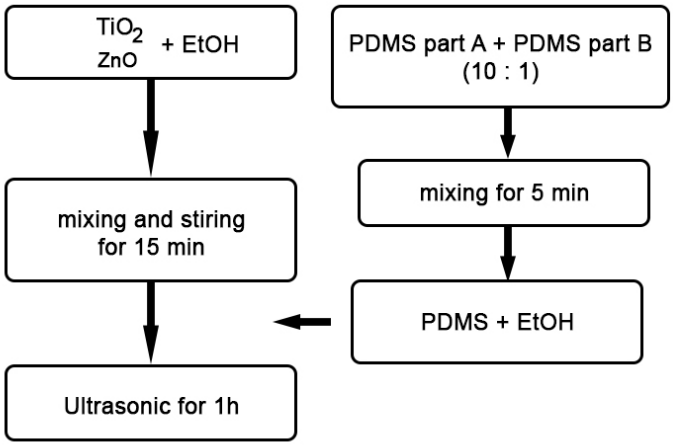

Figure 5-1 Flowchart of the preparation of PDMS/ZnO and PDMS/TiO_2 nanocomposites

5.3.2 PDMS/SiO_2 and PDMS/MWCNT Nanocomposites

The preparation process of PDMS/SiO_2 and PDMS/MWCNT nanocomposites is shown in Figure 5-2. At the first stage, a nanopowder either SiO_2 or MWCNT was dispersed in organic solvent and mixed in an ultrasonic bath at room temperature for 15 min. Afterwards the solution was mixed with the previously produced PDMS. Initially, the solution was hand-mixed for 5 min then to increase the intensity of mixing an ultrasonic bath was applied. The solution was placed in an open container to evaporate excess solvent.

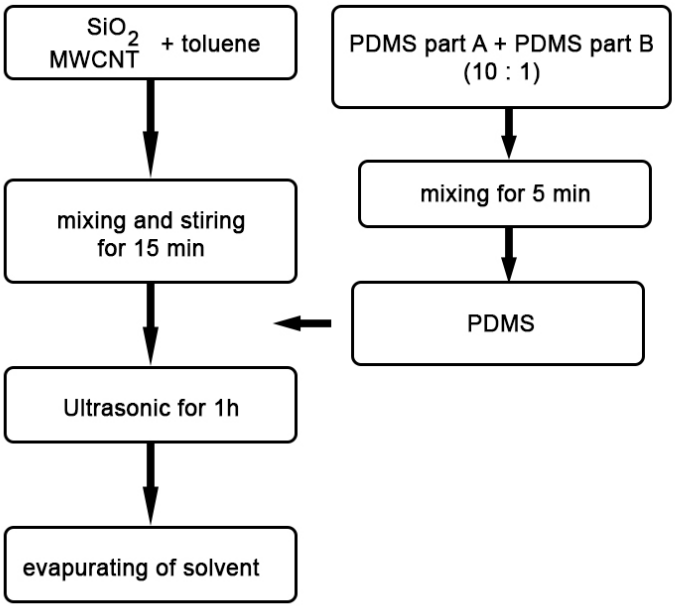

Figure 5-2 Scheme of PDMS/MWCNT and PDMS/SiO_2 nanocomposites preparation

5.3.3 PDMS/NBT Nanocomposite

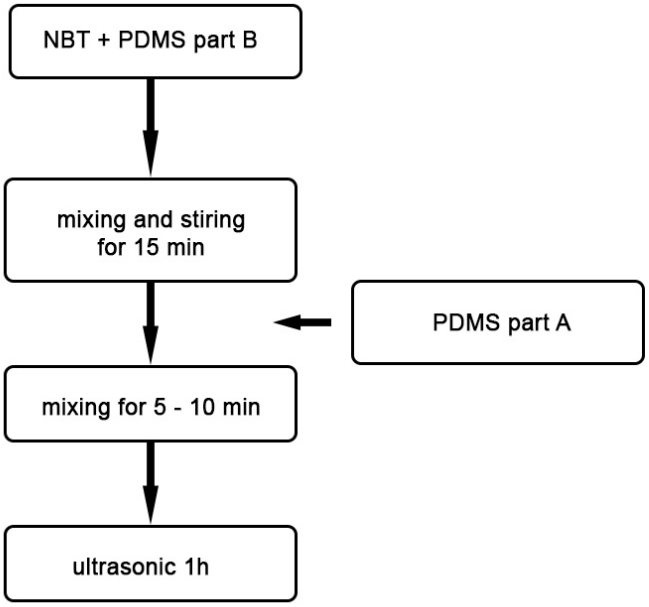

Figure 5-3 Scheme of the preparation of PDMS/NBT nanocomposite

To produce PDMS/NBT nanocomposite, an appropriate amount of previously synthesised NBT nanopowder (Section 4.1) was dispersed in PDMS curing agent (Part B) and sonicated for few minutes. Subsequently, silicone elastomer base (Part A) was poured slowly and mixed manually, followed by sonication.

5.4 Coatings Preparation

5.4.1 Substrate Cleaning

In this work, the standard laboratory glass slides were used as primary substrates. It was necessary to thoroughly remove impurities from substrate before coating application glass slides were washed by soap with deionised water and isopropanol, and dried with N_2.

5.4.2 Coatings Application

The solutions were deposited onto the glass substrate by a micrometer film applicator - doctor blade. During this application technique the thickness of coating can be easily controlled and there is little product waste. The scheme describing the doctor blade deposition method is illustrated in Figure 5-4. To avoid settling of the particles in polymer, nanocomposites were applied directly after preparation. The coated samples were degassed in a desiccator to remove the trapped air bubbles. Finally, the coatings were dried in oven at 80 ºC for 1 h and left to cool at room temperature. The PDMS without nanoparticles was prepared at this same condition for comparison.

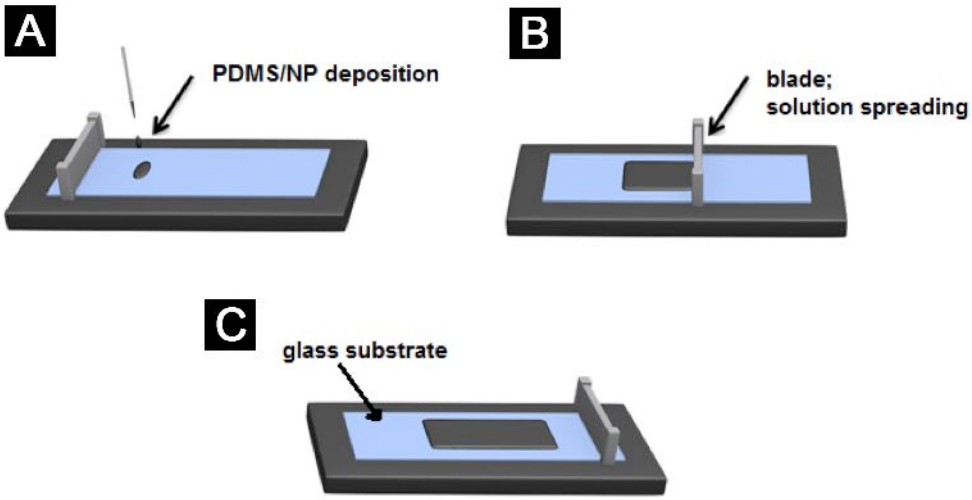

Figure 5-4 Scheme describing the doctor blade deposition method: A) deposition of PDMS/NP on glass slide, B) solution spreading by the doctor blade, C) all surface area covering

5.5 Nanocomposite Coatings Characterisation

In the present study, 10 different coatings were formed (including pure PDMS) as illustrated in Figure 5-5. The image taken with a digital camera demonstrates the homogeneity in colour and uniform coverage of coatings. As presented on Figure 5-5 A-J, two of prepared samples are colourless, highly transparent and the remaining eight coatings have adopted colours of used powders. The presence of MWCNT in the coatings (Figure 5-5 I and J) causes resistant to colour change, which can be a problem in use on an industrial scale.

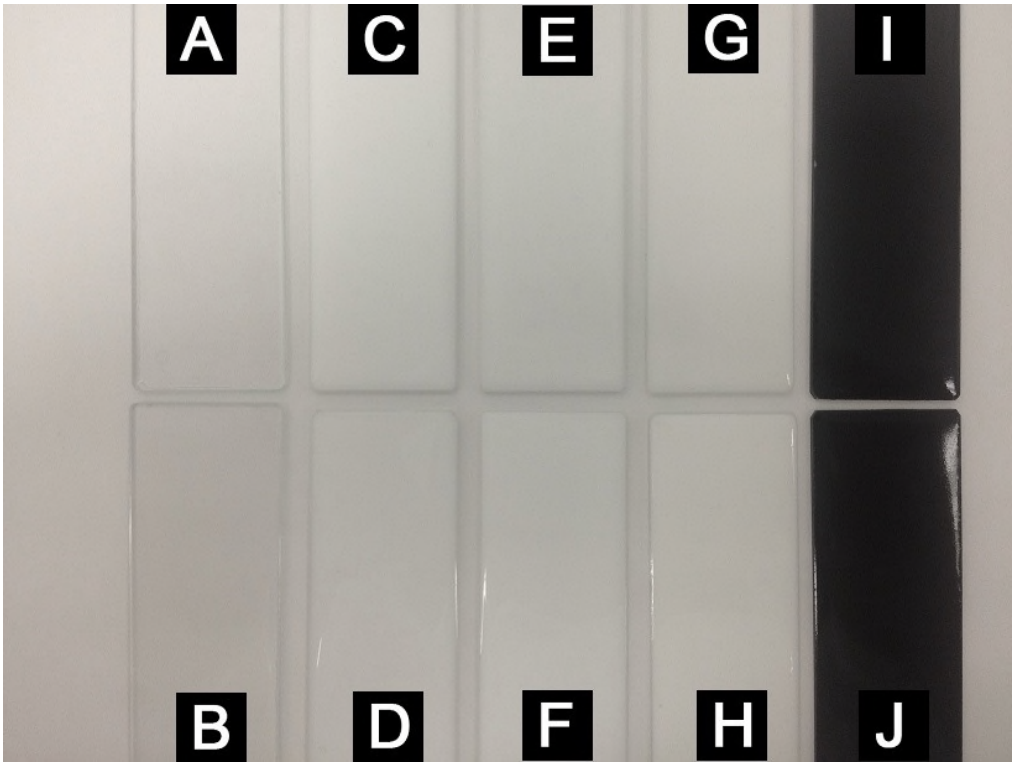

Figure 5-5 The final coatings: A) PDMS, B) PDMS/SiO_2 20:1, C) PDMS/TiO_2 20:1, D) PDMS/TiO_2 10:1, E) PDMS/ZnO 20:1, F) PDMS/ZnO 10:1, G) PDMS/NBT 20:1, H) PDMS/NBT 10:1, I) PDMS/MWCNT 20:1, J) PDMS/MWCNT 10:1

The characterisation and properties of the final coatings were tested and discussed. The phase composition was identified by XRD. SEM and AFM were used to investigate morphology and texture of materials. Subsequently, the wettability was examined and the surface energy calculated. All characterisation methods are described in Chapter 3.

5.5.1 Effect of Nanopowders on the Coatings Morphology

5.5.1.1 PDMS Coating

The studies carried out on PDMS coating were made as a comparative reference to polymer nanocomposite coatings. The result of XRD analysis is

shown in Figure 5-6 and reveals the presence of a characteristic amorphous peak in the range 2Θ = 10-35º from the highest intensity around 12º (Yang D. et al. 2015). The presence of additional peaks was not observed, which proves the purity of the test material.

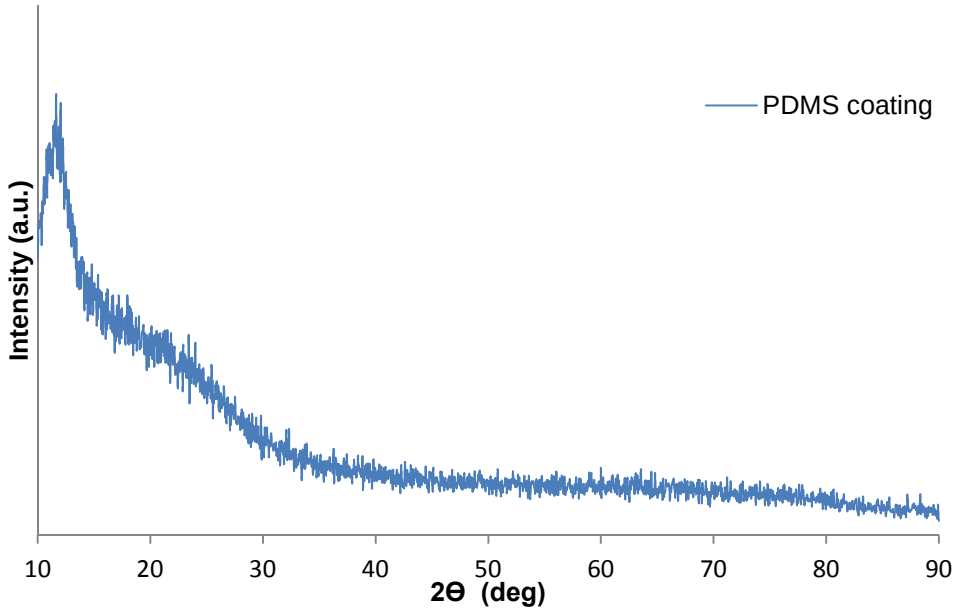

Figure 5-6 X-ray diffraction pattern of PDMS coating

The transparent PDMS coating applied to the glass slide was tested by scanning electron microscope. The microstructures of surface presented on Figure 5-7 show that a perfectly smooth coating, without visible impurities, cracks and distortion was obtained.

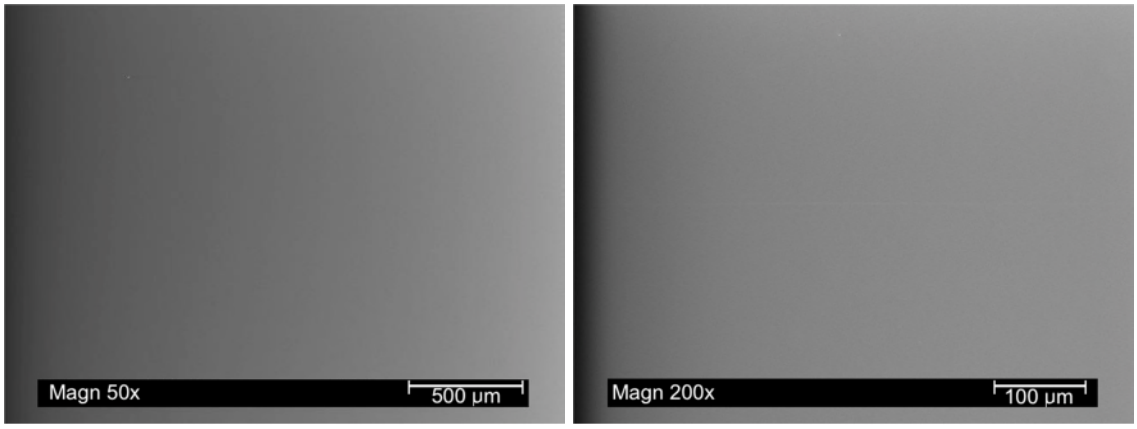

Figure 5-7 SEM micrographs in low magnifications, of PDMS coated on glass slide

5.5.1.2 PDMS/SiO_2 Coating

During the sample preparation it was noted that increasing amounts of silicon dioxide nanopowder prevented polymerisation. For this reason, SiO_2 nanopowder was tested only in one weight ratio (PDMS/SiO_2 20:1).

In order to determine the purity of PDMS/SiO_2 nanocomposite coating, analysis was carried out using XRD. The diffraction patterns presented in Figure 5-8 shows characteristic amorphous peak for silicon dioxide powder and PDMS/SiO_2 nanocomposite coating. The characteristic peak assigned to SiO_2 (JCPDF no. 43-0596) cannot be detected in PDMS/SiO_2 diffraction pattern. This is associated with the presence of silicon in the PDMS bond, as well as with small amount of powder.

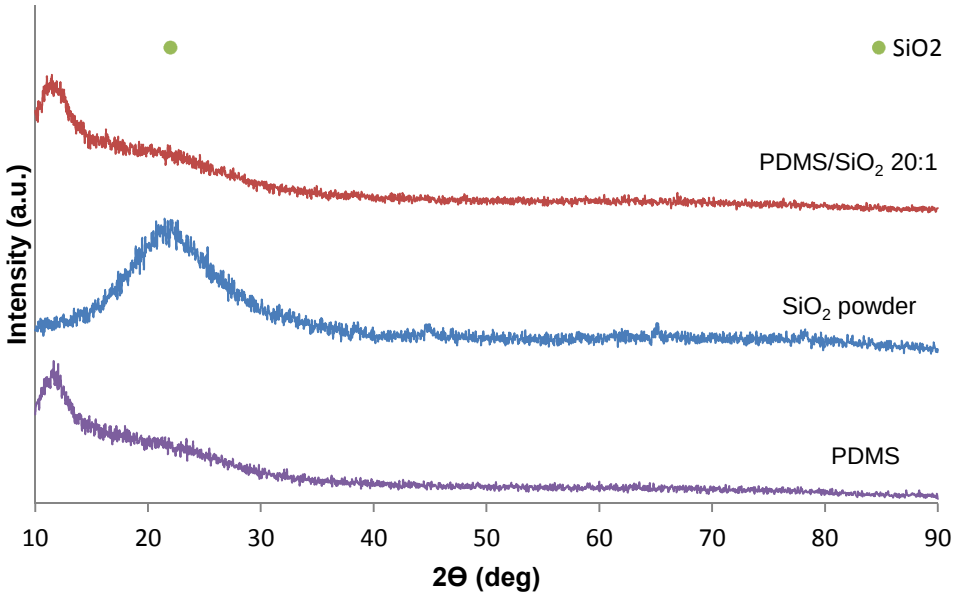

Figure 5-8 XRD spectrum of PDMS, SiO_2 nanopowder and PDMS/SiO_2 20:1 nanocomposite coating

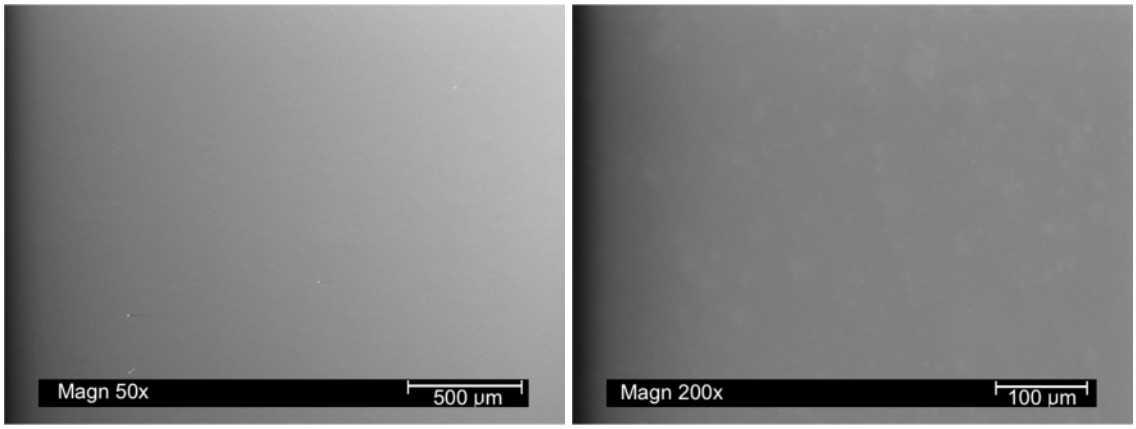

Figure 5-9 Microstructure of PDMS/SiO_2 20:1 coating taken via SEM

Figure 5-9 shows the SEM microstructure of the prepared PDMS/SiO_2 nanocomposite coating. Observations carried out at low magnification revealed the presence of several separate particles on the surface. At a slightly higher-magnification it can be seen that introduction of silicon dioxide to the PDMS

matrix affects the microstructure and particle agglomeration occurs. This indicates that some of the nanoparticles are not dispersed well.

5.5.1.3 PDMS/TiO_2 Coatings

The prepared PDMS/TiO_2 nanocomposite coatings were analysed in order to determine how the material changes with increasing TiO_2. For comparison, the XRD diffraction pattern of titanium dioxide powder is also presented. The results of XRD analysis are shown in Figure 5-10.

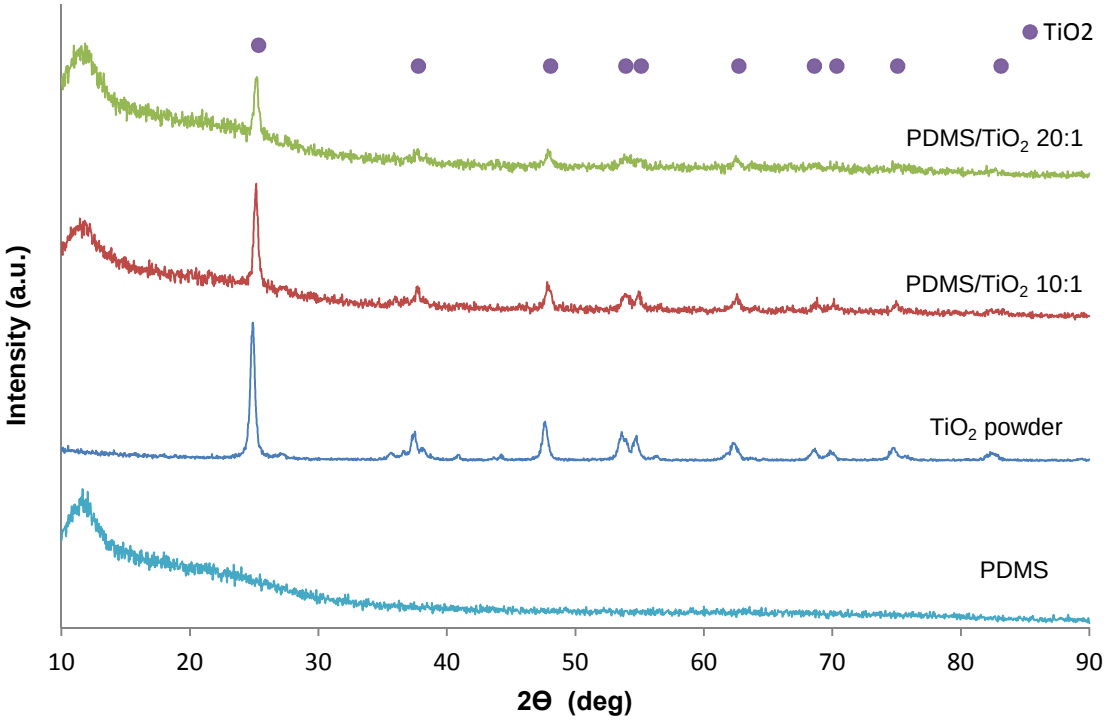

Figure 5-10 X-ray diffraction patterns of TiO_2 nanopowder and PDMS/TiO_2 20:1, PDMS/TiO_2 10:1

The characteristic peak of TiO_2 nanopowder, at 2Θ = 25° (1 0 1), was also detected in PDMS/TiO_2 20:1 and PDMS/TiO_2 10:1 coatings. The intensity of TiO_2 peaks is higher in the case of PDMS/TiO_2 10:1 coating, which is related to

larger amounts of nanopowder. In two cases, there were no additional peaks demonstrating the purity of samples.

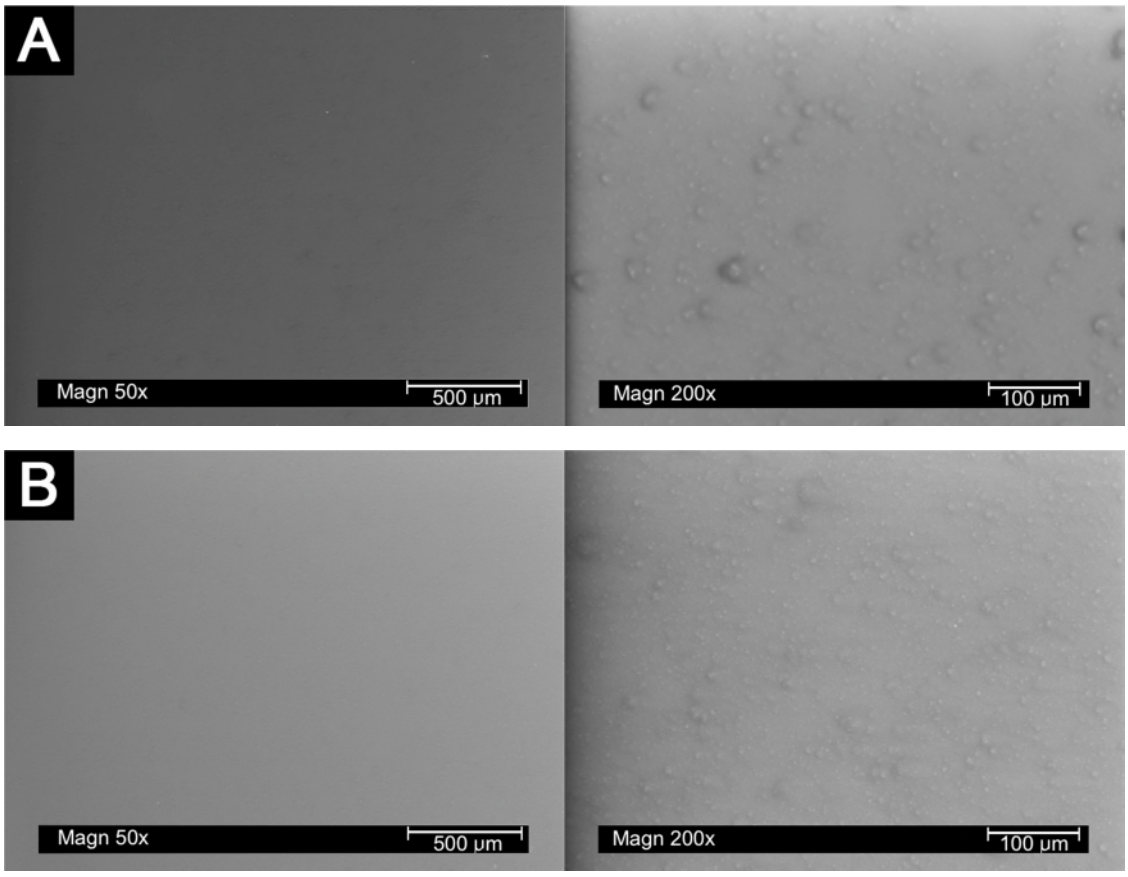

Figure 5-11 Electron microscopy images of PDMS/TiO_2 20:1 (A) and PDMS/TiO_2 10:1 (B) nanocomposites coatings.

Figure 5-11 shows SEM images taken from synthesised PDMS/TiO_2 20:1 and PDMS/TiO_2 10:1 nanocomposites coatings. The micrographs of both samples revealed similar surfaces morphology without visible cracks and distortion, which shows the uniformly distribution of the nanocomposite coatings on the substrate. The changes that can be observed during the observation at higher magnification indicate the dispersion of titanium dioxide in PDMS. The TiO_2 nanoparticles are distributed as aggregates with irregular size. Increasing the

concentration of titanium dioxide in the polymer does not show the difference in the microstructure of the coating.

5.5.1.4 PDMS/ZnO Coatings

In order to determine the microstructure of PDMS/ZnO nanocomposite coatings the X-ray diffraction analysis (XRD) was performed. The Figure 5-12 shows the X-ray diffraction pattern of ZnO powder and PDMS/ZnO nanocomposite coatings.

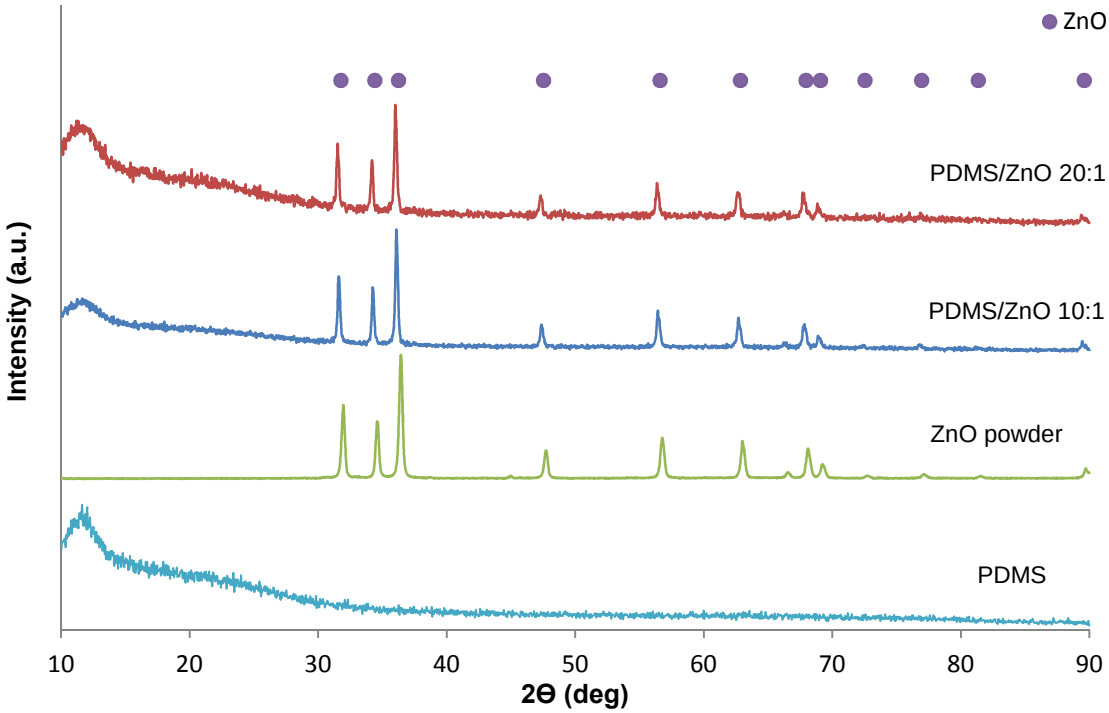

Figure 5-12 X-ray spectrum of PDMS, ZnO nanoparticles and PDMS/ZnO 20:1, PDMS/ZnO 10:1 nanocomposites coatings

Three characteristic peaks of ZnO nanopowder were chosen for comparison: 2Θ = 32º (1 0 0), 34º (0 0 2), 36º (1 0 1). These peaks were detected in

PDMS/ZnO 20:1 and PDMS/ZnO 10:1 nanocomposites coatings. The XRD diffraction patterns of these nanocomposites reveal that ZnO is detected and there is no evidence of extra peaks, what demonstrating the purity of prepared samples.

The SEM microstructures of PDMS/ZnO coatings are shown in Figure 5-13. Two nanocomposites coatings with different weight ratios of ZnO nanopowder were used for characterisation: PDMS/ZnO 20:1 and PDMS/ZnO 10:1. Following SEM analysis it can be observed that ZnO nanoparticles are uniformly distributed in polymer and there are no obvious visible morphological changes. These results provide evidence that smooth surfaces are formed.

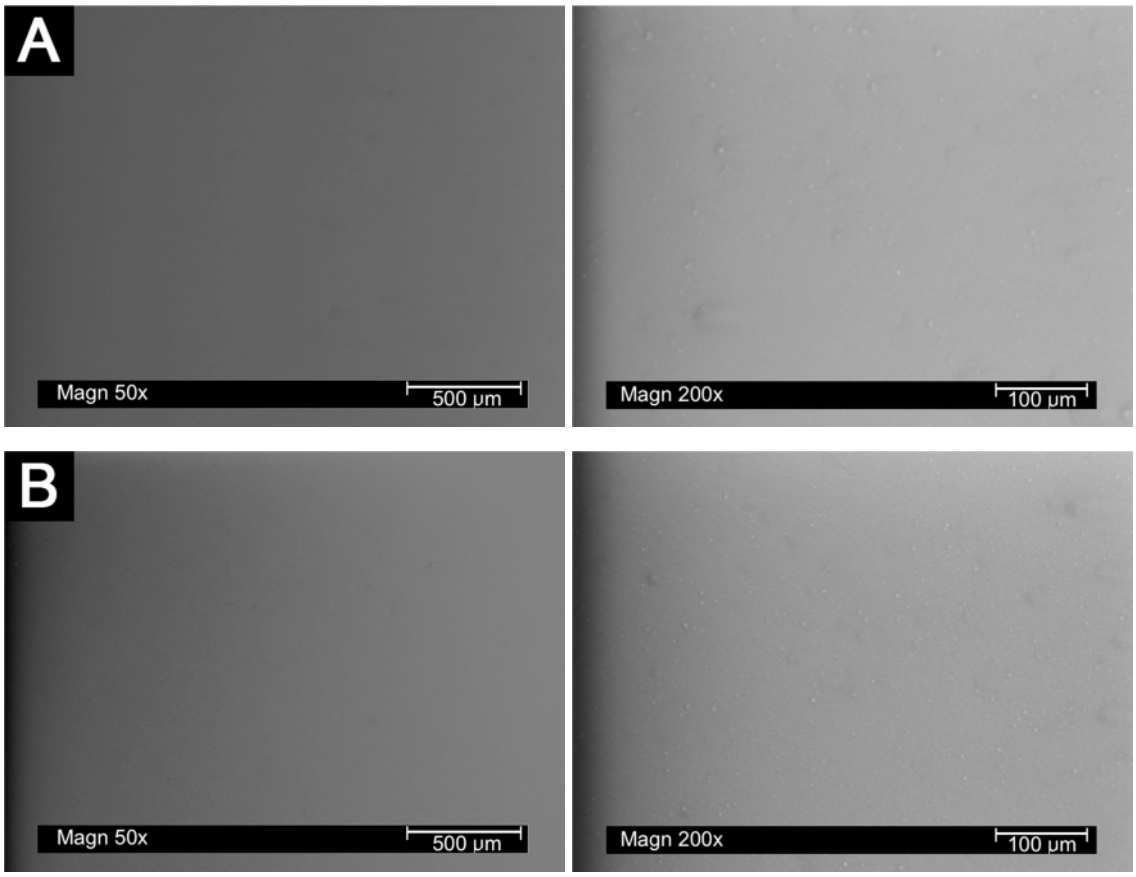

Figure 5-13 SEM micrographs of PDMS/ZnO 20:1 (A) and PDMS/ZnO 10:1 (B) nanocomposites coatings

5.5.1.5 PDMS/MWCNT Coatings

The produced PDMS/MWCNT nanocomposite coatings were subjected to X-ray diffraction analysis. Figure 5-14 shows a reference diffraction pattern of carbon nanopowder with a strong peak at 2Θ = 26,5º (0 0 6). The characteristic peak of carbon cannot be detected in PDMS/MWCNT 20:1 nanocomposite coating due to presence of a low amount of nanopowder in the prepared sample and the presence of carbon in the PDMS bond (what was observed before in the PDMS/SiO_2 20:1 coating). Additional peaks were not observed, suggesting the purity of the tested materials.

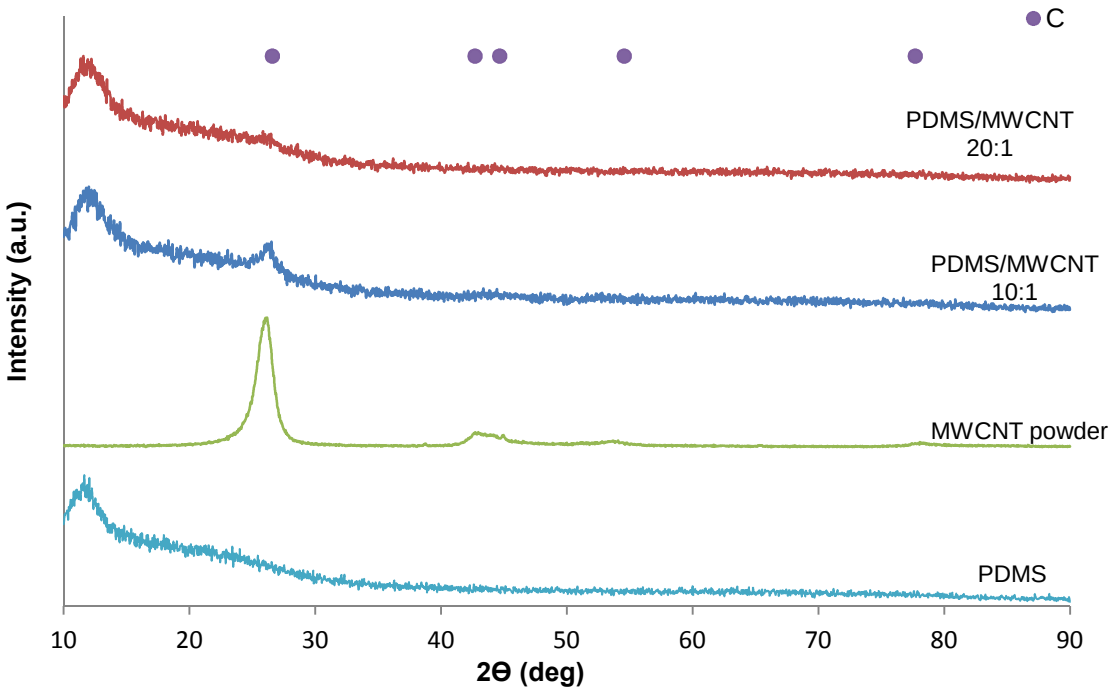

Figure 5-14 X-ray diffraction patterns of PDMS, MWCNT nanopowder, PDMS/MWCNT 20:1 and PDMS/MWCNT 10:1 coatings

Figure 5-15 shows the surface morphology of PDMS/MWCNT nanocomposites coatings deposited on glass substrates. After adding different weight ratios of

MWCNT into the PDMS matrix, some changes in colour can be observed as shown in Figure 5-15. SEM pictures taken at low magnification depicts the dark areas for both surfaces, which correspond to the particle aggregation. However, this has no impact on the general state of coating, in which no larger changes (like e.g. cracks and pores) are observed.

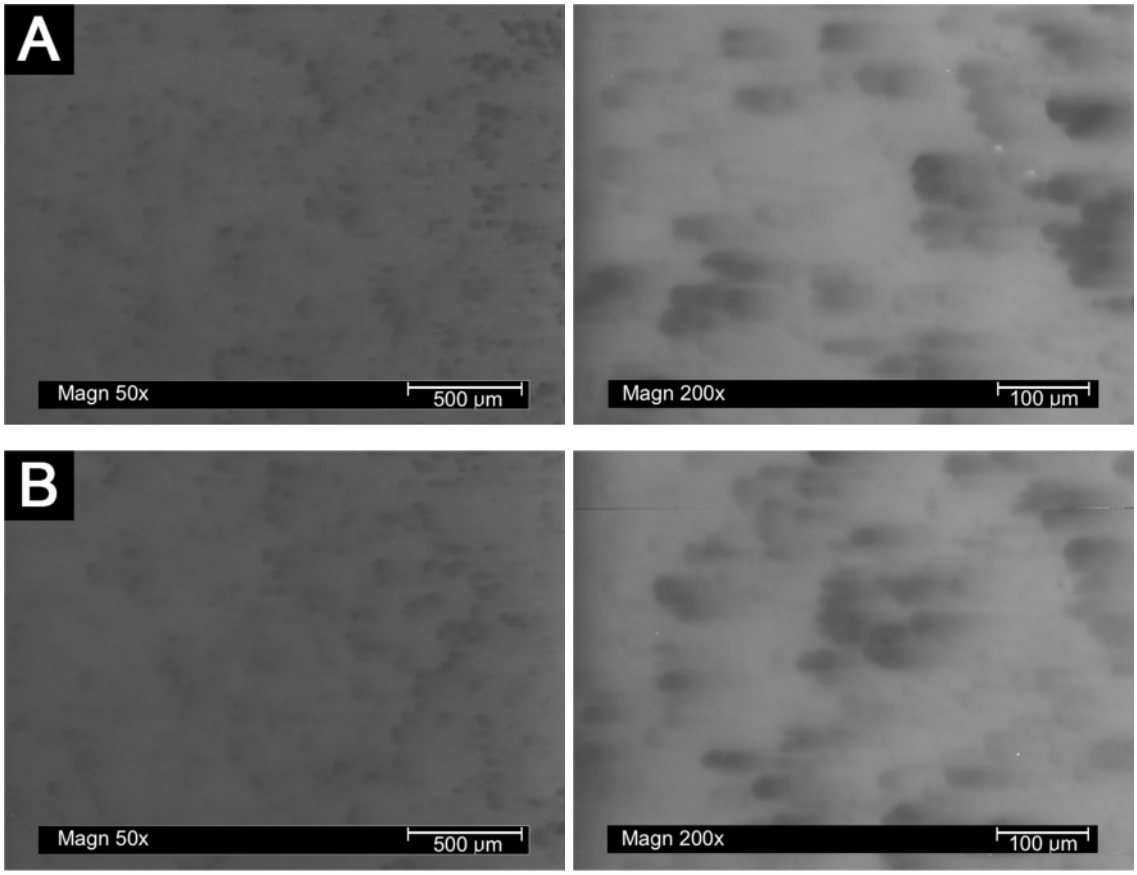

Figure 5-15 Electron microscopy images of PDMS/MWCNT 20:1 (A) and PDMS/MWCNT 10:1 (B) nanocomposites coatings

5.5.1.6 PDMS/NBT Coatings

Figure 5-16 shows a comparison of XRD patterns obtained for NBT nanopowder to PDMS/NBT 20:1 and PDMS/NBT 10:1 nanocomposite. Detected diffraction patterns of NBT reveal the presence of the characteristic

peak at 2Θ = 32.4º (1 0 2), which is detected in PDMS/NBT 20:1 and PDMS/NBT 10:1 coatings. The presence of a low amount of NBT nanoparticles in PDMS/NBT 20:1 causes a reduced intensity of NBT peaks.

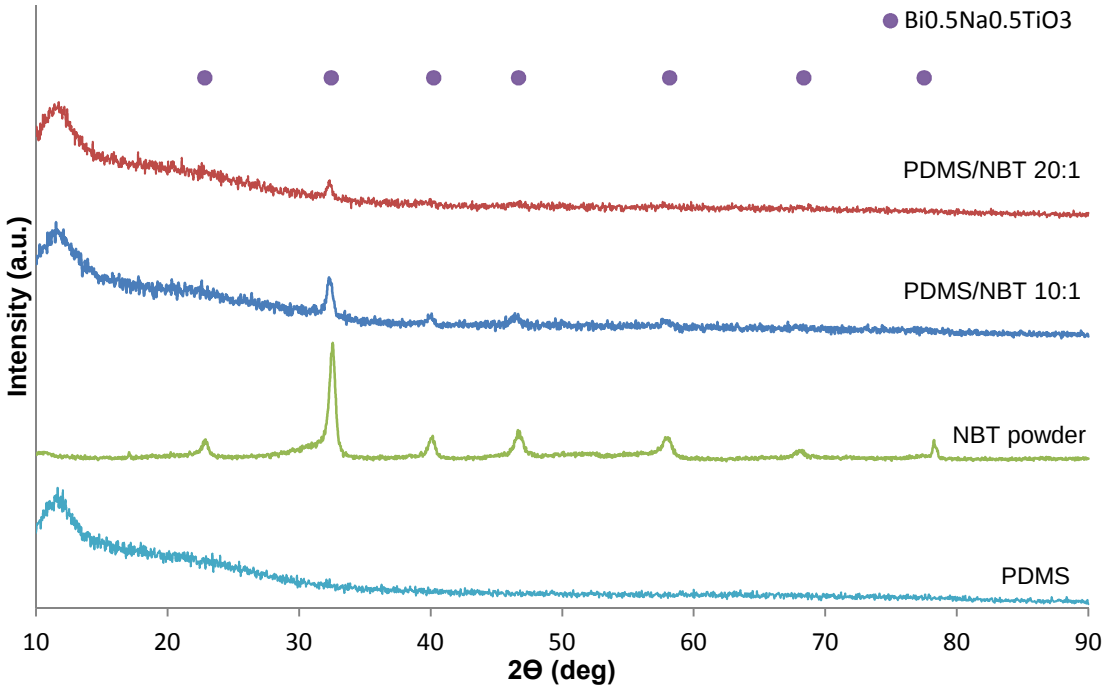

Figure 5-16 X-ray of NBT nanopowder, PDMS and PDMS/NBT 20:1, PDMS/NBT 10:1 nanocomposites coatings

Figure 5-17 shows an SEM micrograph of the microstructure of synthesised PDMS/NBT nanocomposite coatings. It can be seen that NBT nanopowder added to the polymer does not affect the structure of coatings. A highly uniform surface indicates a very good dispersion of particles.

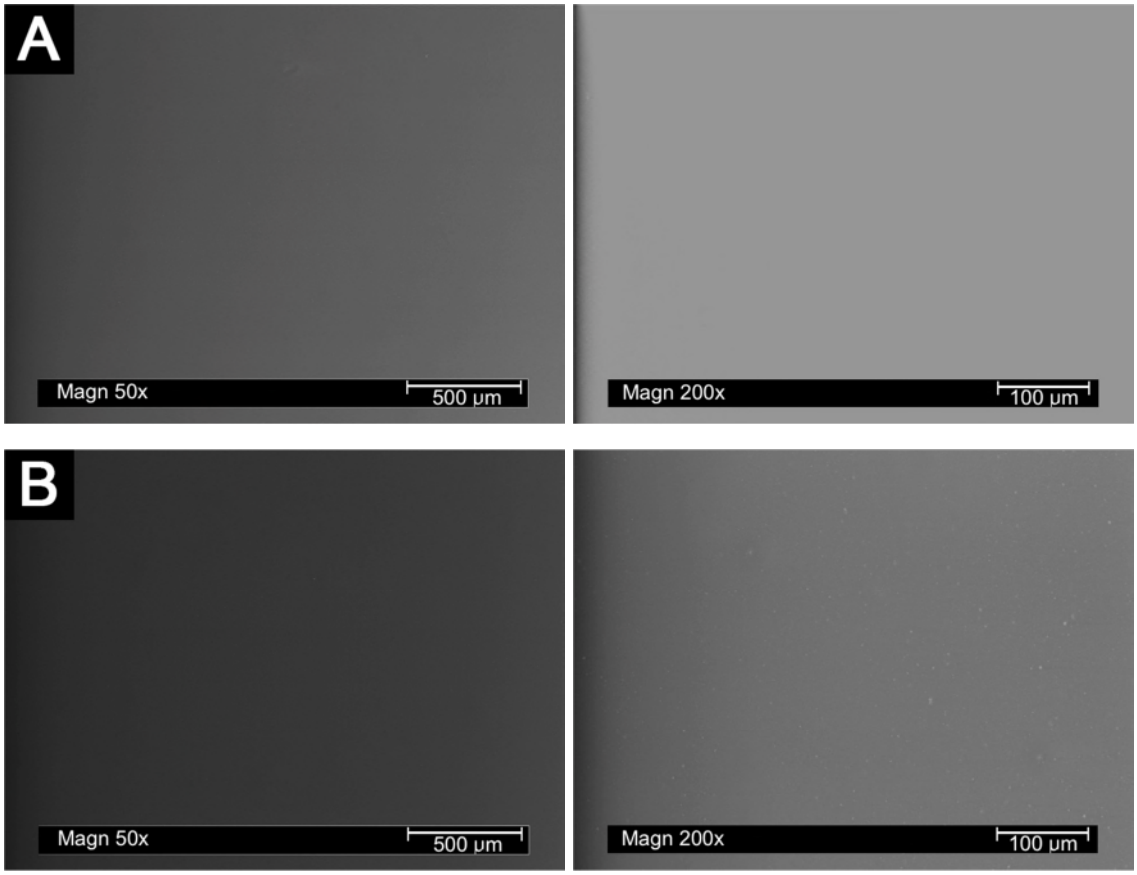

Figure 5-17 SEM micrographs of PDMS/NBT 20:1 (A) and PDMS/NBT 10:1 (B) coatings

5.5.2 Effect of Nanopowders on Surface Topography

The coatings with different chemical compositions may have different surface structure. To provide quantitative information about the topography of the samples and measure surface roughness, an atomic force microscope (AFM) was used. The surface of all 10 coatings were scanned over a 30 μm x 30 μm area and characterised. The Figure 5-18 shows 3D maps of the surfaces profile and the corresponding flat 2D images, in a given location.

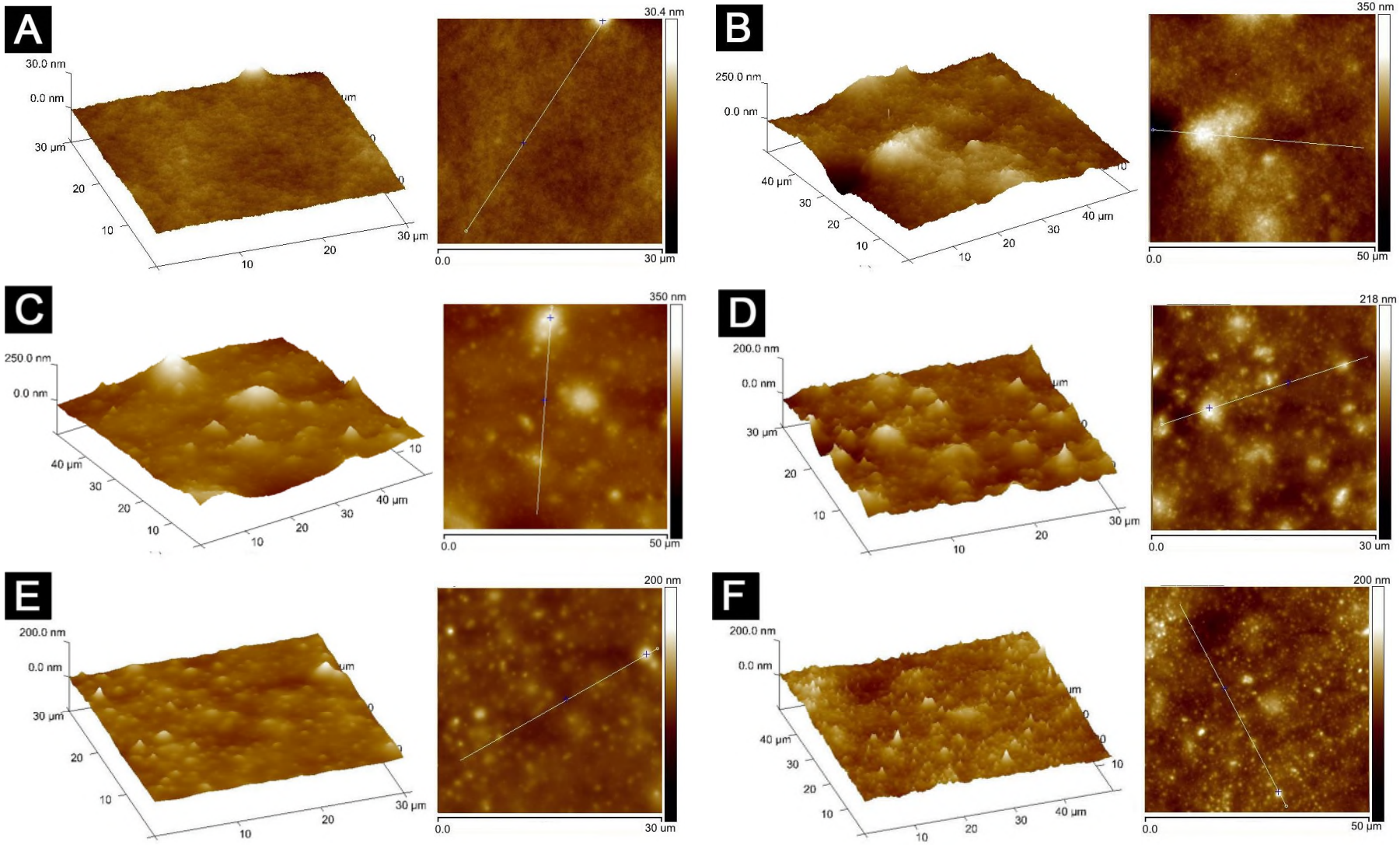
A
30.0 nm
0.0 nm
30 µm
20
10
10
20
30 µm
30.4 nm
0.0
30 µm
B
250.0 nm
0.0 nm
40 µm
30
20
10
10
20
30
40 µm
350 nm
0.0
50 µm
C
250.0 nm
0.0 nm
40 µm
30
20
10
10
20
30
40 µm
350 nm
0.0
50 µm
D
200.0 nm
0.0 nm
30 µm
20
10
10
20
30 µm
218 nm
0.0
30 um
E
200.0 nm
0.0 nm
30 µm
20
10
10
20
30 µm
200 nm
0.0
30 um
F
200.0 nm
0.0 nm
40 µm
30
20
10
10
20
30
40 µm
200 nm
0.0
50 µm

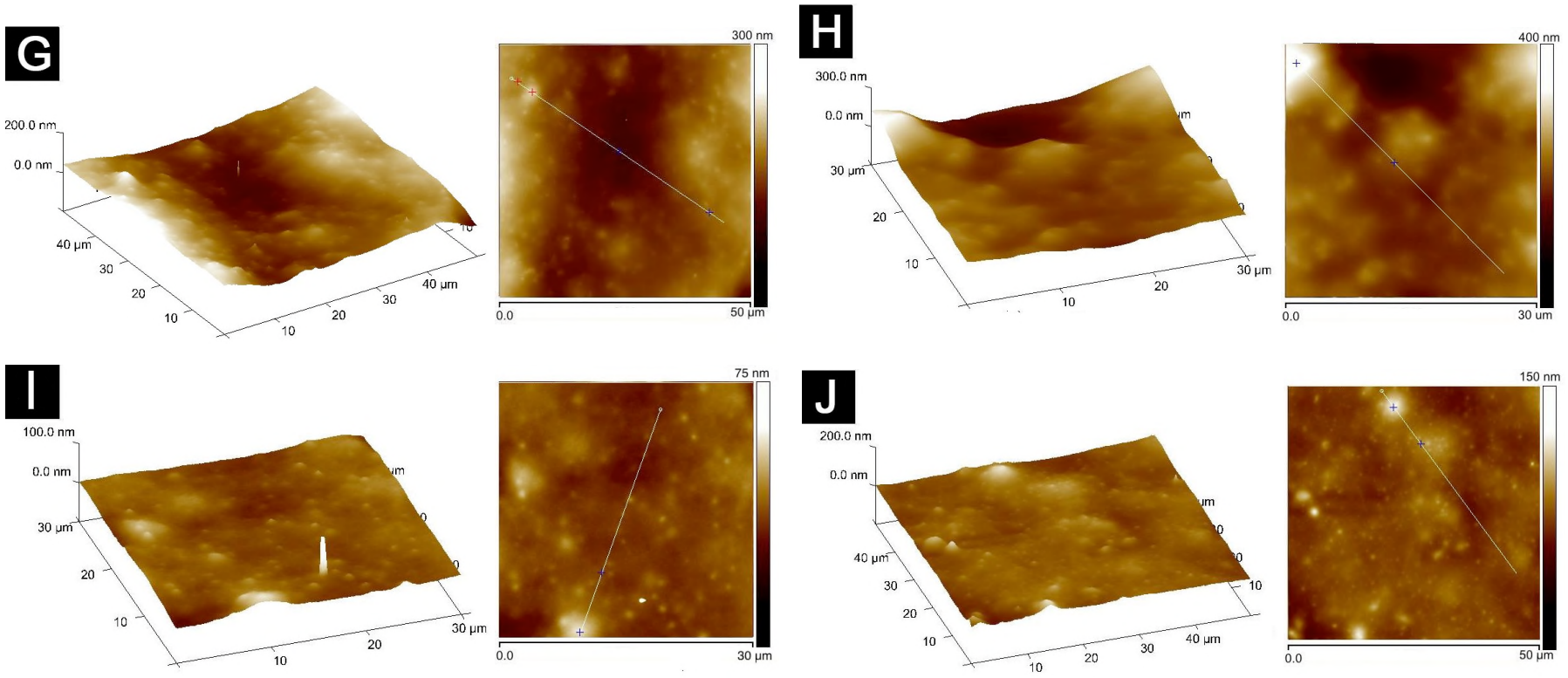

Figure 5-18 AFM topographical analysis of A) PDMS, B) PDMS/SiO_2 20:1, C) PDMS/TiO_2 20:1, D) PDMS/TiO_2 10:1, E) PDMS/ZnO 20:1, F) PDMS/ZnO 10:1, G) PDMS/MWCNT 20:1, H) PDMS/MWCNT 10:1, I) PDMS/NBT 20:1, J) PDMS/NBT 10:1, I)

The obtained results confirm the observations taken from SEM analysis. The coatings are fairly flat, without visible cracks and damages. The surface of pure PDMS coating is extremely smooth and the average roughness (Ra) value is only 0.8 nm. The images shown in Figure 5-18 C and D demonstrated that there is a change in structure and the surface become rougher after adding TiO_2. The roughness measurement of PDMS/TiO_2 20:1 is 9.46 nm and for PDMS/TiO_2 10:1 is 13.2 nm. The surfaces of PDMS/ZnO 20:1 and PDMS/NBT 20:1 coatings are nearly smooth as shown on Figure 5-18 I and E (7.4 nm and 4.6 nm). The roughness slightly increases with increasing amount of nanoparticles in the composite, and is 9.6 nm and 7.2 nm for PDMS/ZnO 10:1 and PDMS/NBT 10:1, respectively. The surface texture of samples containing SiO_2 and MWCNT has changed to a more undulating and the roughness is greater than in case of PDMS and other nanocomposites coatings (PDMS/SiO_2 20:1=20.4 nm, PDMS/MWCNT 20:1=21.8 nm, PDMS/MWCNT 10:1=27.3 nm).

5.5.3 Effect of Nanopowders on Surface Wettability

The hydrophobicity and low surface free energy are very important material properties in aiding the removal of marine organisms from the surface. In this work, the contact angle (CA) was measured on prepared samples and glass substrates to evaluate the wetting properties. In order to calculate surface free energy, three different liquids were used during the test: deionised water (DI), diiodomethane (DM) and ethylene glycol (EG). All results are presented in Table 5-2 and Table 5-3.

The static contact angle of water measured on a glass substrate is relatively low (CA = 20.1±3.2º), which corresponds to hydrophilic surface. However, after applying PDMS and PDMS/NP coatings on substrate it was found that the contact angle increases up to > 90^O and thereby changes of surface nature into hydrophobic. For the better visualisation, the obtained results of contact angle for three liquids are shown in Figure 5-19. The measured water contact angles

of prepared coatings are in the range 104º – 117.6º. The obtained results were used for surface free energy calculations (SFE).

The Table 5-3 shows that the values of SFE for the all coatings are low, which is consistent with literature where surface free energy is ~ 20 mN/m (Berglin and Gatenholm, 1999). Analysing the obtained results can be seen that the selected nanopowders did not have a significant effect in the value of SFE and only small differences for the different coatings can be observed.

Table 5-2 Contact angle of PDMS/NP coatings and glass substrate

Sample	Contact Angle [Θ]			
	Θ^{DI}	Θ^{DM}	Θ^{EG}	Θ^{ASW}
Glass	20.1±3.2	33.3±2.2	34.7±5.2	32±3.4
PDMS	104±3.03	80.7±0.8	97±2.8	91.6±2.2
PDMS/SiO_2	115.2±1.1	79.8±0.5	99.1±1.7	102±1.6
PDMS/TiO_2 20:1	104.8±2.3	80.7±0.5	100.2±1.5	98.3±0.8
PDMS/TiO_2 10:1	109.9±0.8	80.3±0.6	97.5±1.6	100.9±2.3
PDMS/ZnO 20:1	117.6±0.5	81±0.7	99±1.8	103.5±0.9
PDMS/ZnO 10:1	114.7±0.9	79±0.7	101.6±0.9	103.6±1.6
PDMS/MWCNT 20:1	116.2±0.5	80.8±0.4	101.4±0.5	104.3±1.3
PDMS/MWCNT 10:1	115.7±0.7	81.5±0.8	100.9±0.5	107.8±1.1
PDMS/NBT 20:1	114.2±0.4	81.1±0.2	98.8±1.6	99.2±0.9
PDMS/NBT 10:1	115.4±0.2	81.2±0.9	95.9±1.6	103.2±0.9

Table 5-3 Surface free energy components of PDMS/NP coatings and glass substrate

Sample	Surface Free Energy Components [mN/m]		
	γ_s^{tot}	γ_s^{d}	γ_s^{p}
Glass	58.1	34	23
PDMS	16.3	15.5	0.8
PDMS/SiO_2	16.7	16.7	0.005
PDMS/TiO_2 20:1	15.9	15.2	0.7
PDMS/TiO_2 10:1	16.4	16.2	0.2
PDMS/ZnO 20:1	16.4	16.4	0.001
PDMS/ZnO 10:1	15.5	15.5	0.03
PDMS/MWCNT 20:1	17.1	17.1	0.02
PDMS/MWCNT 10:1	15.8	15.8	0.01
PDMS/NBT 20:1	16.1	16.1	0.04
PDMS/NBT 10:1	16.5	16.4	0.03

Additionally, the effect of artificial sea water (ASW) used for algae growth was also tested. Sea salt mix, needed to prepare seawater, was purchased from Aquarium Systems and was prepared according to the manufacturer's recommendations. Figure 5-20 depicts the static contact angle of ASW and water as reference liquid; the dotted line indicates the boundaries of hydrophobicity. The obtained results show that ASW contact angles of the PDMS/NP coatings are lower than water contact angles. Contact angle decreased slightly ~10º. However, all prepared coatings are still hydrophobic in nature with contact angles ranging between 91.5º – 107.8º.

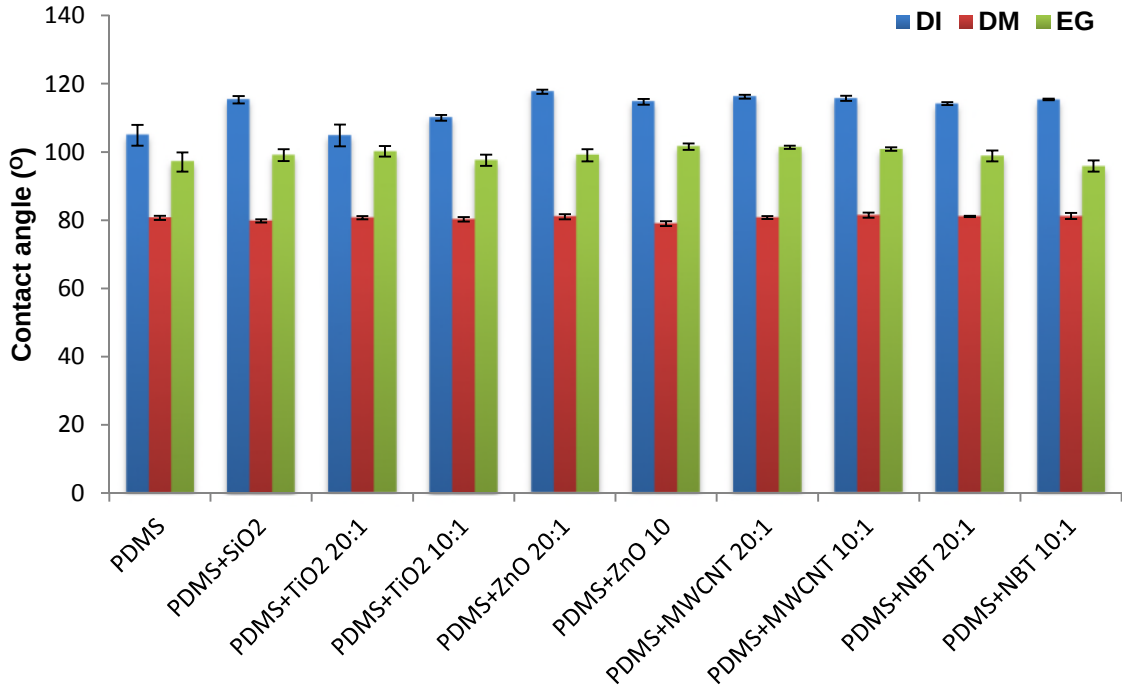

Figure 5-19 Static contact angle of water, diiodomethane and ethylene glycol

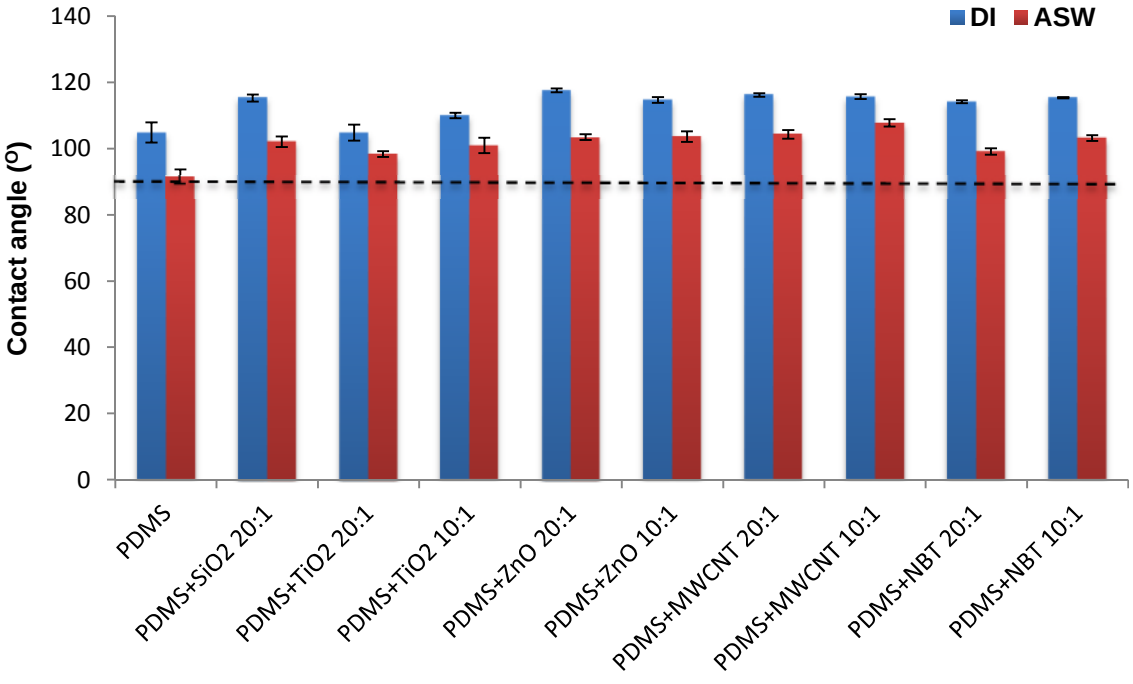

Figure 5-20 Water and artificial sea water contact angle for tested samples

Since surface roughness is a property that can have a big impact on the wetting behavior (Wenzel, 1936), the relationship between water contact angle and roughness was checked. Figure 5-21 shows that the smoothest coating –PDMS with roughness Ra 0.8 nm (as shown on Figure 5-18) has the smallest value of contact angles. The results show that the water contact angles of PDMS/NP coatings do not increase with an increase of surface roughness. This is due to a fact that the roughness values are too low and do not have a significant effect on the hydrophobicity of the coatings.

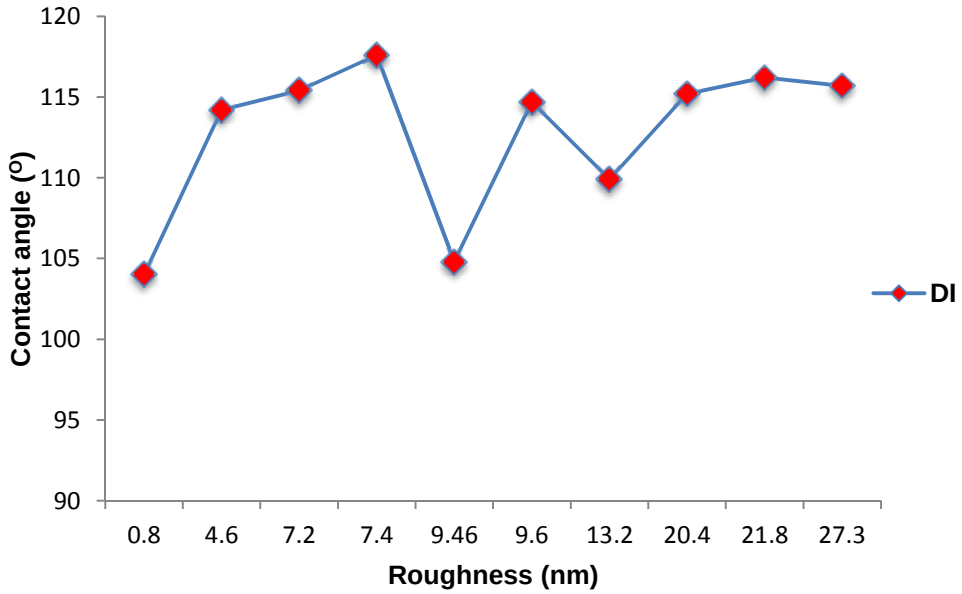

Figure 5-21 Water contact angle vs surface roughness of all coatings

5.5.4 Influence of Water on Nanocomposite Coatings

The presence of nanoparticles in the marine environment could trigger harmful effects on animals and plants. Therefore it is important to create coatings safe for the environment. The influence of water on tested coatings was investigated in order to test whether the metal nanoparticles contained in the PDMS/NP coatings does penetrate to the water. The whole coatings were immersed in 10

ml of distilled water for up to 30 days, at room temperature. After this time the samples were removed from water and the water was tested by ICP-MS spectroscopy (X-series II ICP-MS) to disclose whether there was any trace of elemental composition dissolved in the water. During the test no changes were observed in the elemental composition of water. This demonstrates that the water is still pure and free from tested nanoparticles. This process was repeated a few times to evaluate the repeatability of the finding.

5.6 Conclusion

In summary, a simple and useful method has been developed to produce polymer nanocomposites. With this method PDMS nanocomposite coatings have been successfully created and examined by XRD, SEM and AFM, respectively.

The studies have shown that the X-ray diffraction patterns of tested samples can be easily matched with the standard database of chosen nanopowders (NP). Based on the obtained results, we can say that the reference diffraction patterns of nanopowders were detected in PDMS/NP coatings. The intensity of NP peaks was higher in the case of coatings with larger amounts of nanopowder (PDMS/NP 10:1). Additional peaks were not observed, demonstrating the purity of the examined materials. The SEM microstructure of PDMS/NP nanocomposites coatings deposited on glass substrates show mostly depicts no significant difference in surface structure. Only PDMS/MWCNT show significant changes in color and distortion. It was confirmed by AFM that PDMS/MWCNT coatings were the roughest in comparison to other produced nanocomposite coatings. The effect of nanopowders on the properties of prepared nanocomposites coatings is presented. The studies carried out on glass and PDMS coating were made as a comparative reference to nanocomposites coatings. Based on the results of the surface wettability, it was found that water contact angle for all samples were >90º. This means that after

applying polymer coatings on the substrate with hydrophilic nature, the hydrophobic surfaces were obtained. However, the addition of sea salt to the water causes a decrease in the value of the contact angle (refer to Figure 5-20). Finally, it was proven that surface roughness did not influence wettability of coatings.

6 Bacterial Adhesion Assay

In the marine environment, bacteria are a significant contributor to marine fouling. Bacteria attached to the surface immersed in the sea water generate undesirable secretions known as extracellular polymeric substances (EPS) (Callow et al., 2002). These secretions connect settled cells to each other in addition to the surfaces forming a biofilm, which is hard to remove. Subsequently this biofilm provides a good surface for marine organisms' growth. A key parameter, which influences microbial attachment in the early stage of biofilm formation, is the wettability of the cells. The hydrophobic properties of the bacterial surface may affect adhesion to hydrophobic surfaces and conversely the more hydrophilic cells adhere more to hydrophilic surfaces (Krasowska and Sigler, 2014). Literature has shown increased microbial attachment onto rough surfaces (Callow et al., 2002; Howell and Behrends, 2006; Schultz, 2007). The coatings tested in this research, are comparably smooth compared to those described in the literature and based on Section 5.5.2 roughness is only observable in the nanoscale. However, Mitik-Dineva et al. (2008) found that even minor changes in surface topography can contribute to increased microbial adhesion. Literature more widely comments on the effect of physico-chemical properties on the adhesion of bacteria (Garrett et al. 2008; Renner and Weibel, 2011). Among the various surface properties, a number have been identified, which demonstrares a significant impact on microbial adhesion. These properties include surface wettability and surface free energy.

In this chapter the adhesion of *Bacillus subtilis* to PDMS nanocomposite coatings was evaluated. The influence of contact time, surface topography and the physico-chemical properties of coatings with different nanoparticles was investigated. In addition, the bacterial cells were characterised and contact angles were measured to determine the ability of the bacteria to adhere to the tested coatings.

The bacterial culture and adhesion was cerried out in collaboration with Msc student Richard Onarinde from the School of Energy, Environment and Agrifood (SEEA), Cranfield University.

6.1 Materials and Methods

6.1.1 Bacterial Culture

Bacillus subtilis NCIMB 3610 obtained from NCIMB was used for bacterial adhesion tests. The bacterial strain was cultured in Nutrient broth (Oxoid CM0001) prepared according to the manufacturer's recommendations and sterilised in an autoclave at 121 ºC for 20 min. The bacterial colony was inoculated in cooled NCIMB and grown for 3 h at 37 ºC in an incubation shaker. In order to ensure that the same number of bacteria was used in each test, the optical density (OD) of the bacterial suspension was measured. The growth curve in Figure 6-1 was obtained using the OD measured at 600 nm and number of bacteria colony-forming units (CFU) (Gurd, 2015).

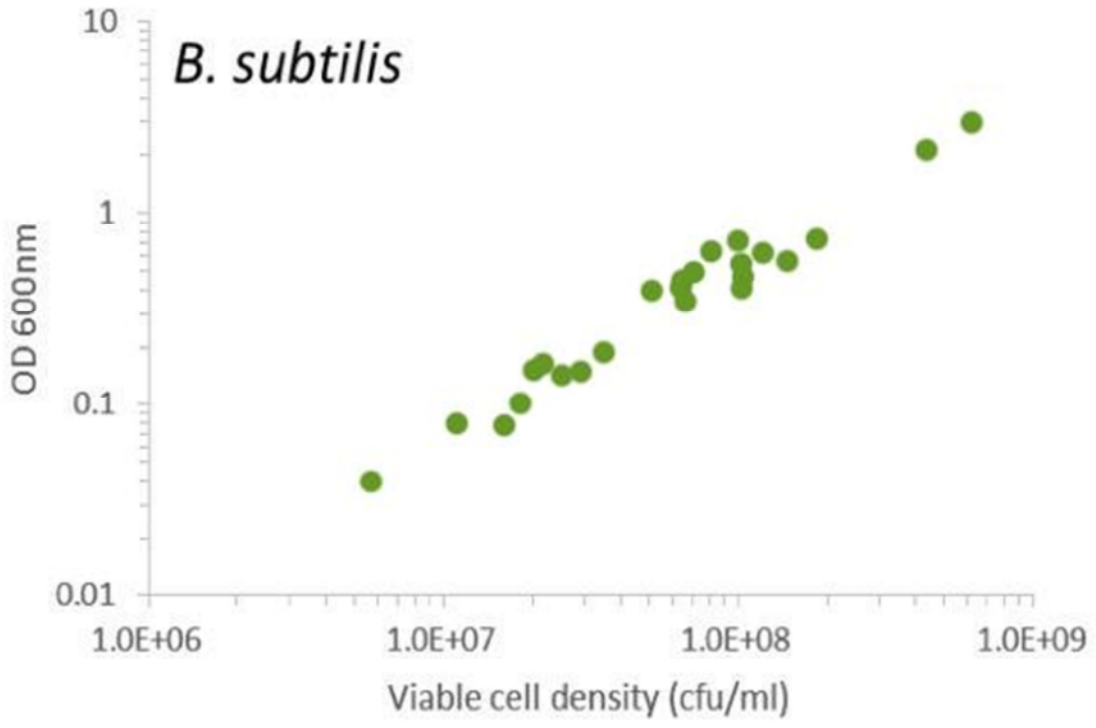

Figure 6-1 Growth curve of *Bacillus subtilis* (Gurd, 2015)

6.1.2 Bacterial Adhesion to PDMS/NP Coatings

The adhesion of *Bacillus subtilis* to PDMS and PDMS nanocomposites coatings were tested in laboratory conditions. Preparation and characterisation of all coatings can be found in Chapter 5. Prior to the investigation, the substrates were sterilised by detergent and isopropanol, and then dried by N_2. When the bacterial suspension reached a suitable concentration (10^7 cell/ml) the substrates were immersed separately for various periods of time: 24 h, 48 h, 72 h and 91 h. Following the completion of incubation, the substrates were removed from suspension and gently rinsed with saline solution (9g/l NaCl in H_2O) to release the loosely adhered cells, and placed vertically in a sterile glass container with 120 ml of saline solution. Such prepared samples were sonicated for one minute and cooled in ice for two minutes. This procedure was repeated six times to ensure the removal of the attached cells from the sample. Subsequently, the total number of adhered bacteria was counted by plate count method (Section 6.1.3).

6.1.3 Cell Counting Method

The total number of bacteria adhered to the substrates was determined by a plate count method. This method involves counting grown colonies after the settling of bacteria onto the surface. Solutions containing a high number of bacteria were diluted before plating so as to contain the cell suspension to countable accurately. The dilution of bacteria released in the saline solution occurs according to the scheme shown in Figure 6-2. 0.1 ml of each diluted solution was deposited onto the solid media plates and incubated at 37 ºC for 15 h (Moat et al., 2002). Three samples for each solution were used to obtain the average bacterial attachment (results are shown in Appendix A). The plates, which possess from 10 to 300 colonies, were counted visually. The number of colony forming units (CFU) could then be calculated using the following equation (Mukherjee and De, 2015) before being divided by the total surface area (CFU/cm^2).

$$CFU\ ml^{-1} = \frac{CFU\ per\ plate \times dilution\ factor}{volume\ of\ sample\ taken} \quad \textbf{(6-1)}$$

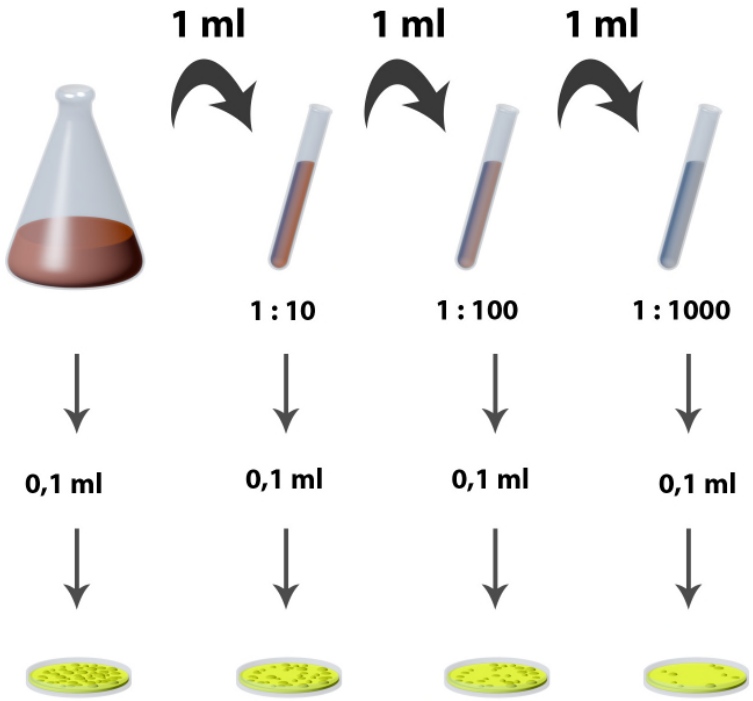

Figure 6-2 Diagram of serial dilution process

6.1.4 Bacterial Cell Morphology Characterisation

The bacteria containing biofilm was coated by gold/palladium and characterised using scanning electron microscopy (SEM, SFEG FEI XL30). To calculate the size and to determine the shape of cells, SEM images were evaluated with the ImageJ software (Rasband, 1997-2016).

6.1.5 Contact Angle and Surface Free Energy Measurements

The hydrophobicity of *B. subtilis* was measured by the sessile drop technique using a Biolin Scientific Theta Lite Attension Tensiometer. The method of measuring contact angle on microbial lawns deposited on filters has been described by Busscher et al. (1984). 120 ml of bacterial culture was washed in distilled water and filtered through cellulose filter paper with a pore diameter of 0.45 μm. Filtered bacterial lawn was left to air dry until the contact angle was stable. Contact angles with three liquids were measured: deionized water (DI), diiodomethane (DM) and ethylene glycol (EG). Each liquid was placed on five different areas on bacterial lawn and contact angles were calculated as an average volume, using OneAttension software. In order to calculate the surface free energy, an Owens-Wendt (OWRK) method was applied.

6.2 Experimental Results and Discussion

6.2.1 Characterisation of Bacterial Cell

The bacteria used in this study are *B. subtilis*, which are rod-shaped as presented in Figure 6-3. The SEM images and ImageJ software were used to measure diameters and circularity of singular cells. Table 6-1 summarises the morphological properties measured on 15 samples. The results indicate that individual species have similar shapes and sizes, measuring approximately 2.78 μm in length and 0.79 μm in diameter.

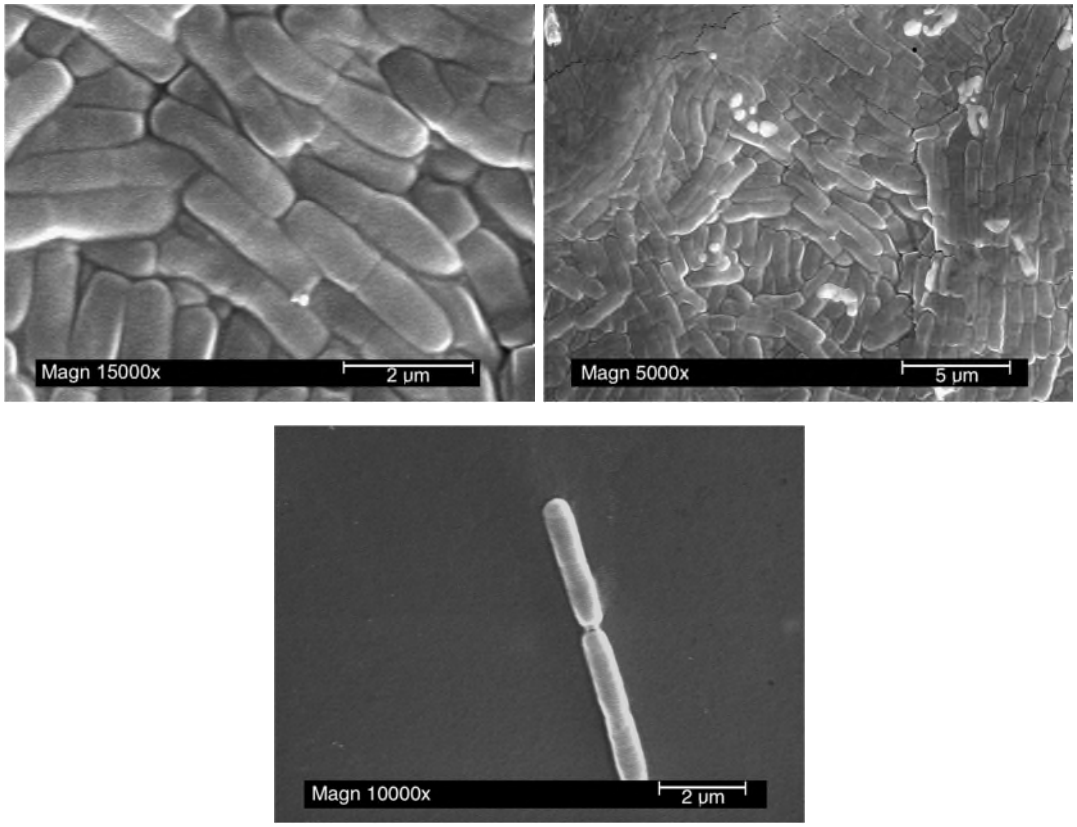

Figure 6-3 Scanning electron microscope micrographs of *Bacillus subtilis*

Table 6-1 Morphological and physic-chemical properties of *Bacillus subtilis*

Shape and Size	**Major diameter [µm]**	**Minor diameter [µm]**	**Equivalent spherical diameter [µm]**	**Circularity**
	2.78	0.79	1.79	0.5
Contact Angle [Θ]		Θ^{DI}	Θ^{DM}	Θ^{EG}
		12.4±1.08	62.1±4.7	24.8±1.24
Surface Free Energy Components [mN/m]		γ_s^{tot}	γ_s^{d}	γ_s^{p}
		62.6	23.3	39.3

Table 6-1 summarises physico-chemical properties of bacteria, such as the contact angle of three different liquids and surface free energy components as computed by Attension Software. The value of the water contact angle formed on a bacterial lawn is significantly low which indicate that the *B. subtilis* cells are hydrophilic. This suggests that the bacteria should adhere more readily to the hydrophilic surfaces (Krasowska and Sigler, 2014).

6.2.2 Influence of Contact Time on Bacterial Adhesion

In this study eight PDMS based coatings were evaluated with *B. subtilis*. The results of the number of bacteria cells detected on PDMS nanocomposite coatings, at a various contact time are tabulated in Table 6-2.

Table 6-2 Number of attached bacteria in CFU/cm^2 at various incubation time

Sample	CFU/cm^2			
	24 h	**48 h**	**72 h**	**96 h**
PDMS	3.63×10^5	1.1×10^6	1.32×10^5	7.6×10^3
PDMS+SiO_2 20:1	2.75×10^6	3.38×10^4	6.5×10^4	5.18×10^3
PDMS+TiO_2 20:1	3.18×10^5	8.87×10^5	1.14×10^5	7.27×10^3
PDMS+TiO_2 10:1	2×10^5	3.26×10^5	8.83×10^3	1.3×10^4
PDMS+ZnO 20:1	6.96×10^5	1.59×10^5	4.68×10^3	7.12×10^3
PDMS+ZnO 10:1	2.34×10^6	6.86×10^5	1.89×10^5	3.56×10^3
PDMS+MWCNT 20:1	1.56×10^5	1.41×10^5	9.43×10^4	1.64×10^4
PDMS+MWCNT 10:1	8×10^5	1.79×10^5	2.27×10^4	7.15×10^4

For adequate understanding of the effect of contact time on bacterial adhesion, the results were presented as log CFU/cm^2 versus time in Figure 6-4. Figure 6-4 shows that all coatings have similar antifouling properties. However, the adhesion of *B. subtilis* showed considerable variability over time. The number of bacteria attached to the PDMS based coatings after 24 h ranged from 10^5 to 10^6 CFU/ cm^2, and this value changed during the contact time.

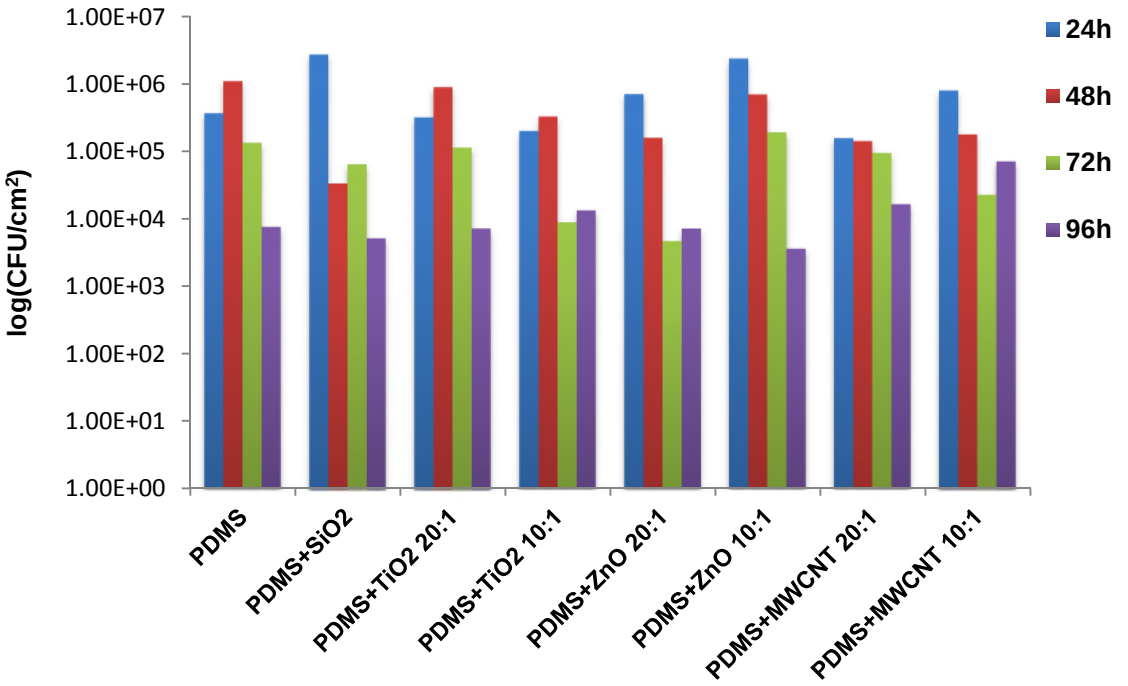

Figure 6-4 Chart of *Bacillus subtillis* attachment to PDMS nanocomposites coatings at various incubation time.

Comparing the shortest contact time of 24 h and the longest of 96 h (Figure 6-5) an interesting correlation can be noted; the number of bacteria decreases over the time. For an incubation time of 24 h, the number of adhered bacteria showed an initial increase and then decreased to 10^3 CFU/cm^2. A similar trend is observed for the majority of coatings after 96 h. Coatings with MWCNT and PDMS+TiO_2 10:1 showed a higher number of bacteria was (10^4 CFU/ cm^2). A

possible explanation proposed could be the fact that adhesion of microorganisms can be reversible. Garrett et al. (2008) explained that bacteria cells detach from the solid surface if the attractive forces are lower than the repulsive forces.

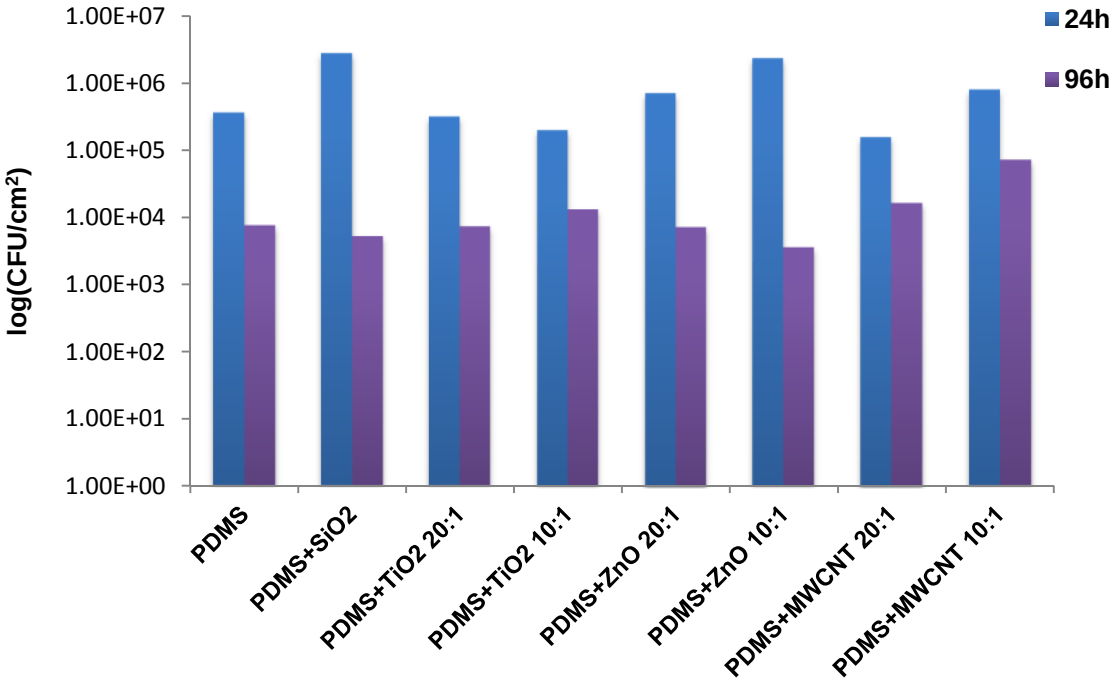

Figure 6-5 Chart of *Bacillus subtilis* attached to PDMS nanocomposite coatings after 24 h and 96 h incubation time

6.2.3 Influence of Surface Coating types on Bacterial Adhesion

The various nanoparticles used during synthesis of polymer nanocomposites resulted in changes to the surface properties. The detailed characterisation of tested coatings was described in Chapter 5.5. As shown in Table 5-2 and Table 5-3, all tested coatings are hydrophobic with a low surface free energy, it means that microbial adhesion should not take place (Krasowska and Sigler, 2014).

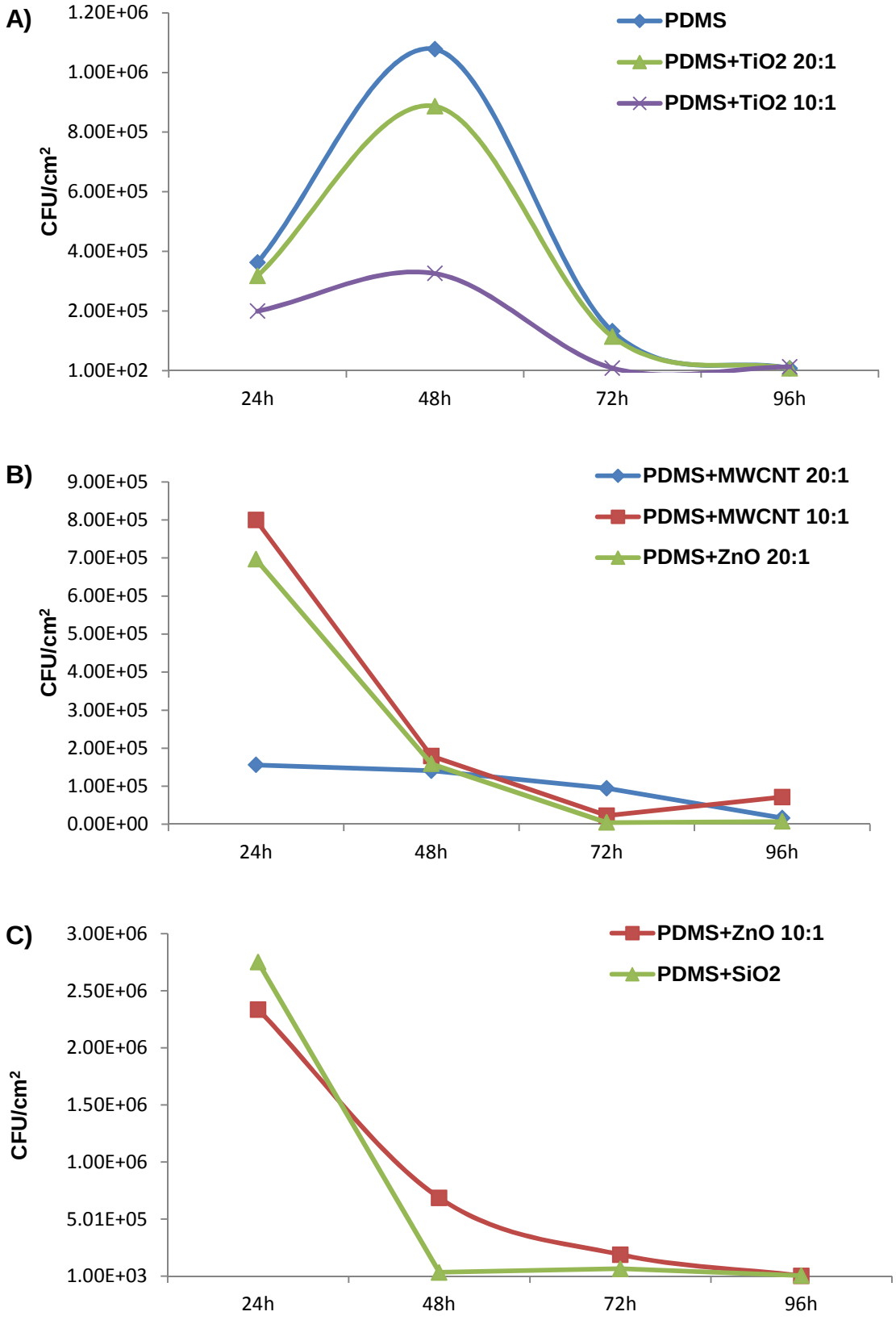

Figure 6-6 Effect of contact time (24 h, 48 h, 72 h and 96 h) on *B. subtillis* adhesion to PDMS/NP coatings

Figure 6-6 shows the comparison of *B. subtilis* attached to different PDMS based coatings over time. For better visualisation and understanding of results, PDMS/SiO_2 20:1 and PDMS/ZnO 10:1 coatings are presented on a separate chart, due to their higher number of attached cells after 24 h of incubation.

The number of bacteria adhered to the control surface (PDMS) is in the range 10^5 CFU/cm^2 after 24 h of incubation. The PDMS coating achieved similar inhibition of bacterial attachment as those coatings containing nanoparticles. Significant differences among the CFU's number were only observed on the coatings containing SiO_2 (PDMS/SiO_2 20:1) and greater amount of ZnO (PDMS/ZnO 10:1); the bacterial number was in the range of 10^6 CFU/cm^2.

As presented on Figure 6-6 A, PDMS coatings showed very similar behaviour to bacterial attachment when compared to the coatings containing titanium dioxide. The CFU counting of *B. subtilis* increased during the contact time and reached the highest values at 48 h. Subsequently, after this time there was a significant decrease in the adhesion of bacteria. The passible explanation can be detachment of cells. Picioreanu et al. (2000) proved that microbial cells are able to detach from the solid substrate under stress conditions such as liquid flow or rapid growth. Material features provide favourable niches for microbial attachment, which are less affected by shear rate (Characklis, 1990). In the case of the remaining coatings (Figure 6-6 B C) a decrease of adhered bacteria occurred after 24 h. Since bacterial adhesion can be a reversible process (Bos et al., 1999; Garrett et al., 2008), it can be assumed that CFU number for these coatings have reached their maximum before 24 h. To confirm this more experiments for the different incubation times are required.

Comparing the experimental results in Figure 6-6 with the surface analysis in Table 5-2, it can be observed that, such results of bacterial attachment can be correlated with the surface wettability of coatings. Although all of the tested coatings are hydrophobic, it was noted that the contact angle for PDMS and PDMS containing TiO_2 is less than 110º. The coatings, which showed a decrease in bacterial attachment after 24 h, possess contact angles >115º. This

data indicates that some coatings are more hydrophobic which has a significant impact on bacterial adhesion.

Based on previous reports, another important parameter that affects microbial attachment is surface free energy (Liu and Zhao, 2005). The experimental results showed that all PDMS based coatings have similar, low surface energies <17 mN/m (Table 5-3), which does not affect bacterial adhesion. However, it was noted that tested coatings have different polar components, and the number of cells attached to the surfaces with lower $\boldsymbol{\gamma_s^p}$ (<10^{-2} mN/m) decreases after 24 h. When the $\boldsymbol{\gamma_s^p}$ of the coatings reached 10^{-2} mN/m, bacterial adhesion increased after initial time 24 h. Thus, it can be concluded that surface polarity plays an important role in adhesion of bacteria to polymer coatings.

Overall, the above results show that the number of adhered *B. subtillis* cells decreased with increasing contact time. Previous studies also indicated that the incubation time have significant influence on bacteria attachment (Zhao et al., 2007a; Zhao et al., 2007b). Zhao et al. 2007a observed this behavior with *P. aeruginosa*, *S. epidermidis* and *S. aureus* adhesion to ion-implanted surfaces. They found that bacterial attachment depends of the surface energy, surface roughness and contact angle. The results presented in this study, indicate there was apparent correlation between contact angle and *B. subtillis* adhesion. However, no correlation was found between total surface energy of coatings and bacteria attachment. A possible explanation could be the fact that the SFE values of PDMS/NP coatings were comparable, while the materials with different SFE was used in literature. The authors finally concluded that the increase and the later decrease of bacteria fouling may reflect three processes: initial bacteria attachment, detachment and biofilm formation. In this order, further investigation is needed.

6.2.4 Influence of Surface Roughness on Bacterial Adhesion

Another important parameter, which affects attachment of bacteria, is the roughness of the coatings. It has been reported that surface texture plays a significant role and is one of determining factors in marine microorganisms attachment. Microbial cells prefer to grow on rougher surfaces compared to smooth surfaces (Callow et al., 2002).

In order to examine the effect of surface roughness on *B. subtilis* adhesion, coatings with different texture were investigated. Experimental results indicate (Section 5.5.2) that nanoparticles have a huge influence on surface texture roughness. After AFM analysis, it was found that tested coatings have low surface roughness and Ra values are in the range of 0.8 nm (PDMS) to 27.3 nm (PDMS/MWCNT 10:1). Figure 6-7 shows the influence of coating roughness on adhesion after specific times (24 h, 48 h, 72 h and 96 h). The results showed that there is no significant connection between lower roughness and number of attaching bacteria. However, looking more closely at particular incubation times some correlation can be observed after 96 h. The results presented on Figure 6-8 showed a higher number of bacteria attached to rough surfaces (Ra>13 nm) when compare to the smoothest surfaces. These observations demonstrate that roughness on the nanoscale can have an impact on bacterial attachment, however the adhesion time plays a significant role in this.

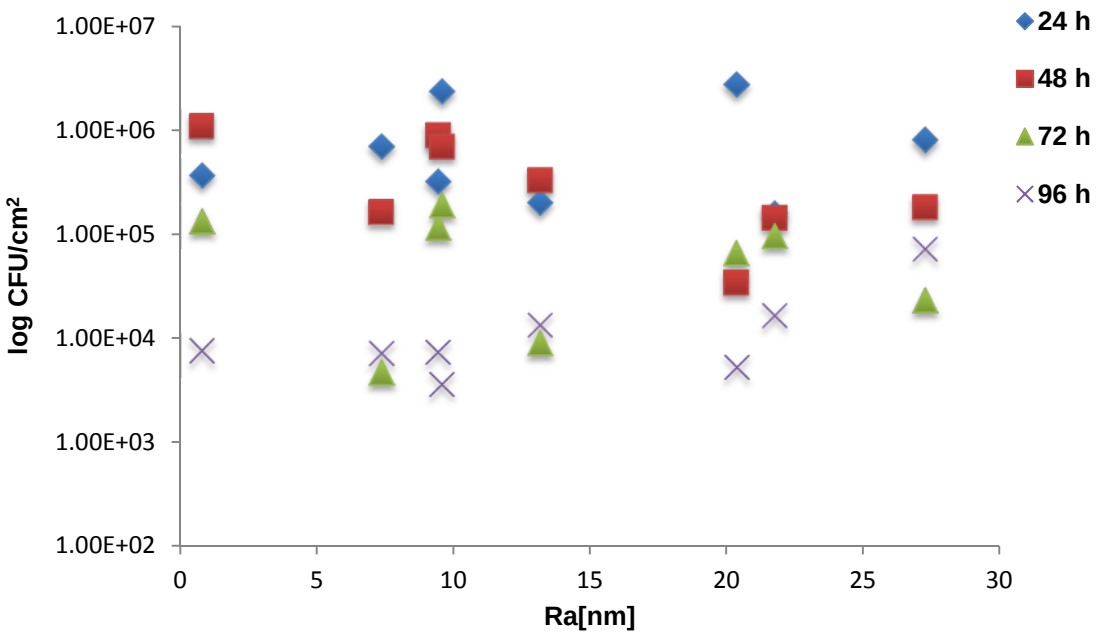

Figure 6-7 Bacteria attachment vs. substrates roughness after various incubation time

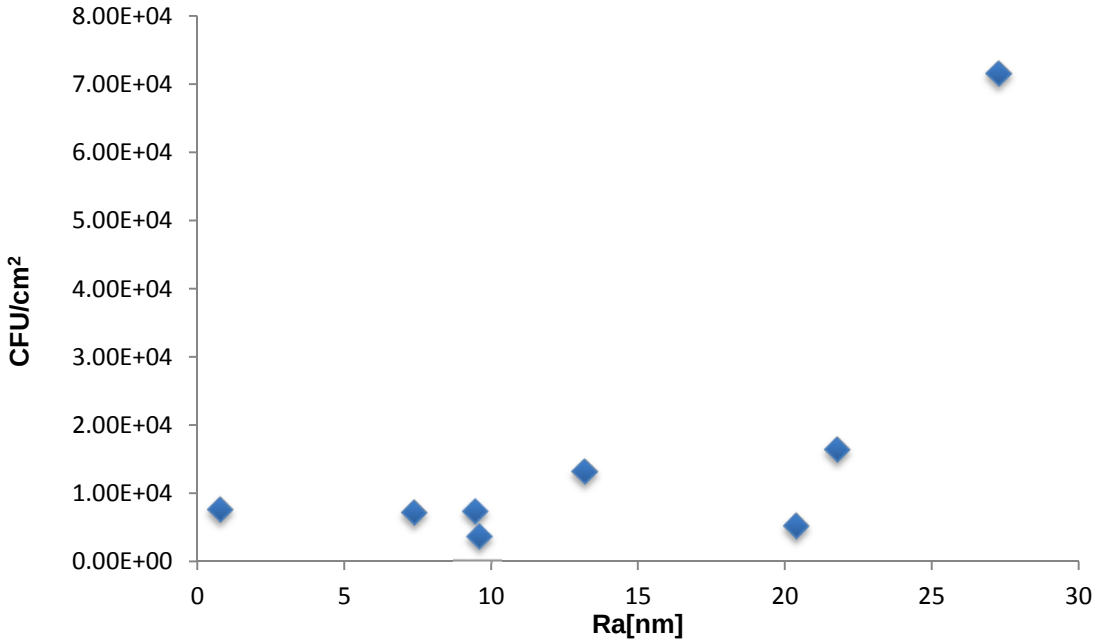

Figure 6-8 Bacterial attchament vs. substrates roughness after 96 h incubation time

6.3 Conclusion

In conclusion, the adhesion of *Bacillus subtilis* to PDMS nanocomposite coatings was investigated. Bacteria were successfully cultured and tests were undertaken using laboratory conditions.

It was found that the tested bacteria were hydrophilic, suggesting that they should not adhere to the produced hydrophobic surfaces. No correlation was observed between surface free energy of substrates and the number of adhered bacteria, due to the relatively low surface free energies (<17 mN/m). However, a direct relationship between the polar components of surface free energies and the number of attached cells were seen to increase.

Moreover, results show that the surface hydrophobicity of the produced coatings plays an important role for *Bacillus subtilis* colonisation. It was noted that the bacteria settles faster on the surfaces with contact angles higher than 150º and a decrease in adhesion is taking place after 24 h.

The experimental results indicated that even though, the coatings produced are relatively smooth and their roughness is in the nanoscale they are still attractive to *B. subtilis*. It was observed that the bacterial adhesion occurred on rougher surfaces after longer incubation time.

Finally, it was proven that incubation time plays an important role in bacterial colonisation. The cells of *Bacillus subtilis* need 24 h to fully settle into most of the coatings and 48 h into PDMS and both coatings containing TiO_2. After these times, a reduction in the number of attached bacteria was observed.

7 Algae Adhesion Assay

It is assessed that in fouling communities there exists 1700 species comprising more than 4000 organisms (Almeida, 2007).

Microalga are unicellular organisms encased in the siliceous shell (frustule). They are an important component of biofilm, which may live in all types of water and on most solid soils.

The purpose of this study was to investigate the effect of PDMS nanocomposite coatings on the microalgae adhesion. Antifouling tests, with the principal representatives of marine fouling microalgae: *Skeletonema sp., Amphora sp. and D. Salina,* were undertaken using laboratory conditions and results are discussed in this chapter. The first part describes the cells attachment for different durations and performance of previously prepared coatings. The subsequent section investigates surface properties, which can influence the settling process, such as wettability or surface topography. Since it is known that PDMS coatings work only in the case of high-speed vessels, the last part of this chapter focuses on investigating whether the changes made during the coatings synthesis have improved the fouling release properties.

7.1 Materials and Methods

7.1.1 Microalgae Species

Three saltwater microalgal strains were selected for use in this study: *D. Salina* (19/12), *Amphora sp.* (1001/3) and *Skeletonema sp*. (1077/1B) were obtained from the Culture Collection of Algae and Protozoa, UK (CCAP). Images of representative algae species are shown in Figure 7-1.

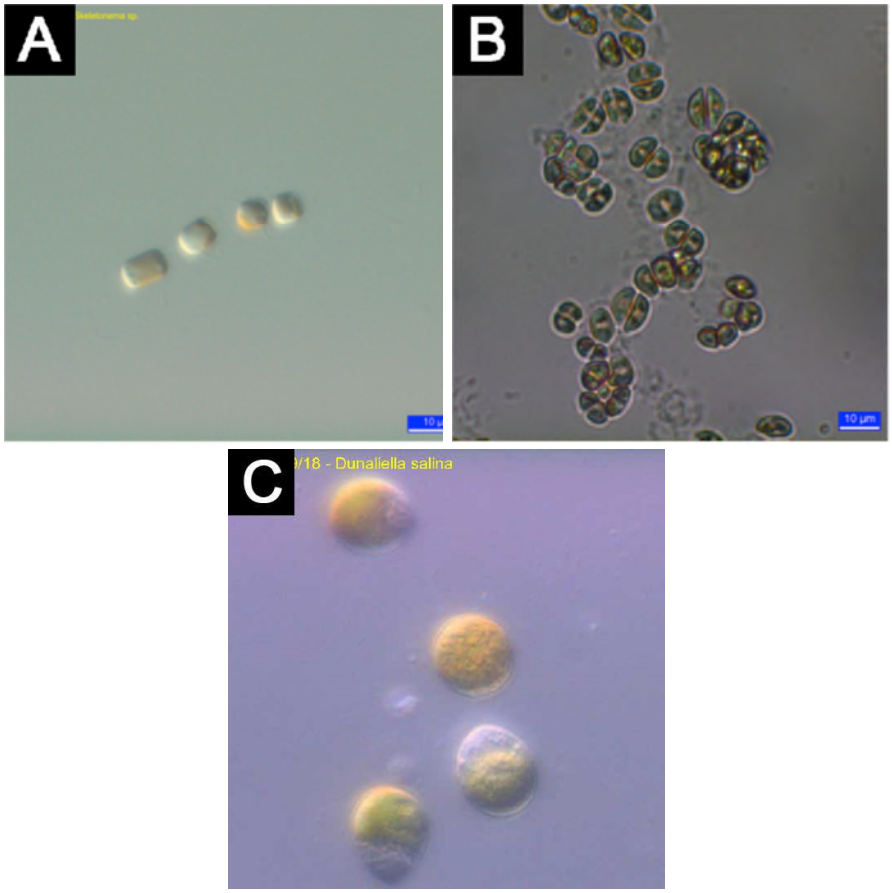

Figure 7-1 A) *Sceletonema sp.,* B) *Amphora sp.*, C) *D. Salina* (CCAP)

7.1.2 Microalgae Culture

The algae cultures were grown in a flask (1000 ml) and then transferred to fifty litres glass tanks**.** Prior to experimentation the tanks were filled with 40 l deionized water. Additionally, water was treated with a sea salt mix (Aquarium Systems) in order to create artificial seawater (ASW) providing an environment suitable for living marine organisms. ASW allows for easy preparation of an environment suitable for living marine organisms. Each algal species was cultivated in Cell Hi f/2 + Si medium (Varicon Aqua Solutions Ltd). A description of the medium is presented in Appendix B. The salinity was kept in optimal range 20 - 25 psu (practical salinity units). Each tank includes a lid with 15 Watt white lamps in order to avoid stressing the algae and to optimise growth by

allowing 12 h : 12 h light and dark periods. The temperature of the ASW was regulated by a 50 Watt water heater, which gives the opportunity to obtain optimal conditions (approximately 20 ± 2 ºC). Aeration of water was achieved by supplying air bubbling using an airstone connected to filtration pumps. The pH in the algae growth tanks were kept in optimal range (pH = 7-9), and measurements of pH were taken periodically.

7.1.3 Microalgae Adhesion Assays

Antifouling properties of the tested samples were examined on a laboratory scale. Coated glass slides were cleaned with isopropanol and deionised water, then dried and placed randomly in the rack holders. Afterwards, rack holders were placed in the mid-depth of previously prepared tanks. Produced coatings were incubated with algae at different time intervals: 1 week, 6 weeks and 12 weeks. After the expiration of the time, samples were gently rinsed with DI water to remove loosely bound microalga.

7.1.4 Comparative assay

To examine if slow water movement may have an effect on the cells adhesion, a rotor set-up (Figure 7-2) was used. The samples were mounted randomly on the slowly rotating disk using double-sided tape and incubated with *Skeletonema sp.* During the test, the rotor speed was at 0.5 knots for 12 weeks. The ASW was kept in optimal conditions as described in Section 7.1.2.

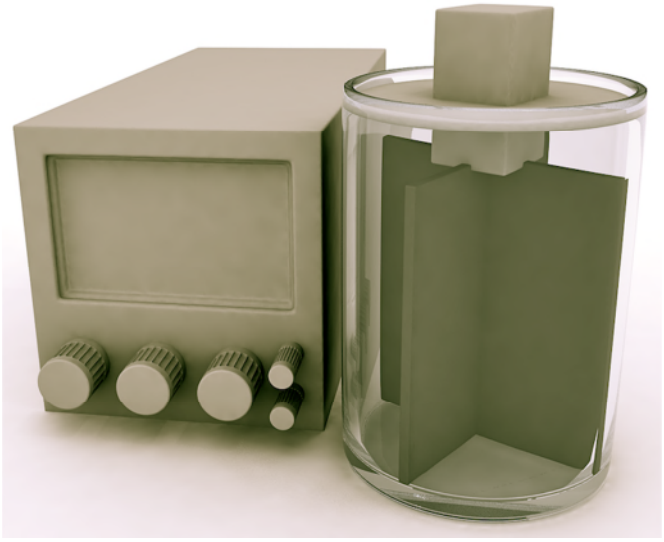

Figure 7-2 Schematic illustration of rotor set-up

7.1.5 Cell Counting Method

Microalgae cell density was measured by a cell count method using a haemocytometer (Guillard and Sournia, 1978). Before observation, samples were placed in beakers with 40 ml of deionised water and sonicated for 15 minutes. Afterwards, small drops of sample were placed in chamber of haemocytometer and checked under a microscope. The results are presented as number of cells divided by surface area (cell/cm^2).

7.1.6 Microalgae Morphology

The morphological properties of microalgal strains settled on coated substrates were evaluated based on SEM images obtained by SEM, SFEG FEI XL30 microscopy. An optical microscope (GXML 320 1 LED, GX Optical UK) was used for observation of algae on coated substrates and during the cell count method.

7.2 Experimental Results and Discussion

7.2.1 Microalgae Adhesion to the PDMS/NP Coatings

The settlement of *Skeletonema sp., Amphora sp.* and *D. Salina* was studied on PDMS nanocomposite coatings and two control surfaces (PDMS coating and glass slides). The number of microalgae cells attached to each coating shows how resistant the coating is to adhesion. Figure 7-3 depicts the number of microalgae attached to the coatings after 12 weeks of incubation time. The results are presented as number of cells divided by surface area (cell/cm^2).

The adhesion of *Skeletonema sp.* (Figure 7-3 A) showed a significant difference among the type of coatings. A quantitative assessment of cells made on control surfaces indicated that the greatest number of algae was settled. Cell count for these samples were PDMS = 4 x 10^3 and glass = 5.3 x 10^3. However, a significantly higher number of cells were also observed during the test of PDMS/SiO_2 coating (3.1 x 10^3). The lowest settlement was observed on coatings containing MWCNT nanopowders (PDMS/MWCNT 20:1 = 7.9 x 10^2, PDMS/MWCNT 10:1 = 8.5 x 10^2).

The amount of *D. Salina* cells adhered to the coatings is presented in Figure 7-3 B. After 12 weeks, the number of attached cells on the control surfaces and PDMS/SiO_2 was very similar to the *Skeletonema sp*. attachment. The settlement assay also found that the coatings containing NBT nanopowder demonstrated the best antifouling properties.

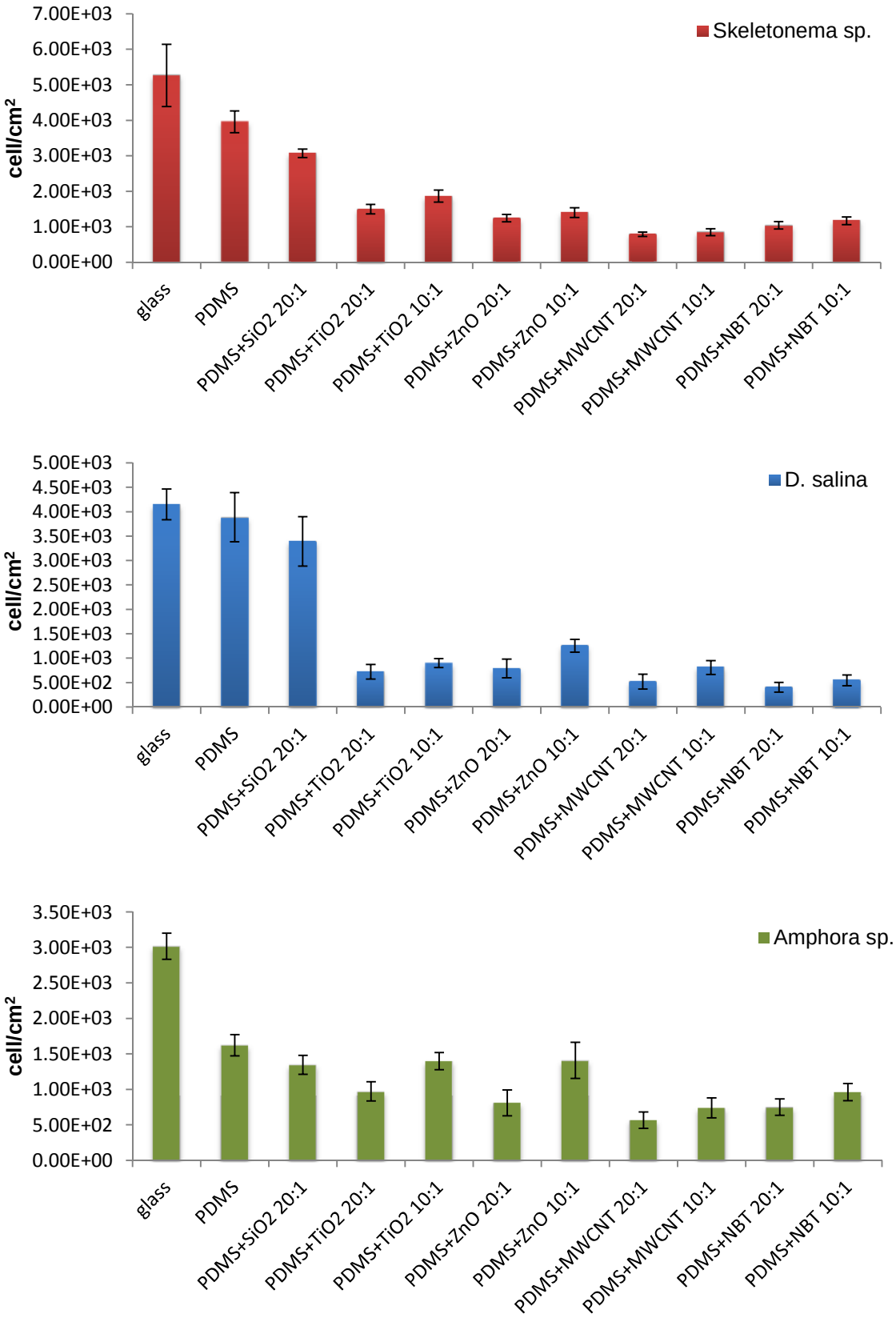

Figure 7-3 Number of cells attached to control surfaces and PDMS/NP coatings after 12 weeks incubation time, A) *Skeletonema sp.*, B) *D. Salina*, C) *Amphora sp.*

For the settlement of Amphora sp. significant differences were observed after applying coatings containing PDMS on glass (Figure 7-3 C). The highest colonisation was observed on a glass slide (3×10^3), while after applying PDMS coating the decline in the number of cells was approximately 50%. The lowest adhesion was observed on PDMS/MWCNT 20:1 coating (5.6×10^2). For the PDMS/MWCNT 10:1, PDMS/NBT, PDMS/TiO_2 20:1 and PDMS/ZnO coatings the number of attached microorganisms was slightly larger ($\approx 8 \times 10^2$).

Antifouling investigations on three types of algae showed that the presence of nanoparticles in a polymer coating changes the settlement behavior of microalgae. After 12 weeks of incubation, visual differences in morphology were observed on all tested surfaces (Appendix C).

Taking a closer look at the microalgae fouling it turns out that all three algae seem to show different adhesion properties (Figure 7-4). The attachment on controlled surfaces and PDMS/SiO_2 after 12 weeks of growth was significantly lower for *Amphora sp.* when compared to *Skeletonema sp.* and *D. Salina*. For remaining coatings, the lowest adhesion was observed for *D. Salina*. *Skeletonema* sp. performed the highest adhesive properties to tested surfaces. Therefore, this strain was selected as a main representative for further experiments. Attachment assays also showed that the rate of settlement on coatings, which shows the best antifouling properties for *D. Salina* (NBT coatings) is relatively higher for *Skeletonema sp.* and *Amphora sp.* The comparable, low settlement levels for all investigated species were observed for coatings PDMS/MWCNT 20:1 and PDMS/MWCNT 10:1. According to some recent study (Woods and Fletcher, 1991), each microorganism has its own preferences of attachment to surface. This involves production rate of EPS by various species. Cui et al. (2013) proved that the shape and size of microalgae may be another factor responsible for the different fouling properties. Therefore, the properties of settled organisms must be taken into consideration in future work.

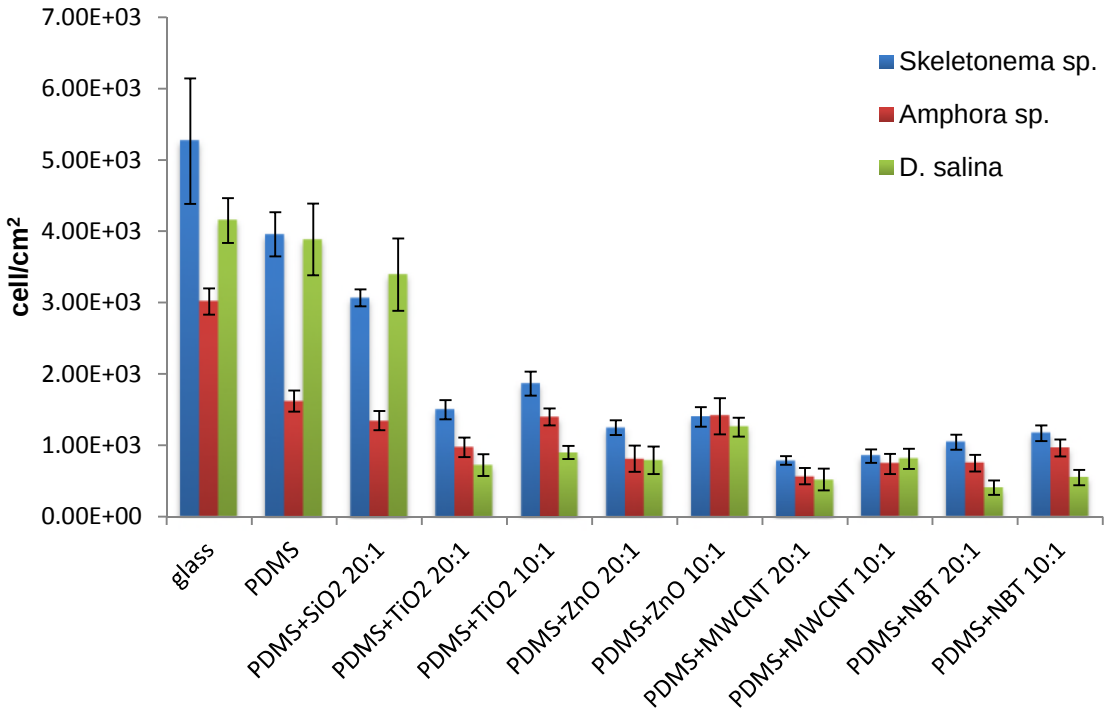

Figure 7-4 Number of cells attached to control surfaces and PDMS/NP coatings after 12 weeks incubation time

7.2.2 Influence of Contact Time on Microalgae Adhesion

The settlement of microalgae was examined at various incubation times. The relation between adhesion of tested algae and contact time is presented in Figure 7-5. As can be observed, initial attachment on tested coatings was lower then after 12 weeks. The number of cells increased slowly after 1 week and then increased greatly after 6 weeks. This phenomenon can be observed for most of the tested surfaces. While the adhesion on control surfaces increased significantly after 6 weeks, the number of cells on coatings containing MWCNT and NBT remained at comparable level. The increased settlement during the contact time was also observed for other spores and substrates in recent studies (Callow et al., 1997; Cooper et al. 2011).

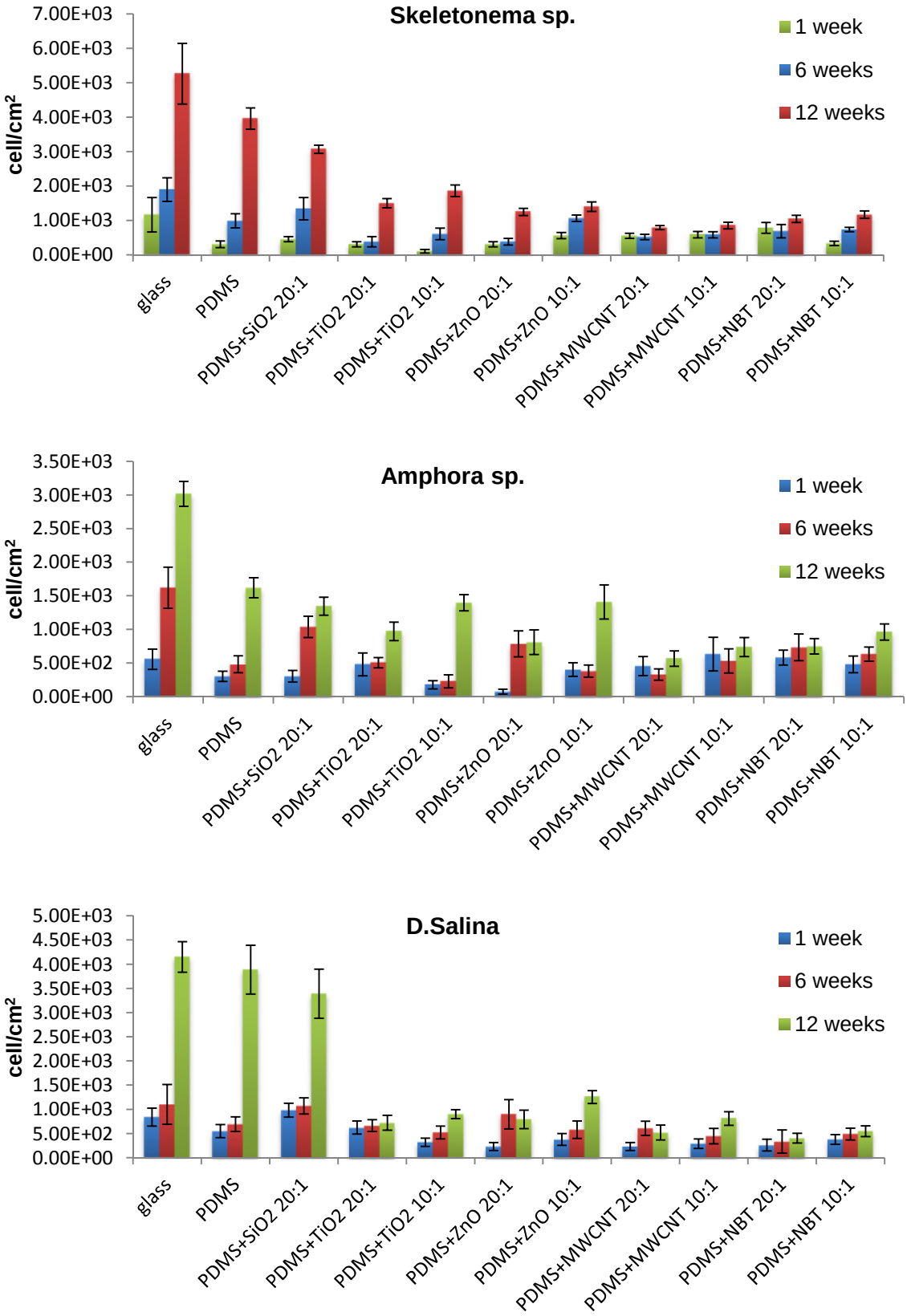

Figure 7-5 Number of cells attached to control surfaces and PDMS/NP coatings after various incubation time, A) *Skeletonema sp.,* B) *D. Salina*, C) *Amphora sp.*

Those results show that with an increase in incubation time, some cells may start to adhere on top of previously attached cells. The initially attached cells are starting to form ligands, which may be an excellent substrate for next attachment (Dunne Jr., 2002). The settled spores lead to a change in the chemical properties of the coatings, as well as surface topography. This may explain the increase in number of cells after a longer incubation time.

7.2.3 Influence of Surface Properties

The contact angle and surface free energy of control surfaces and PDMS/NP coatings are shown in Table 5-2 and Table 5-3. It was found that the glass substrate is relatively hydrophilic and after applying PDMS and PDMS/NP coatings on substrate the contact angle increases > 90º and thereby changes of surface nature into hydrophobic. In this study, no correlation was found between the wetting properties of coatings and the microalgae attachment, as some hydrophobic coatings have similar number of settled cells to hydrophilic glass slides. This lack of correlation corresponds with the previous literature, where the surface wettability of the coatings also does not affect the adhesion of microorganisms (Irving and Allen 2011).

Another surface property that can influence the attachment of fouling organisms is the topography of surface. Many authors reported that microorganisms prefer to settle on rougher surfaces in comparison to smooth surfaces. Callow et al. (2002) concluded that algae attach better to the coatings with channels or pillars with similar or larger size then the fouled organism. However, some authors suggest that even minor changes in surface topography can contribute to increased microbial adhesion (Mitik-Dineva et al., 2008). In order to examine the impact of surfaces roughness on cell attachment, all three types of algae were tested.

The roughness (Ra) of coatings used in the current study is presented in Section 5.5.2. Results show that the Ra of the PDMS/NP coatings only ranges from 0.8 nm to 27.3 nm, which is much smaller than the algae cell.

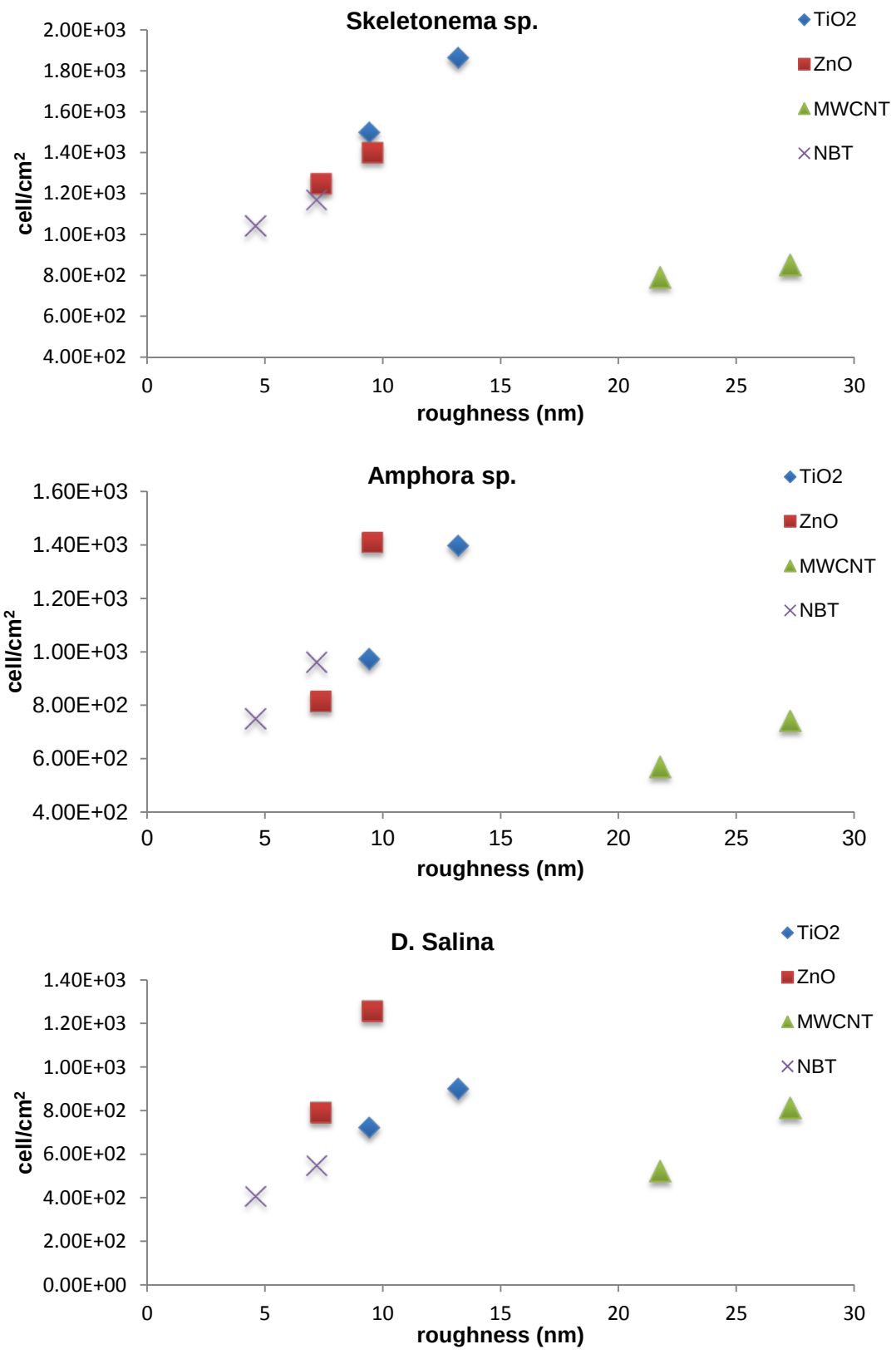

Figure 7-6 Number of cells attached to surfaces with different roughness, A) *Skeletonema sp.* B) *Amphora sp.*, C) *D.Salina*

No considerable influence was observed between surfaces roughness and settled cells, as the differences in the change in topography are not so large. When the coatings that contain the same nanopowder were examined, interaction appears. The relationship between the surface roughness and attachment of microalgae is presented in (Figure 7-6). Overall, the results suggest that the settlement of tested microalgae is higher on rougher surfaces in the case of coatings with similar composition. However, as the coatings roughness was broadly equivalent, the topography influence on the settlement of microalgae is still not obvious and further tests need to be performed.

7.2.4 Comparative Adhesion Assay

The coatings based on silicone matrix elastomers possess foul release properties, and are the most promising possibilities to control biofouling (Swain, 1999). However, PDMS coatings are still restricted to fast moving vessels, this is due to the need for shear forces created by hydrodynamic flow over the surface which are required for the detachment of fouling species (AMBIO, 2010). In this study, a slowly rotating disk (0.5 knots) was used to test if slow water movement may have effect to the cells adhesion. *Skeletonema* sp. performed the highest adhesive properties to tested coatings as shown in Section 7.2.1. Therefore, this strain was selected as main representative for fouling release performance. The differences presented in Figure 7-7 indicate the ability of cells attachment to the coatings after slow water movements for 12 weeks immersion time. It can be observed that number of attached cells is lower for PDMS/SiO_2 coating and the decrease was approximately 65%. Significant fouling release properties of the *Skeletonema sp.* attachment was also noted on PDMS/TiO_2 10:1 (58%), followed by PDMS/TiO_2 20:1 (46%). A possible reason for the decrease in attachment on those coatings can be attributed to the presence of SiO_2 and TiO_2 nanoparticles, which may improve fouling release properties of PDMS. The results obtained on the remaining surfaces showed that the microalgae growth is independent of the low-speed water movement.

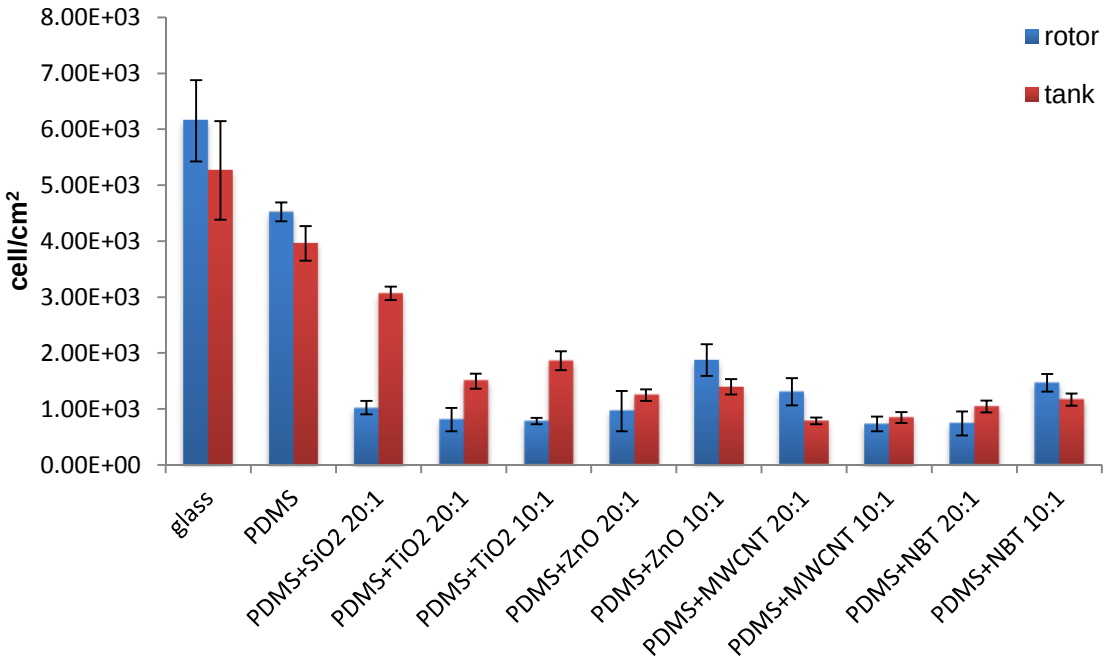

Figure 7-7 Rotor growth vs static growth results of *Skeletonema sp.*

7.3 Conclusion

In conclusion, the attachment of *Skeletonema sp., Amphora sp.* and *D. Salina* was found to be greater on control surfaces and PDMS/SiO_2 20:1 coating. The observations indicated the potential of using MWCNT nanoparticles in antifouling coatings, as the PDMS/MWCNT coatings demonstrated the best antifouling properties, for all tested organisms. Though, further research into the properties of the microorganisms need to be taken for consideration, as all three algae show different adhesion properties. *D. Salina* cells show the lowest settlement to the PDMS/NP coatings compared to *Skeletonema sp.* and *Amphora sp*. However, adhesion to glass slides and PDMS coating was significantly lower for *Amphora sp*.

The experimental results show that the incubation time plays an important role in microalgae attachment. It was noted that the number of cells increased slowly

after 1 week and then increased greatly after 6 weeks. This leads to the fact that fouling is significantly higher after 12 weeks.

In this study, no correlation was found between the wetting properties of coatings and the microalgae attachment, as contact angles of the coatings were broadly equivalent. It was shown that the settlement of tested spores was higher on rougher surfaces in the case of coatings with a similar composition.

Finally, laboratory scale rotor set-up showed promising results using PDMS/SiO_2 and PDMS/TiO_2, as significant fouling release properties of the *Skeletonema sp.* attachment was observed.

8 Thermodynamic Analysis of Microbial Attachment to PDMS/NP Coatings

Marine fouling is a complex mechanism, which begins with the initial microbial attachment, then the biofilm formation and finally is followed by the macrofouling. Physico-chemical methods can be used to explain the microbial adhesive interactions. When microbial cell approaches to a substratum surface located in an aquatic environment, three interfaces with their interfacial free energies taking places (cell-liquid, substratum-liquid, cell-substratum) (Bos et al., 1999). Therefore, there is considerable interest in the influence of different surface free energy on adhesion. There exist experimental evidence to support the hypothesis that the low-energy surfaces have a low biofouling tendency (Dexter et al., 1975; Bakker et al., 2003; Hamza et al., 1997). Baier and Meyer (1992) reported that bacterial adhesion is minimal when the surface free energy of substrate is in the range between 20-30 mJ/m^2. However, some authors indicated that microbial attachment is decreasing with increasing surface free energy of material (Fletcher and Pringle, 1985; Brink et al., 1993; Cui et al., 2015).

The thermodynamic approach is a helpful method to understand the microbial adhesion. The thermodynamic modelling uses the interaction, which occurs between microbial and materials located in the aquatic environment to determine the work of attachment. It has been proven that there is a correlation between cell attachment and work of attachment (Li and Logan, 2004; Cui and Yuan, 2013); favourable and unfavourable adhesion can be determined.

In this chapter, the process of microbial cell attachment to PDMS/NP coatings was simulated through a thermodynamic model. As a result, the work of attachment was calculated and compared to the laboratory results, to assess the potential for initial attachment prediction.

8.1 Materials and Methods

8.1.1 Thermodynamic Approach

When man-made structures are submerged in marine environments they become colonised by unwanted organisms. During this process, three interfacial interactions, which have their own interfacial free energy (Figure 8-1), take place (Bos et al., 1999)

- microorganism-liquid, γ_{ml}
- substratum-liquid, γ_{sl}
- microorganism-substratum, γ_{ms}

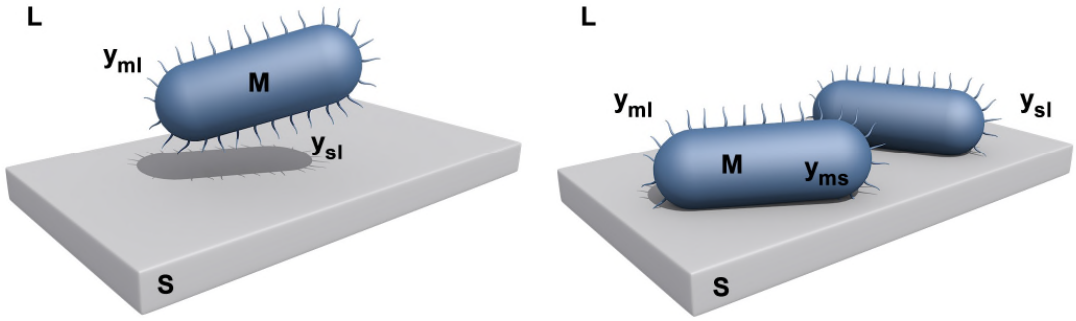

Figure 8-1 Schematic illustration of the interfacial free energies involved during microorganism (M) adhesion to a solid surface (S) in aquatic environment (L)

The thermodynamic approach offers a useful method to explain an interaction occurring in the process of a microorganisms adhesion, and can be expressed by the equation of work of attachment (Cui and Yuan, 2013)

$$W = \gamma_{ml} + \gamma_{sl} - \gamma_{ms} \quad \textbf{(8-1)}$$

where *W* is the work of attachment. According to thermodynamic model, the adhesion of microorganisms is energetically unfavourable if (Li and Logan, 2004; Cui and Yuan, 2013; Ozkan and Berberoglu, 2013).

$$W < 0 \quad \textbf{(8-2)}$$

In order to calculate interfacial free energy, an Owens-Wendt (OWRK) method was applied. According to this theory (Fowks, 1962) the total free energy can be calculated based on two components, dispersive γ^d and polar γ^p:

$$\gamma_m = \gamma_m^d + \gamma_m^p \quad \textbf{(8-3)}$$

$$\gamma_s = \gamma_s^d + \gamma_s^p \quad \textbf{(8-4)}$$

$$\gamma_l = \gamma_l^d + \gamma_l^p \quad \textbf{(8-5)}$$

where, the subscripts s, m, l are relates to substrate, microorganism and liquid, respectively.

OWRK theory suggests the following relationship for interfacial free energy between microorganism and substrate:

$$\gamma_{ms} = \gamma_m + \gamma_s - 2\sqrt{\gamma_m^d \gamma_s^d} - 2\sqrt{\gamma_m^p \gamma_s^p} \quad \textbf{(8-6)}$$

Similarly, the microorganism-liquid and substrate-liquid interaction, interfacial free energies can be obtained from:

$$\gamma_{ml} = \gamma_m + \gamma_l - 2\sqrt{\gamma_m^d \gamma_l^d} - 2\sqrt{\gamma_m^p \gamma_l^p} \quad \textbf{(8-7)}$$

$$\gamma_{sl} = \gamma_s + \gamma_l - 2\sqrt{\gamma_s^d \gamma_l^d} - 2\sqrt{\gamma_s^p \gamma_l^p} \quad \textbf{(8-8)}$$

Combining Eq. (8-1) with Eqs. (8-6) - (8-8), the microorganism work of attachment can be express as follow:

$$W = 2\left(\sqrt{\gamma_m^d} - \sqrt{\gamma_l^d}\right)\left(\sqrt{\gamma_s^d} - \sqrt{\gamma_l^d}\right) + 2\left(\sqrt{\gamma_m^p} - \sqrt{\gamma_l^p}\right)\left(\sqrt{\gamma_s^p} - \sqrt{\gamma_l^p}\right) \quad \textbf{(8-9)}$$

According to Eq. (8-9) work of attachment can be expressed as:

$$W = W^d + W^p \quad \textbf{(8-10)}$$

where:

$$W^d = 2\left(\sqrt{\gamma_m^d} - \sqrt{\gamma_l^d}\right)\left(\sqrt{\gamma_s^d} - \sqrt{\gamma_l^d}\right) \quad \textbf{(8-11)}$$

$$W^p = 2\left(\sqrt{\gamma_m^p} - \sqrt{\gamma_l^p}\right)\left(\sqrt{\gamma_s^p} - \sqrt{\gamma_l^p}\right) \quad \textbf{(8-12)}$$

8.1.2 Microbial Culture

In this study *B. subtilis* and three types of microalgae species: *Skeletonema sp., Amphora sp.* and *D. Salina* were used. Cultivation methods for bacteria and microalgae were described in Section 6.1.1 and 7.1.2, respectively.

8.1.3 Microbial Adhesion

Adhesion assays were carried out on previously prepared PDMS/NP coatings and control PDMS, as has been detailed in Section 6.1.2 for bacteria and in Section 7.1.3 for microalgae.

8.1.4 Contact Angle and Surface Free Energy Measurements

8.1.4.1 Surface Wettability

Contact angle and surface free energy components of PDMS/NP were calculated using the same method as detailed in Section 3.6.

8.1.4.2 Microorganisms Wettability

Surface properties of microbial species were obtained by the sessile drop technique according to Busscher et al. (1984). Contact angles of three liquids: deionized water (DI), diiodomethane (DM) and ethylene glycol (EG) (Liu and Zhao, 2005), were measured by a tensionmeter (Biolin Scientific Theta Lite Attension Tensiometer). The surface tension values of tested liquids are given in Table 3-2. Prior to measurements microorganism cells were washed with distilled water and filtered through a cellulose acetate filter paper with a pore diameter of 0.45 µm. The species lawn was dried under room temperature until the water contact angle was stable. Microliter sized drops of each probe liquid were placed in five different areas on the microbial lawn and contact angle values were recorded after 2 seconds (Ozkan and Berberoglu, 2013). The

surface free energy and their components were calculated based on contact angle values (OWRK method), using OneAttension software.

8.1.4.3 Liquid medium

The surface free energy of both liquid mediums was measured using the Du Noüy Ring method with a Krüss K6 ring tensiometer. This method is based on measurement of the force, which is required to detach the ring from the liquid surface (Figure 8-2 B). On the outer circumference of the ring made of a thin platinum wire, acts a force of surface tension that holds the ring in contact with the liquid (du Nouy, 1925). During the research, five measurements at room temperature were taken and the average was documented for further tests.

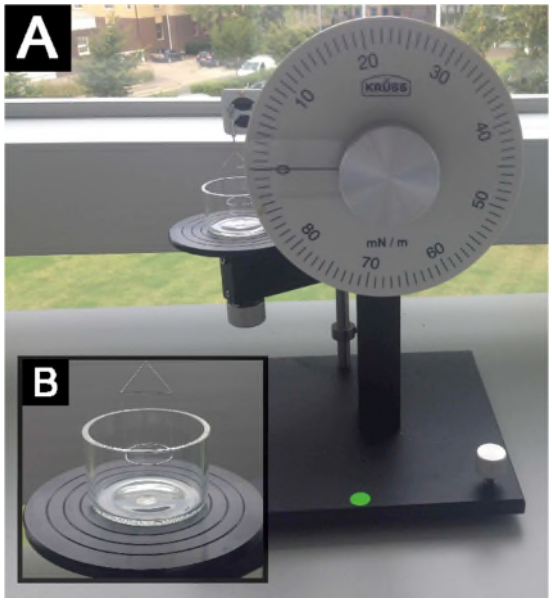

Figure 8-2 Krüss K6 ring tensiometer

8.2 Experimental Results and Discussion

In the present study, physico-chemical properties of microorganisms, substrates and liquid mediums were used for thermodynamic approach. Figure 8-3 shows

images taken by a digital camera of tested microalgae deposited on cellulose filter before contact angle measurements (SEM micrograph of bacteria is presented in Figure 6-3 A). As can be observed, filters are completely covered with microorganism layers, which allowed for determining the physico-chemical properties. The contact angle values and calculated individual components of surface free energy of tested liquids are presented in Table 8-1. It appears that measured contact angles are below 90º, therefore, all species are considered to be hydrophilic. The surface free energies and their components of the used mediums are given in Table 8-2.

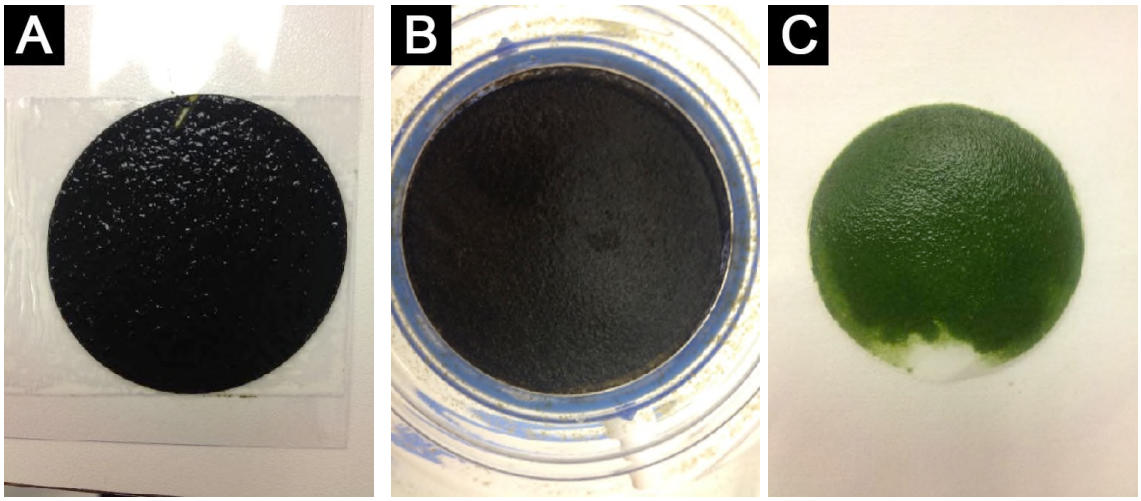

Figure 8-3 Microalgae cells deposited on filter paper; A) *Skeletonema sp.* B) *Amphora sp.* C) *D. Salina*

Table 8-1 Physico-chemical properties of microorganisms

Microorganism	θ^{DI}	θ^{DM}	θ^{EG}	γ_m^{tot}	γ_m^{d}	γ_m^{p}
B. subtilis	12.4±1.1	62.1±4.7	24.8±1.2	62.6	23.3	39.3
Skeletonema sp.	59.8±0.6	78±1.6	62.2±1.7	36.4	15.8	20.6
Amphora sp.	65.8±2.8	52.9±4.6	83.2±5.5	33.3	25.6	7.8
D. Salina	41.6±4.2	74.4±2	47.9±1.2	47.7	17.9	29.8

Table 8-2 Surface free energy components of liquid mediums

Liquid	γ_l^{tot}	γ_l^{d}	γ_l^{p}
F2	68.3±0.9	20.5±0.3	47.8±0.6
Nutrient Broth	63.3±0.3	18.9±0.1	44.4±0.2

Table 8-3 summarises the physico-chemical properties of the control PDMS and synthesised PDMS/NP coatings. Combining these results with the wettability properties of tested species presented in Table 8-1, it can be assumed that the adhesion should not take place, as according to Krasowska and Sigler (2014), the hydrophilic properties of the microbial surface may not affect adhesion to hydrophobic surfaces and conversely. Literature also demonstrated that a smaller number of cells adhere to materials with low surface energy (Dexter, 1979; Milne and Callow, 1985; Brady, 2000). For example, Fletcher et al. (1984) found that microbial cells were easy to remove from materials with low surface energies. As was thoroughly described in Section 5.5.3, all tested coatings are hydrophobic with low surface free energy and microorganisms should be easy to detach from the surface.

Table 8-3 Physico-chemical properties of coatings

Sample	Contact Angle [^{O}]			Surface Free Energy Components [mN/m]		
	θ^{DI}	θ^{DM}	θ^{EG}	γ_s^{tot}	γ_s^{d}	γ_s^{p}
PDMS	104±3.03	80.7±0.8	97±2.8	16.3	15.5	0.8
PDMS/SiO_2	115.2±1.1	79.8±0.5	99.1±1.7	16.7	16.7	0.005
PDMS/TiO_2 20:1	104.8±2.3	80.7±0.5	100.2±1.5	15.9	15.2	0.7
PDMS/TiO_2 10:1	109.9±0.8	80.3±0.6	97.5±1.6	16.4	16.2	0.2
PDMS/ZnO 20:1	117.6±0.5	81±0.7	99±1.8	16.4	16.4	0.001
PDMS/ZnO 10:1	114.7±0.9	79±0.7	101.6±0.9	15.5	15.5	0.03
PDMS/MWCNT 20:1	116.2±0.5	80.8±0.4	101.4±0.5	17.1	17.1	0.02
PDMS/MWCNT 10:1	115.7±0.7	81.5±0.8	100.9±0.5	15.8	15.8	0.01
PDMS/NBT 20:1	114.2±0.4	81.1±0.2	98.8±1.6	16.1	16.1	0.04
PDMS/NBT 10:1	115.4±0.2	81.2±0.9	95.9±1.6	16.5	16.4	0.03

Cui and Yuan (2013) suggested another link between cell attachment and surface free energy. According to this research, adhesion depends on which surface free energy component is greater: γ_m^d or γ_l^d and γ_m^p or γ_l^p**.** Comparing results from Table 8-1 and Table 8-2 two different cases for three algae species and bacteria can be observed. For *B. subtilis* and *Amphora sp.* $\gamma_m^d > \gamma_l^d$ and $\gamma_m^p < \gamma_l^p$, this means that adhesion can be more favourable (W>0) on surfaces with higher dispersive and lower polar surface free energy. For *Skeletonema sp.* and *D. Salina* $\gamma_m^d < \gamma_l^d$ and $\gamma_m^p < \gamma_l^p$**,** cell adhesion should take place on surfaces with lower dispersive and lower polar surface free energies. As can be observed in Table 8-3, all coatings have low total surface free energies, higher dispersive

and lower polar component. According to this, attachment of all tested microorganisms should take place. This theory is in contrast to previous assumptions, therefore the influence of surface free energy on cell adhesion is discussed further below.

The experimental results were applied in the thermodynamic model to obtain a work of attachment and their corresponding components. The work of attachment values between tested strains and coatings were calculated using Eq. (8-10) and are listed in Table 8-4 for bacteria and Table 8-5 for microalgae. As can be observed, the work of attachment values obtained for *B. subtilis* are above 0, which according to the thermodynamic theory indicates that the attachment of a larger number of cells would be expected. No significant difference was found for different PDMS/NP coatings, and *W* value ranged from 4.1 to 4.9. The same trend was obtained for tested microalgae; results show that *W* is positive which theoretically suggests significantly favourable adhesion. Again, all PDMS based coatings indicated similar work of attachment for each microalgae species. However, obtained data has shown that in theory, the microalgae should adhere better to PDMS based coatings then *B. subtilis*, as they have such greater *W* values.

Table 8-5 is summarised in Figure 8-4 and compared to the results described in Section 7.2.1. Based on thermodynamic modeling results, the highest work of attachment was observed for *Amphora sp.,* followed by *Skeletonema sp.* and *D. Salina,* for all tested coatings. The experimental data (Section 7.2.1) confirmed that *D. Salina* has the lowest adhesion to PDMS based coatings, which was predicted by calculated *W* values. However, work of attachment did not reflect the attachment of other microalgae, as *Skeletonema* sp. performed the highest adhesive properties to tested coatings. One possible factor contributing to these results is a fact that the thermodynamic model does not consider additional properties of a species. Previous research has shown that the age of the microbial strain (Fletcher M., 1977) and morphological properties, like size and

shape of cells (Ozkan and Berberoglu, 2013) can affect the attachment ability, therefore should be taken into consideration in further investigation.

Table 8-4 Work of attachment between PDMS and PDMS/NP coatings and *B.subtilis*

Substrate	B. subtilis		
	W	W^d	W^p
PDMS	4.1	-0.39	4.53
PDMS/SiO_2 20:1	4.91	-0.25	5.16
PDMS/TiO_2 20:1	4.13	-0.43	4.56
PDMS/TiO_2 10:1	4.53	-0.31	4.84
PDMS/ZnO 20:1	4.9	-0.29	5.19
PDMS/ZnO 10:1	4.7	-0.39	5.09
PDMS/MWCNT 20:1	4.9	-0.21	5.1
PDMS/MWCNT 10:1	4.79	-0.36	5.15

Table 8-5 Work of attachment between PDMS and PDMS/NP coatings and microalgae

Substrate	Skeletonema sp			Amphora sp.			D. Salina		
	W	W^d	W^p	W	W^d	W^p	W	W^d	W^p
PDMS	29.2	0.63	28.6	49.1	-0.62	49.7	17.9	0.34	17.5
PDMS+SiO_2 20:1	32.9	0.48	32.4	55.9	-0.47	56.4	20.1	0.26	19.9
PDMS+TiO_2 20:1	29.5	0.69	28.8	49.3	-0.67	50	18	0.37	177
PDMS+TiO_2 10:1	31	0.55	30.5	52.5	-0.53	52.9	18.9	0.29	18.7
PDMS+ZnO 20:1	33.1	0.52	32.6	56.2	-0.5	56.7	20.3	0.28	19.9
PDMS+ZnO 10:1	32.6	0.64	31.9	54.9	-0.62	55.6	19.9	0.34	19.6
PDMS+MWCNT 20:1	32.5	0.42	32.1	55.3	-0.41	55.7	19.9	0.23	19.7
PDMS+MWCNT 10:1	32.9	0.59	32.3	55.6	-0.58	56.2	20.1	0.32	19.8
PDMS+NBT 20:1	32.3	0.56	31.8	54.7	-0.55	55.2	19.8	0.3	19.5
PDMS+NBT 10:1	32.4	0.5	31.9	55	-0.5	55.5	19.9	0.28	19.6

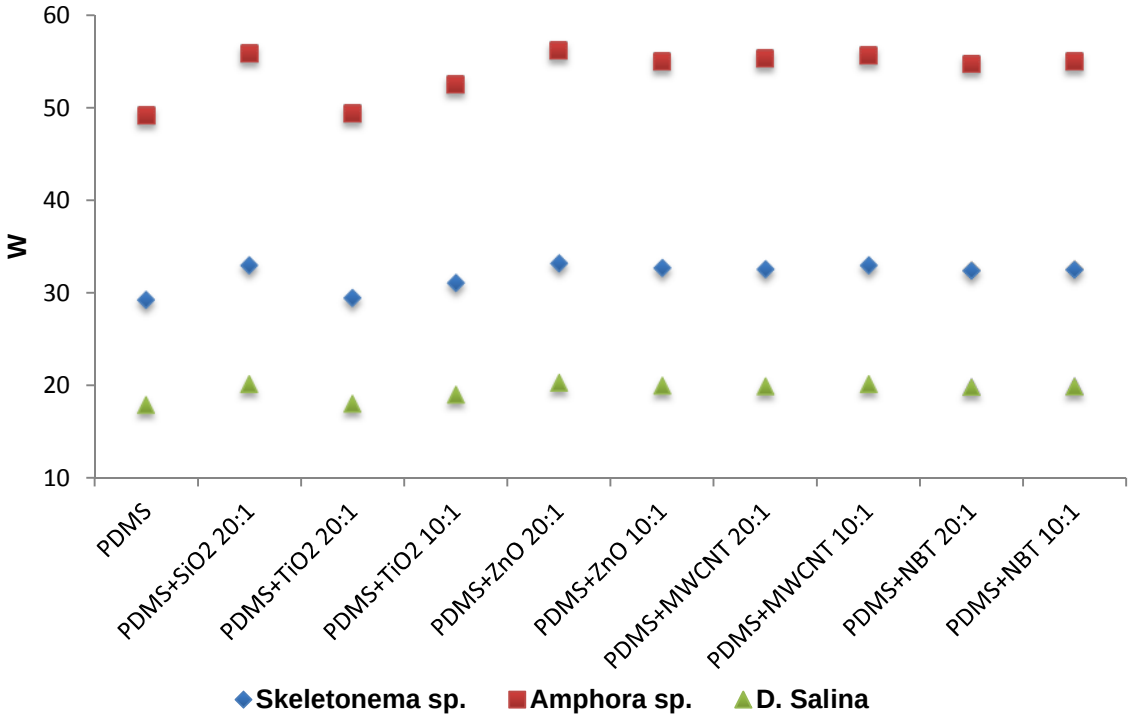

Figure 8-4 Work of attachment for all microalgae species

Figure 8-5 shows the laboratory scale and thermodynamic modelling results of microbial cells attached to tested surfaces. The positive correlation can be observed between bacteria adhesion and *W*, for some coatings (Figure 8-5 A). Settled cells on four PDMS based coatings are in order of PDMS/TiO_2 20:1 < PDMS < PDMS/ZnO 10:1 < PDMS/SiO_2 20:1 and this same trend was predicted by the calculated work of attachment. However, this correlation cannot be observed when all materials are tested together, as the experimental results did not match with the order of *W* values for remaining coatings.

As expected, similar results were obtained for all tested microalgae. Positive correlation between the work of attachment and settled cells cannot be observed if the coatings are examined together. When the coatings are divided into different parts, the thermodynamic approach can predict unfavourable cell attachment. For example, based on the modelling and laboratory results of *Skeletonema sp.* attachment (Figure 8-5 B), the total numbers of cells increase in order PDMS/TiO_2 10:1 < PDMS/NBT 10:1 < PDMS/MWCNT 20:1 <

PDMS/ZnO 10:1 < PDMS/MWCNT 10:1 and PDMS < PDMS/TiO_2 20:1 < PDMS/SiO_2 20:1, and these same orders were indicated for calculated *W* values. Similar trends were obtained for *Amphora sp.* and *D. Salina.* There was a correlation coefficient of cell adhesion and work of attachment, but only if coatings were not tested together. For all examined species, Appendix D summarises results presented in Figure 8-5.

Similar results were obtained by Cui & Yuan (2013), who analysed the process of cells adhesion to different surfaces simulated by the thermodynamic model. Authors also observed that works of attachment values are correlated with experimental results if tested materials are placed separately. Generally, they concluded that the thermodynamic model can predict cell attachment to the surfaces, if the surface free energies of materials are varied greatly. In the present study, the total surface free energies of all coatings are in this same range (Table 8-3), and this can be one possible factor causing the lack of correlation between calculated *W* values and laboratory results of microorganisms cell attachment.

Figure 8-6 depicts the experimental results of cell attachment to the tested surfaces and corresponding W^d and W^p values. It can be observed that the polar component of work of attachment has a similar trend to total work of attachment, which is understandable as the values of *W* and W^p are similar (Table 8-4, Table 8-5). Those results indicate that the polar component has a greater impact on microbial fouling than the dispersive element (Cui & Yuan, Thermodynamic modeling of algal cell–solid substrate interactions, 2013).

Overall, the relationship between work of attachment and number of attached cells is not clear and adhesion cannot be accurately predicted, for all examined species and coatings. Results reported here are in contrast with many previous studies, where the thermodynamic model successfully predicted adhesion of microorganisms (Brady Jr. and Singer, 2000; Cui and Yuan, 2013; Ozkan and Berberoglu, 2013).

One possible reason may be due to the fact that the thermodynamic model is focused on contact angle and surface free energy components of

microorganisms, substrates and liquid mediums. It should be noted that coatings with comparable physico-chemical properties were tested in this research, while the group of different materials were used in literature. The experimental results indicate no correlation of microbial fouling, contact angles and surface free energies, which may be cased by different growth conditions and used species (Gross et al., 2016).

Another factor which has not been concerned, is the influence of surface topography on microbial adhesion. It has been proven that surface roughness has an impact on microbial adhesion. For example, Cao et al. (2002) proved that there was correlation between microroughness and cell attachment, as larger number of cells was observed on metals with dimpleds. Cui et al. (2004) observed that organisms prefer to adhere to the surfaces of the comparable size pillars. Also, roughness on nanoscale can increase microbial attachment to the surfaces, as it was reported that even minor changes in surface topography can contribute to microbial adhesion (Mitik-Dineva et al. 2008). In the present study, it was proven that PDMS/NP coatings could be attractive to tested species even though surfaces are relatively smooth. However, it should be noted that different attachment was observed by tested species.

Furthermore, the topography of microbial surface is not taken into consideration. Although, the technique described by Busscher et al. (1984) was considered to be correct and was used by many authors (Brady Jr. and Singer, 2000; Cui and Yuan, 2013; Ozkan and Berberoglu, 2013), it is impossible to create a smooth surface on the filters. Despite the fact that filter papers were completely and homogeneously covered by tested species, they have a roughness comparable to diameter of the cells (Ozkan and Berberoglu, 2013).

The above discussion shows that texture of both material and microorganism surface also has an impact on microbial fouling. Therefore, physico-chemical properties of rough surfaces should be corrected by a roughness factor (Wanzel, 1936). It has also been shown that other factors could affect initial cell attachment and further research should be conducted to confirm proposed explanations.

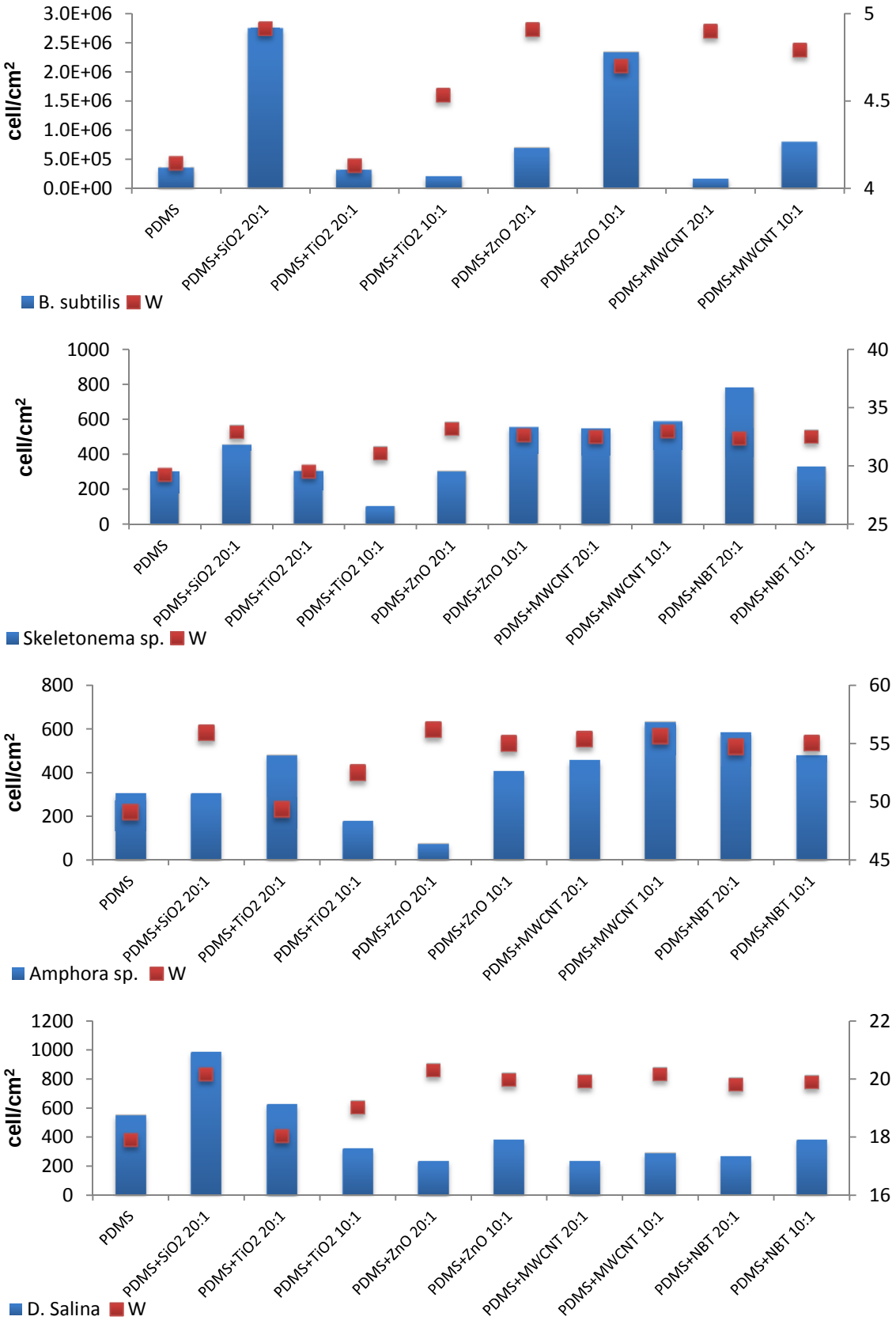

Figure 8-5 Initial attachment of microorganisms vs. work of attachment (*W*)

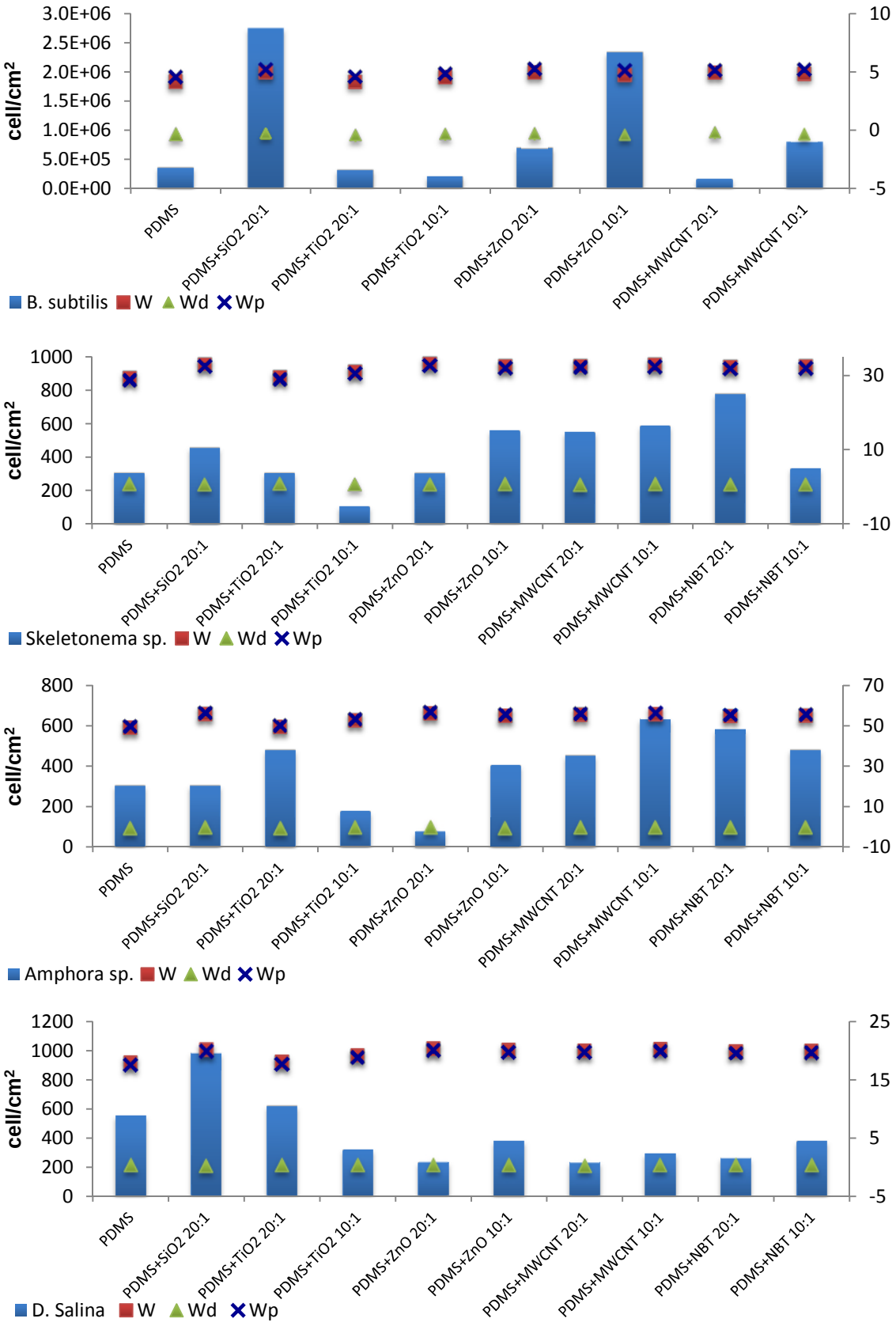

Figure 8-6 Initial attachment of microorganisms vs. work of attachment (*W*) and their components: polar *Wp* and dispersive *Wd*

8.3 Conclusion

The thermodynamic approach including interfacial free energies between microbial and material located in the aquatic environment was used to determine the prediction of initial microorganisms adhesion. In theory, all microorganisms are able to attach to PDMS/NP coatings, as results indicated positive work of attachment values. The results show that polar component has a greater impact on microbial fouling than the dispersive element, as has a similar trend to total work of attachment.

Based on the model, *D. Salina* has the lowest adhesion to PDMS/NP coatings, which was matched with experimental results. However, calculated work of attachment did not predict the attachment of other microalgae, as *Skeletonema* sp. performed higher attachment then *Amphora sp.*

The positive correlation between the work of attachment and attached cells was observed when the coatings were divided into different parts. This correlation was not observed when all materials were tested together.

The thermodynamic modelling tested in this study show that the relationship between work of attachment and number of attached cells is not clear and adhesion cannot be accurately predicted, for all examined species and PDMS based coatings. The used method was not suitable to explain the microbial adhesion and further research on the texture of both material and microorganism may improve stimulated growth.

9 Conclusions and Recommendations for Future Work

The investigations into the potential of using polymer nanocomposites coatings to control marine biofouling were presented. It is evident from the literature that the growth of unwanted organisms on surfaces submerged in marine water is a worldwide phenomenon bringing negative effects for marine environment and industries. Environmental friendly coatings are required to prevent fouling of marine organisms.

The experimental work is focused on developing the new method for the synthesis of polymer nanocomposites. An aim of present research was to develop coatings for prevention on marine biofouling. Three simple methods of synthesis PDMS/NP have been used in order to achieve the goal. The uses of these methods were dependent on the type of nanoparticles and required a solvent. The preparation and investigation of polymer nanocomposites coatings with antifouling properties were described. The objective was to understand how structure and surface properties influence the adhesion of microorganisms. To examine the influence of different materials, the applicability of silica dioxide, zinc oxide, titanium dioxide, multi walled carbon nanotubes and sodium bismuth titanate nanoparticles as precursors for PDMS in antifouling coatings has been tested. For the first time, NBT nanopowder was used for antifouling coatings. NBT nanoparticles with a size of 10 nm were successfully synthesised using hydrothermal method. Characterisation techniques included XRD and SEM confirmed the purity of chosen nanoparticles.

Eight PDMS nanocomposite coatings were successfully applied on the glass substrate. Using surface analytical techniques, namely XRD, SEM and AFM, formation and structure of coatings were examined. Contact angles measurements indicated that presence of PDMS changes the hydrophilic nature of glass substrate into the hydrophobic surface. The wettability coefficients of different materials decreased after using artificial water drop. Smooth PDMS/NP coatings were successively created and the surface roughness was on the nanoscale. It was confirmed that small surface roughness did not influence wettability of coatings.

Since bacteria is causing a biofilm formation in the early stages of marine biofouling, the settlement behavior of the *Bacillus subtilis* spores on PDMS/NP coatings were investigated. Coatings were exposed to contact with bacteria for 24 h to 96 h. It was found that incubation time has a huge influence on *Bacillus subtilis* adhesion. A number of attachment for all samples tested in this research was larger after 24 h then after 96 h. The experimental results indicated that *Bacillus subtilis* need 48 h to achieve the maximum of attachment onto PDMS, PDMS/TiO_2 20:1 and PDMS/TiO_2 10:1 coatings, while for other coatings this time is 24 h is needed. After these times, a decrease in bacteria adhesion was observed. It means that coatings containing ZnO, SiO_2, MWCNT and NBT are better for longer incubation time. It was proven that the influence for these results has surface wettability. The bacteria needs more time to fully adhere to the coatings with contact angle lower than 150^o and the polar component of surface free energy higher than 10^{-2}. Comparing the AFM results with *Bacillus subtilis* adhesion it is revealed that the roughness on nanoscale may still have influence on bacteria colonisation, however incubation time plays here an important role.

Following the examination of bacteria attachment on the PDMS/NP coatings, the antifouling properties were tested on the adhesion of microalgae spores. Three different types of microalgae: *Skeletonema sp*., *Amphora sp. and D. Salina* were used to perform adhesion assays. The effects of incubation time, surface properties and structure have been intensively studied. Antifouling investigations proved that the presence of nanoparticles in a polymer coating changed microbial settlement behaviour. After a long time of incubation (12 weeks), the degree of attached cells was found to be greater on control surfaces (glass and PDMS) and PDMS/SiO_2 20:1 coating. The best antifouling properties, for tested microalgae were observed in coatings containing MWCNT. The observations also indicated the potential of using NBT nanoparticles, as PDMS/NBT coatings demonstrate a low adhesion of *D. Salina* cells.

Settlement of microalgae on PDMS/NP coatings was performed to investigate the influence of topography. The results show that cells attachment is lower on surfaces with lower surface roughness in the case of coatings with a similar composition. Although some effect of surface roughness on the microbial attachment was observed, the topography influence is still not obvious and further examination needs to be performed.

Fouling-release properties of PDMS/NP coatings were examined on laboratory scale rotor set-up. Results showed a promising use of PDMS/SiO_2 20:1 and both PDMS/TiO_2, as the lower number of attached *Skeletonema sp.* was observed. A recommendation based on this would be to investigate different marine organisms.

The thermodynamic approach did not predict microorganisms adhesion well. The reason may be the fact that the physic-chemical properties of coatings are comparable and thermodynamic model is focused only on the surfaces free energy. In this order, future recommendations should include testing the extended DVLO theory. This model may be a better approach for the prediction of microorganisms as is accommodates for Lifshitz-van der Waals, electrostatic, Lewis acid-base and Brownian motion forces**.**

If coatings inhibit the adhesion of microorganisms tested in this research, it doesn't mean a general inhibition to other marine species. More marine species should be tested. Furthermore, it would be interesting to expose the coatings in the natural marine environment, due to the fact that the marine organisms include a diverse range of species that may affect fouling.

The doctor blade method is a straightforward alternative in coating application as demonstrated in this thesis. Different application methods should be investigated to find the optimal solution for commercial uses. The use of suitable surfactants could change the viscosity of the nanocomposites resulting in the spray application.

REFERENCES

Abarzua, S., & Jakubowski, S. (1995). Biotechnological investigation for the prevention of biofouling. I.Biological and biochemical principles for the prevention of biofouling. *Marine Ecology Progress Series , 123*, 301-312.

Almeida, E. (2007). Marine paints: the particular case of antifouling paints. *Progress in Organis Coatings , 59*, 2-20.

AMBIO Final report, 2010.

Baier, R. E. (1972). Influence of the initial surface sondition of materials onbioadhesion. *Congress on Marine Corrosion and Fouling* , 633-639.

Bakker, D. P., Huijs, F. M., de Vries, J., Klijnstra, J. W., Busscher, H. J., & van der Mei, H. C. (2003). Bacterial depositionto fluoidated and nonfluoidated polyurethane coatings with different elastic modulus and surface thension in a parallel plate and a stagnation point flow chamber. *Colloids Surfaces , 32*, 179-190.

Bakker, D. P., Klinstra, W. J., Busscher, J. H., & Van der Mei, H. C. (2003). The effect of dissolved organic carbon on bacterial adhesion to conditioning films adsorbed on glass from natural seawater collected during different seasons. *Biofoling , 19*, 391-397.

Ball, P. (1999). Engineering shark skin and other solutions. *Nature , 4000* (6744), 507-509.

Beigbeder, A., Degee, P., Conlan, S. L., Mutton, R. J., Clare, A. S., Pettitt, M. E., et al. (2008). Preparation and characterisation of silicone-based coatings filled with carbon nanotubes and natural sepiolite and their application as marine fouling-release. *Biofouling: The Jouurnal of ~Bioadhesiona and Biofilm Research , 24* (4), 291-302.

Beigbeder, A., Labruyere, C., Viville, P., Pettitt, M. E., Callow, M. E., Callow, J. A., et al. (2011). Surface and fouling-release properties of

silicone/organomodified montmorillonite coatings. *Jurnal of Adhesion Science and Technology , 25*, 1689-1700.

Berglin, M., & Gatenholm, P. (1999). The nature of bioadhesive bonding between barnacles and fouling-release silicone coatings. *Journal of Adhesion Science and technology , 13* (6), 713-727.

Bos, R., Mei, H. C., & Busscher, H. J. (1999). Physico-chemistry of initial microbial adhesive interactions - its mechanisms and methods for study. *FEMS Microbiology Reviews , 23*, 179-230.

Bott, T. R., & Pienheiro, M. (1977). Biological fouling: velocity and temperature effects. *Canadian Jurnal of Chemical Engineering , 55*, 473-474.

Brady Jr, R., & Singler, I. (2000). Mechanical factors favoring release from fouling release coatings. *Biofouling , 15*, 73-81.

Brady Jr., R. F. (1999). Properties which influence marine fouling resistance in polymers containing silicon and fluorine. *Progress in Organic Coatings , 35*, 31-35.

Brink, L. E., Elbers, S. J., Robbertson, T., & Both, P. J. (1993). The anti-fouling action of polymers preadsorbed on ultrafiltration and microfiltration membranes. *Jurnal of Membrane Science , 76* (2-3), 281-291.

Bryers, J. D. (2008). Medical biofilms. *Biotechnology and Bioengineering , 100*, 1-18.

Burns, A., Dannenfelser, F., & Mueller, R. (1946). A future of U.S. navy plastic type antifouling paints in commercial shiping. *Pacific Marine* , 218-227.

Busscher, H. J., & Weerkamp, A. H. (1987). Specific and non-specific interactions in bacterial adhesion to solid substrata. *FEMS Microbiology Letters , 46*, 165-173.

Busscher, H. J., Weerkamp, A. H., van der Mei, H. C., van Pelt, A. W., de Jong, H. P., & Arends, J. (1984). Measurement of the surface free energy of bacterial

cell surfaces and its relevance for adhesion. *Applied and Environmental Microbiology , 48* (5), 980-983.

Busscher, H., Weerkamp, A., van der Mei, H., van Pelt, A., de Jong, H., & Arends, J. (1984). Measurement of the surface free energy of bacterial cell surfaces and its relevance for adhesion. *Applied and Environmental Microbiology* , 980-983.

Byrappa, K., & Yoshimura, M. (2001). *Handbook of Hydrothermal Technology.* New Jersey, USA: Noyes Publications.

Callow, J. A. (2010). *Advanced nanostructured surfaces for the control of biofouling.* Birmingham: AMBIO.

Callow, M. E., & Callow, J. A. (2002). Marine biofouling: a sticky problem. *Biologist , 49*.

Callow, M. E., Jennings, A. R., Brennan, A. B., Seegert, C. E., Gibson, A., Wilson, L., et al. (2002). Microtopographic cues for settlement of zeospores of the green fouling alga Enteromorpha. *Biofouling , 18*, 237-245.

Callow, M., Callow, J., Ista, L., Coleman, S., Nolasco, A., & Lopez, G. (2000). Use of self-assembled monolayers of different wettabilities to study surface selection and primary adhesion processes of green algal (Enteromorpha) zoospores. *Appl. Environ. Microbiol. , 66*, 3249-3254.

Callow, M., Callow, J., Pickett-Heaps, J., & Wetherbee, R. (1997). Primary adhesion of Enteromorpha(Chlorophyta, Ulvales) propagules: quantitative settlement studies and video microscopy. *Journal of Phycology , 33* (6), 938-947.

Chambers, L. D., Stokes, K. R., Walsh, F. C., & Wood, R. (2006). Modern approaches to marine antifouling coatings. *Surface and Coating Technologies , 201*, 3642-3652.

Candries, M. (2000). *Paint systems for the marine industry.* Notes to Complement the External Seminar on Antifouling.

Chan, C. M. (1994). *Polymer surface modification and characterization.* New York: Hanser Publishers.

Cho, Y., Sundaram, H. S., Weinman, C. J., Paik, M. Y., Dimitriou, M. D., Finlay, J. A., et al. (2011). Triblock copolymerswith grafted fluorine-free, amphiphilic, non-ionic side chains for antifouling and fouling-release applications. *Macromolecules , 44*, 4783-4792.

Christensen, B. (1999). Physical and chemical properties of extracellular polysaccharides associated with biofilms and related systems. In J. Wingender, T. Neu, & H. Flemming, *Microbial extracellular polymeric substances* (pp. 143-154). Springer.

Compere, C., Bellon-Fontaine, M. N., Bertrand, P., Costa, D., Marcus, P., Poleunis, C., et al. (2001). Kinetics of conditioning layer formation on stainless steel immersed in seawater. *Biofouling* , 129-145.

Cooper, S., Finlay, J., Cone G., Callow, M., Callow, J., & Brennan, A. (2011). Engineered antifouling microtopographies: kinetic analysis of the attachment of zoospores of the green alga Ulva to silicone elastomers. *Biofouling , 27* (8), 881-891.

Costerton, J. (1999). Introduction to biofilm. *International Journal of Antimicrobial Agents , 11* (3-4), 217-221.

Cui, Y., & Yuan, W. (2013). Thermodynamic modeling of algal cell–solid substrate interactions. *Applied Energy , 112*, 485–492.

Cui, Y., Yuan, W., Cheng, J., & Wang, B. (2015). The effects of solid carrier material and surface roughness on microalgal cell attachment. *American Society of Agricultural of Biological Engineers , 58*, 161-168.

Dexter, S. C. (1979). Influence of substratum critical surface thensionon bacteria adhesion - in situ studies. *Coloid Interface Sci. , 70*, 346-354.

Dexter, S. C., Sullivan, J. D., Williams, J., & Watson, S. W. (1975). Influence of substratum wettability on the attachment of marine bacteria to various surfaces. *Appl. Microbiol. , 30*, 298-308.

Dunne Jr., W. (2002). Bacterial adhesion:seen any good biofilm lataly. *Clin. Microbiol. Rev. , 15* (2), 155-166.

Ederth, T., Nygren, P., Pettitt, M. E., Ostblom, M., Du, C. X., Broo, K., et al. (2008). Anomalous settlement behavior of Ulza linza zoospores on cationic oligopeptide surfaces. *Biofouling , 24* (4), 303-312.

Epstein, N. (1983). Thinking about heat transfer fouling: A 5x5 matrix. *Heat Transfer Engineering , 4*, 43-56.

Evans, S. M. (1999). TBT or not TBT?: That is the question. *Biofouling , 14* (2), 117-130.

Fletcher, M. (1977). The effects of culture concentration and age, time, and temperature on bacterial attchment to polystyrene. *Canadian Journal of Microbiology , 23* (1), 1-6.

Fletcher, M., & Pringle, J. H. (1985). The effect of surface free energy and medium surface tension on bacterial attachment to solid surfaces. *Jurnal of Colloid and Interface Science , 104*, 5-14.

Fletcher, R. L., Baier, R. E., & Fornalik, M. S. (1984). The influence of surface energy on spore development in some common marine fouling, in Proceedings 6th Inter. Congress on Marine Corrosion and Fouling algae. *Marine Biology* , 129-144.

Fowks, F. (1962). Determination of interfacial tensions, contact angles, and dispersion forces in surfaces by assuming additivity of intermolecular interactions in surfaces. *J. Phys. Chem. , 66*, 382.

Garg, A., Jain, A., & Bhosle, N. B. (2009). Chemical characterization of a marine conditioning film. *63*, 7-11.

Garg, A., Jain, A., & Bhosle, N. (2009). Chamical characterization of a marine conditioning film. *International Biodeterioration & Biodegradation , 63*, 7-11.

Garrett, T. R., Bhakoo, M., & Zhang, Z. (2008). Bacterial adhesion and biofilms on surfaces. *Progress in Natural Science , 18*, 1049-1056.

Genzer, J., & Efimenko, K. (2006). Recent developments in superhydrophobic surfaces and their relevance to marine fouling: a review. *Biofouling , 22*, 339-360.

Giaouris, E., Chorianopoulos, N., & Nychas, G. (2005). Effect of temperature, ph, and water activity on biofilm formation by Salmonella enterica Enteritidis PT4 on stainless steel surfaces as indicated by the bead vortexing method and conductance measurements. *Journal of Food Protection , 10*, 2012-2241.

Gross, M., Zhao, X., Mascarenhas, V., & Wen, Z. (2016). Effect of the surface physico-chemical properties and the surface textures in the initial colonization and the attachment growth in algal biofilm. *Biotechnology and Biofuels* , 9:38.

Guillard, R., & Sournia, A. (1978). *Counting slides. Phytoplankton manual.* UNESCO.

Gurd, C. (2015). *nine months review (unpublished PhD thesis).* Cranfield University.

Hamza, A., Pham, V. A., Matsuura, T., & Santerre, J. P. (1997). Development of membranes with low surface energy to reduce the fouling in ultrafiltration applications. *Jurnal of Membrane Science , 131* (1-2), 217-27.

Hellio, C., & Yebra, D. *Advances in marine antifouling coatings and technologies.* Oxford, Camridge, New Delhi: Woodhead Publishing Limited.

Howell, D., & Behrends, B. (2006). A review of surface roughness in antifouling coatings illustrating the importance of cutoff length. *Biofouling , 22* (6), 401-410.

Hoch, M. (2001). Organotin compounds in the environment- an overview. *Applied Geochemistry , 16*, 719-743.

Huggett, M., Williamson, J., de Nys, R., Kjelleberg, S., & Steinberg, P. (2006). Larval settlement of the common Australian sea urchin heliocidaris erthrogramma in response to bacteria from the surface of coralline algae. *Oecologia , 149* (4), 604-619.

IMO, 2. (2001). *Anti-fouling systems: international convention on the control of harmful antifouling systems on ships.* London: International Martime Organisation Publications.

Irving, T., & Allen, D. (2011). Species and material considerations in the formation and development of microbial biofilm. *Appl. Microbiol. Biotechnol. , 92*, 283-294.

Ista, L., Callow, M., Finlay, J., Coleman, S., Nolasco, A., Simons, R., et al. (2004). Effect of substratum surface chemistry and surface energy on attachment of marine bacteria and algal spores. *Appl. Environ. microbiol. , 70* (7), 4151-4157.

Jaworski, A., Serwecinska, L., & Straczek, P. (2005). Quorum sensing - bacterial cell - to -cell communication using chemical signal molecules. *Postepy Biologii Komorki , 32* (2), 231-256.

Jain, A., & Bhosle, N. (2009). Biochemical composition of marine conditioning film: implications for bacterial adhesion. *Biofouling , 25* (1), 13-19.

Jenner, G., Longerich, H., Jackson, S., & Fryer, B. (1990). ICP-MS- a powerful tool for high-precision trace-element analysis in Earth sciences: Evidence from analysis of selected U.S.G.S. reference samples. *Chamical Geplogy , 83* (1-2), 133-148.

Jiang, X., Lin, M., Tu, N., Chen, C., Zhou, S., & Zhan, H. (2011). Simple hydrothermal synthesis and sintering of Na0.5Bi0.5TiO3 nanowires. *Journal of Alloys and Compounds , 509*, 9346-9350.

Kesel, A., & Liedert, R. (2007). Learning from nature: non-toxic biofouling control by shark skin effect. Comparative biochemistry and physiology Part A: molecular & interative. *Physiology , 146* (4), 130.

Khatiwala, S., Primeau, F., & Hall, T. (2009). Reconstruction of the history of antropogenic CO2 concentrations in the ocean. *Nature , 462*, 346-349.

Krasowska, A., & Sigler, K. (2014). How microorganisms use hydrophobicity and what does this mean for human needs. *Frontiers in Cellular and Infection Microbiology , 4* (112).

van Loosdrecht, M., Norde, W., & Zehnder, A. (1990). Pchysical chemical description of bacterial adhesion. *Journal of Biomaterials Applications , 5* (2), 91-106.

Lange, G. (1967). *Lange's handbook of chemistry.* McGraw Hill Book Company.

Li, B., & Logan, B. (2004). Bacterial adhesion to glass and metal-oxide surfaces. *Colloids Surf. B. , 36*, 81-90.

Little, B. (1984). Succession in microfouling. In J. Caslow, & R. Tipper, *Marine biodeterioration: an interdisciplinary study* (pp. 63-67). London: E & FN Spon Ltd.

Loeb, G. I., & Neihof, R. A. (1975). Marine conditioning film. *Advanced Chemical Series , 145*, 319-335.

Lopez, D., Vlamakis, H., & Kolter, R. (2010). Biofilms. *Cold Spring Harbor in Biology , 2*.

Liu, Y., & Zhao, Q. (2005). Influence of surface energy of modified surfaces on bacterial adhesion. *Biophisical Chemistry , 117*, 39-45.

Liu, Y., & Zhao, Q. (2005). influence of surface energy on modified surfaces on bacterial adhesion. *Biophysical Chemistry , 117* (1), 39-45.

Liu, Y., & Tay, J. (2001). Detachment forces and their influence on the structure and metabolic behavior of biofilms. *Journal of Microbiology and Biotechnology , 17*, 111-117.

Ma, X., Zhang, W., Xue, L., Yin, S., Wan, L., & Yan, Y. (2013). Hydrothermal synthesis of bismuth sodium titanate particles with different morphologies. *Material Science , 48*, 6878-6884.

Marine fouling and its prevention. George Banta Publishing Co.

Marhaeni, B., Rajasa, O., Bengen, D., & Kaswadji, D. (2009). Screening of bacterial symbionts of seagrass Enhalus sp. against biofilm-forming bacteria. *Journal of Coastal Development , 13*, 126-132.

Melo, L. F., & Bott, T. R. (1997). Biofouling in water system. *Experimental Thermal and Fluid Science , 14*, 375-381.

Milne, A., & Callow, M. E. (1985). Non-biocidal antifouling process, in: R. Smith (Ed.), Polymers in marine environment. *The Institute of Marine Engineers* , 229-233.

Mitik-Dineva, N., Wang, J., Mocanasu, R., Stoddart, P., Crawford, R., & Ivanova, E. (2008). Impact of nano-topography on bacterial attachment. *Biotechnology , 3* (4), 536-544.

Moat, A. G., Foster, J. W., & Spector, M. P. (2002). *Microbial Physiology,* (4th ed.). Wiley.

Mukherjee, M., & De, S. (2015). Reduction of microbial contamination from drinking water using an iron oxide nanoparticle-impregnated ultrafiltration mixed matrix membrane: preparation, characterization and antimicrobial properties. *Environmental Science: Water Research & Technology , 1*, 204-217.

du Nouy, P. L. (1925). An interfacial tensiometer for universal use. *The Journal of General Physiology , 7* (5), 625-633.

Novak, L. (1982). Comparison of the Rhine river and the Oresund sea water fouling and its removal by chlorination. *Journal of Heat Transfer , 104* (4), 663-669.

Ozkan, A., & Berberoglu, H. (2013). Adhesion of algae cells to surfaces. *Biofouling , 29* (4), 469-482.

Ozkan, A., & Berberoglu, H. (2013). Physico-chemical surface properties of microalgae. *Colloids and surfaces B: Biointerfaces , 112*, 287-293.

Percival, S. L., Malic, S., Cruz, H., & Williams, D. (2011). Introduction to biofilms. *Biofilms and Veterinary Medicine , 6*, 41-68.

Percival, S., Walker, J. T., & Hunter, P. (2000). *Microbial aspects of biofilms and drinking water.* CRC Press.

Picioreanu, C., van Loosdrecht, M., & Heijnen, J. (2000). Effect of diffusive and convective substrate transport on biofilm structure formation: a two-dimensional modeling study. *Biotechnology and Bioengineering , 96* (5), 504-515.

Pompermayer, D., & Gaylarde, C. (2000). The influence of temperature on the adhesion of mixed cultures of Staphylococcus aureus and Escherichia coli to polypropylene. *Foud Microbiology , 17* (4), 361-365.

Rabenau, A. (1985). Role of hydrothermal synthesis in preparative chemistry. *Angewandte Chemie International Edition in English , 24*, 1026-1040.

Rasband, W. S. (1997-2016). ImageJ. *U.S. National Institute of Health* . Bethesda, Maryland, USA. From https://imagej.nih.gov/ij/

Renner, L., & Weibel, D. (2011). Physicochemical regulation of biofilm formation. *MRS Bull , 36* (5), 347-355.

Rittschof, D. (2000). Natural product antifoulants: one perspective on the challenges related to coatings development. *Biofouling , 15* (1-3), 119-127.

Rutherford, S. T., & Bassler, B. L. (2012). Bacterial quorum sensing: its role in virulence and possibilities for its control. *Cold Spring Herb Perspect Med , 2* (11).

Schultz, M. (2007). Effects of coating roughness and biofouling on ship resistance and powering. *Biofouling* , 331-341.

Schultz, M. P., Bendick, J. A., Holm, E. R., & Hertel, W. M. (2011). Marine biofouling is a worldwide problem, defined as unwanted accumulation and

growth of seawater organisms on all surfaces exposed in the marine environment with negative consequences. *Biofouling , 27*, 87-98.

Setinc, T., Spreitzer, M., Logar, M., & Suvorov, D. (2011). Hydrothermal Synthesis of Nanosized Na0.5Bi0.5TiO3. *Jurnal of the Americam Ceramic Society , 94* (11), 3793-3799.

Strand, J., & Jocobsen, J. (2005). Accumulation and trophic transfer of organotins in marine food web from the Danish coastal waters. *Sci. Total Environ. , 350* (1-3), 72-85.

Swain, G. (1999). Redefining antifouling coating. *Oceanography and Ocean Engineering* , 26-35.

The woods hole oceanographic institution 1952.

Thomas, K. V., & Brooks, S. (2010). The environmental fate and effecys of antifouling paint biocides. *Biofouling , 26*, 73-88.

Tribou, M., & Swain, G. (2010). The use of proactive in-water grooming to improve the performance of ship hull antifouling coatings. *Biofouling , 26*, 47-56.

Walt, D. R., Smulow, J. B., Turesky, S. S., & Hill, R. G. (1985). The effect of gravity on initial microbial adhesion. *Journal of Colloid and Interface Sciencew , 107* (2), 334-336.

Wanzel, R. N. (1936). Resistance of solid surfaces to wetting by water. *Industrial and Engineering Chemistry , 28* (8), 988-994.

Wilson, D. P. (1955). the role of micro-organisms in the settlement of Ophelia Bicornis Savigny. *J. Mar. biol. Ass. UK , 34*, 531-543.

Woods, D., & Fletcher, R. (1991). Studies on the strength of adhesion of some common fouling diatoms. *Biofouling , 3*, 287-303.

Yebra, D. M., Kiil, S., & Dam-Johanson, K. (2004). Antifouling technology—past, present and future steps towards efficient and environmentally friendly antifouling coatings. *Progress in Organic Coatings , 50*, 75-104.

Young, T. (1805). An essay on the cohesion of fluids. *Philosophical Transactions of the Royal Society of London , 95*, 65-87.

Zhao, Q., Liu, Y., Wang, C., & Wang, S. (2007b). Evaluation of bacterial adhesion on Si-doped diamond-like carbon films. *Applied Surface Science , 253* (17), 7254-7259.

Zhao, Q., Liu, Y., Wang, C., Wang, S., Peng, N., & Jeynes, C. (2007a). Bacterial adhesion on ion-implanted stainless steel surfaces. *Applied Surface Science , 253* (21), 8674-8681.

Zobell, C. E., & Allen, E. C. (1934). The significance of marine bacteria in the fouling of submerged surfaces. *Scrippe Institution of Oceanography of University of California* .

APPENDICES

Appendix A

Bacteria quantification after 24 h

PDMS				
cells per plate	10^{0}	10^{-1}	10^{-2}	10^{-3}
Plate 1	TMTC	47	4	1
Plate 2	TMTC	62	3	1
Plate 3	TMTC	475	3	28
PDMS/SiO_2 20:1				
cells per plate	10^{0}	10^{-1}	10^{-2}	10^{-3}
Plate 1	TMTC	TMTC	384	60
Plate 2	TMTC	TMTC	473	37
Plate 3	TMTC	TMTC	521	39
PDMS/TiO_2 20:1				
cells per plate	10^{0}	10^{-1}	10^{-2}	10^{-3}
Plate 1	TMTC	491	59	5
Plate 2	TMTC	483	53	2
Plate 3	TMTC	497	45	6
PDMS/TiO_2 10:1				
cells per plate	10^{0}	10^{-1}	10^{-2}	10^{-3}
Plate 1	TMTC	369	54	0
Plate 2	TMTC	269	30	1
Plate 3	TMTC	254	24	5
PDMS/ZnO 20:1				
cells per plate	10^{0}	10^{-1}	10^{-2}	10^{-3}
Plate 1	TMTC	642	202	1
Plate 2	TMTC	514	53	3
Plate 3	TMTC	508	89	7

PDMS/ZnO 10:1				
cells per plate	10^0	10^{-1}	10^{-2}	10^{-3}
Plate 1	TMTC	TMTC	160	15
Plate 2	TMTC	TMTC	167	19
Plate 3	TMTC	TMTC	512	113
PDMS/MWCNT 20:1				
cells per plate	10^0	10^{-1}	10^{-2}	10^{-3}
Plate 1	TMTC	653	27	0
Plate 2	400	520	17	0
Plate 3	TMTC	107	33	1
PDMS/MWCNT 10:1				
cells per plate	10^0	10^{-1}	10^{-2}	10^{-3}
Plate 1	TMTC	TMTC	128	9
Plate 2	TMTC	TMTC	112	6
Plate 3	TMTC	TMTC	155	13

Bacteria quantification after 48 h

PDMS				
cells per plate	10^0	10^{-1}	10^{-2}	10^{-3}
Plate 1	TMTC	TMTC	125	13
Plate 2	TMTC	TMTC	128	7
Plate 3	TMTC	TMTC	112	50
PDMS/SiO_2 20:1				
cells per plate	10^0	10^{-1}	10^{-2}	10^{-3}
Plate 1	TMTC	41	6	0
Plate 2	534	56	7	2
Plate 3	425	70	7	0
PDMS/TiO_2 20:1				

cells per plate	10^0	10^{-1}	10^{-2}	10^{-3}
Plate 1	TMTC	532	52	62
Plate 2	TMTC	598	65	5
Plate 3	TMTC	542	69	2
PDMS/TiO_2 10:1				
cells per plate	10^0	10^{-1}	10^{-2}	10^{-3}
Plate 1	TMTC	462	56	6
Plate 2	TMTC	513	46	7
Plate 3	TMTC	441	59	4
PDMS/ZnO 20:1				
cells per plate	10^0	10^{-1}	10^{-2}	10^{-3}
Plate 1	TMTC	224	18	2
Plate 2	TMTC	345	35	2
Plate 3	TMTC	247	22	3
PDMS/ZnO 10:1				
cells per plate	10^0	10^{-1}	10^{-2}	10^{-3}
Plate 1	TMTC	476	70	2
Plate 2	TMTC	542	73	3
Plate 3	TMTC	TMTC	196	9
PDMS/MWCNT 20:1				
cells per plate	10^0	10^{-1}	10^{-2}	10^{-3}
Plate 1	TMTC	279	19	2
Plate 2	TMTC	240	21	2
Plate 3	TMTC	202	27	4
PDMS/MWCNT 20:1				
cells per plate	10^0	10^{-1}	10^{-2}	10^{-3}
Plate 1	TMTC	279	19	2
Plate 2	TMTC	240	21	2
Plate 3	TMTC	202	27	4

PDMS/MWCNT 10:1				
cells per plate	10^0	10^{-1}	10^{-2}	10^{-3}
Plate 1	TMTC	279	38	6
Plate 2	TMTC	179	40	1
Plate 3	336	340	19	0

Bacteria quantification after 72 h

PDMS				
cells per plate	10^0	10^{-1}	10^{-2}	10^{-3}
Plate 1	TMTC	105	83	3
Plate 2	381	84	9	0
Plate 3	341	116	8	0
PDMS/SiO_2 20:1				
cells per plate	10^0	10^{-1}	10^{-2}	10^{-3}
Plate 1	TMTC	89	12	0
Plate 2	TMTC	105	5	1
Plate 3	TMTC	127	4	0
PDMS/TiO_2 20:1				
cells per plate	10^0	10^{-1}	10^{-2}	10^{-3}
Plate 1	TMTC	109	15	3
Plate 2	TMTC	110	22	0
Plate 3	TMTC	340	20	0
PDMS/TiO_2 10:1				
cells per plate	10^0	10^{-1}	10^{-2}	10^{-3}
Plate 1	80	10	0	0
Plate 2	88	21	1	1

Plate 3	74	32	4	0
PDMS/ZnO 20:1				
cells per plate	10^{0}	10^{-1}	10^{-2}	10^{-3}
Plate 1	88	8	1	0
Plate 2	67	6	1	0
Plate 3	76	8	0	0
PDMS/ZnO 10:1				
cells per plate	10^{0}	10^{-1}	10^{-2}	10^{-3}
Plate 1	TMTC	448	92	2
Plate 2	TMTC	198	9	9
Plate 3	TMTC	119	3	2
PDMS/MWCNT 20:1				
cells per plate	10^{0}	10^{-1}	10^{-2}	10^{-3}
Plate 1	TMTC	79	14	1
Plate 2	TMTC	109	5	1
Plate 3	TMTC	278	4	0
PDMS/MWCNT 10:1				
cells per plate	10^{0}	10^{-1}	10^{-2}	10^{-3}
Plate 1	TMTC	43	2	0
Plate 2	TMTC	30	5	0
Plate 3	TMTC	39	4	0

Bacteria quantification after 96 h

PDMS				
cells per plate	10^{0}	10^{-1}	10^{-2}	10^{-3}
Plate 1	186	7	1	0
Plate 2	118	14	2	0
Plate 3	132	10	3	0

PDMS/SiO_2 20:1				
cells per plate	10^0	10^{-1}	10^{-2}	10^{-3}
Plate 1	93	10	0	0
Plate 2	84	5	2	0
Plate 3	79	7	4	0
PDMS/TiO_2 20:1				
cells per plate	10^0	10^{-1}	10^{-2}	10^{-3}
Plate 1	81	6	1	0
Plate 2	81	5	0	0
Plate 3	192	7	1	0
PDMS/TiO_2 10:1				
cells per plate	10^0	10^{-1}	10^{-2}	10^{-3}
Plate 1	213	22	7	3
Plate 2	211	27	6	0
Plate 3	210	18	2	0
PDMS/ZnO 20:1				
cells per plate	10^0	10^{-1}	10^{-2}	10^{-3}
Plate 1	143	10	2	0
Plate 2	119	11	1	0
Plate 3	101	13	4	1
PDMS/ZnO 10:1				
cells per plate	10^0	10^{-1}	10^{-2}	10^{-3}
Plate 1	71	11	0	0
Plate 2	46	4	0	0
Plate 3	59	5	0	0
PDMS/MWCNT 20:1				
cells per plate	10^0	10^{-1}	10^{-2}	10^{-3}
Plate 1	127	60	2	0
Plate 2	167	17	1	1

Plate 3	349	21	5	2
PDMS/MWCNT 10:1				
cells per plate	10^{0}	10^{-1}	10^{-2}	10^{-3}
Plate 1	TMTC	70	4	0
Plate 2	TMTC	67	5	0
Plate 3	361	216	5	2

Appendix B

f/2 +Si Algal medium recipe

Component	Concentration
NA_2 EDTA	4.16 g
$FeCl_3 \cdot 6H_2O$	3.15 g
$CuSO_4 \cdot 5H_2O$	0.01 g
$ZnSO_4 \cdot 7H_2O$	0.022 g
$CoCl_2 \cdot 6H_2O$	0.01 g
$MnCl_2 \cdot 4H_2O$	0.18 g
$Na_2Mo_4 \cdot 2H_2O$	0.006 g
Cyanocobalamin (Vitamin B12)	0.0005 g
Thiamine HCl (Vitamin B1)	0.1 g
Biotin	0.0005 g
$Na_2SiO_3 \cdot 9H_2O$	30.0g

Appendix C

Microalgae fouling after 12 weeks of incubation

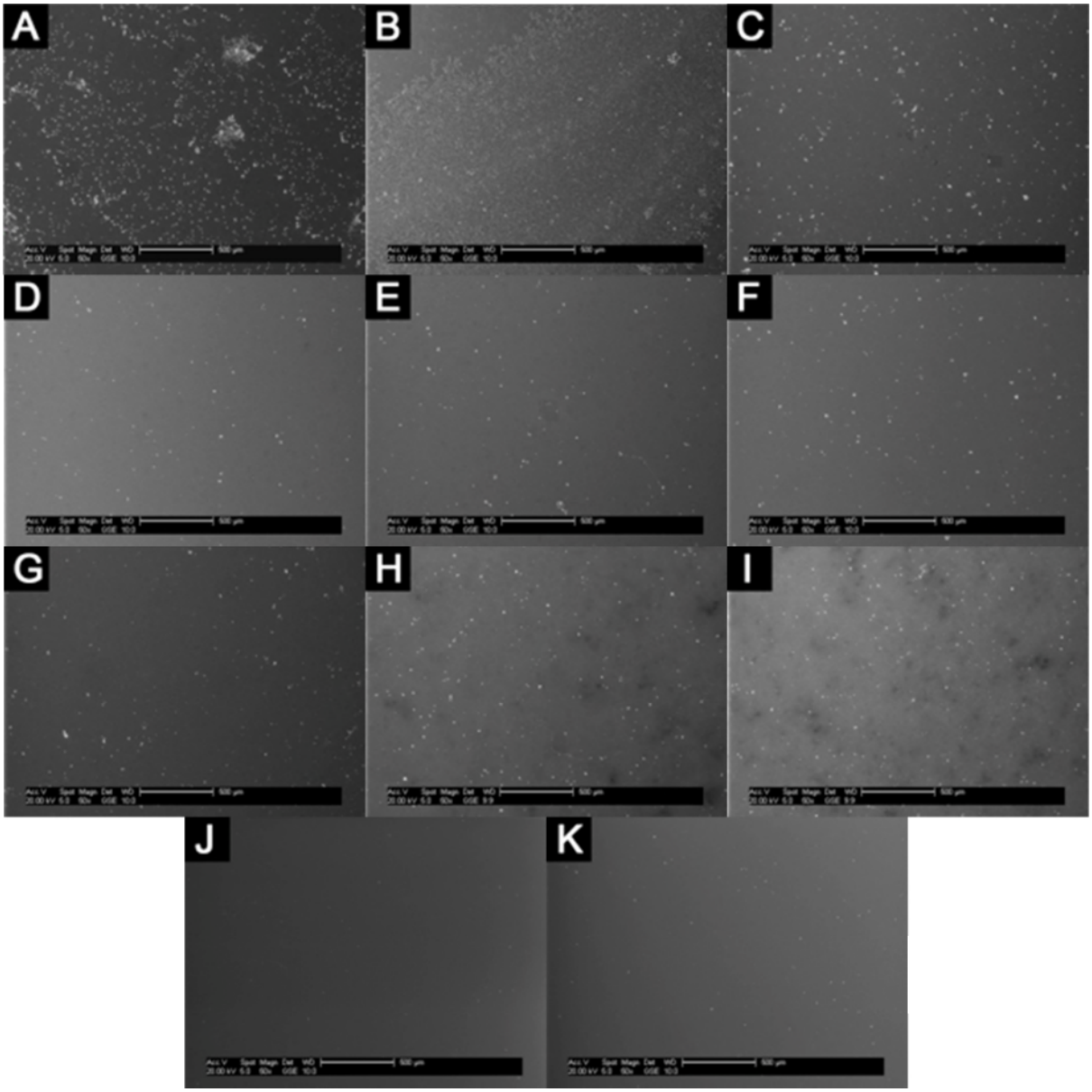

Figure 9-1The measurements of tested samples after 9 weeks of incubation with *Skeletonema sp.*: glass (A), PDMS (B), PDMS/SiO_2 20:1 (C), PDMS/TiO_2 20:1(D), PDMS/TiO_2 10:1 (E), PDMS/ZnO 20:1 (F), PDMS/ZnO 10:1 (G), PDMS/MWCNT 20:1 (H), PDMS/MWCNT 10:1 (I), PDMS/NBT 20:1 (J), PDMS/NBT 10:1 (K).

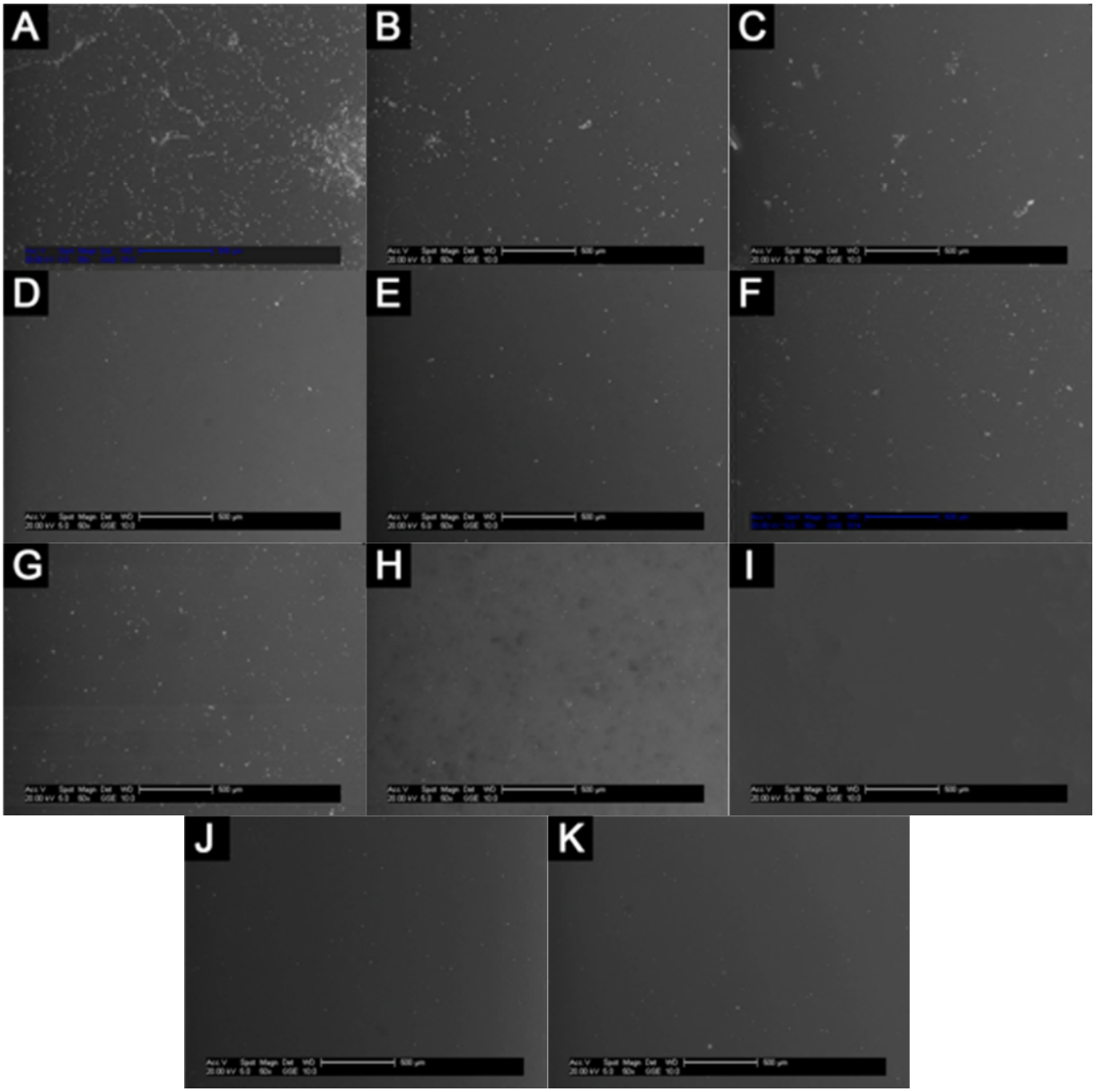

Figure 9-2 The microstructures of tested samples after 9 weeks of incubation with *D. Salina:* glass (A), PDMS (B), PDMS/SiO_2 20:1 (C), PDMS/TiO_2 20:1(D), PDMS/TiO_2 10:1 (E), PDMS/ZnO 20:1 (F), PDMS/ZnO 10:1 (G), PDMS/MWCNT 20:1 (H), PDMS/MWCNT 10:1 (I), PDMS/NBT 20:1 (J), PDMS/NBT 10:1 (K).

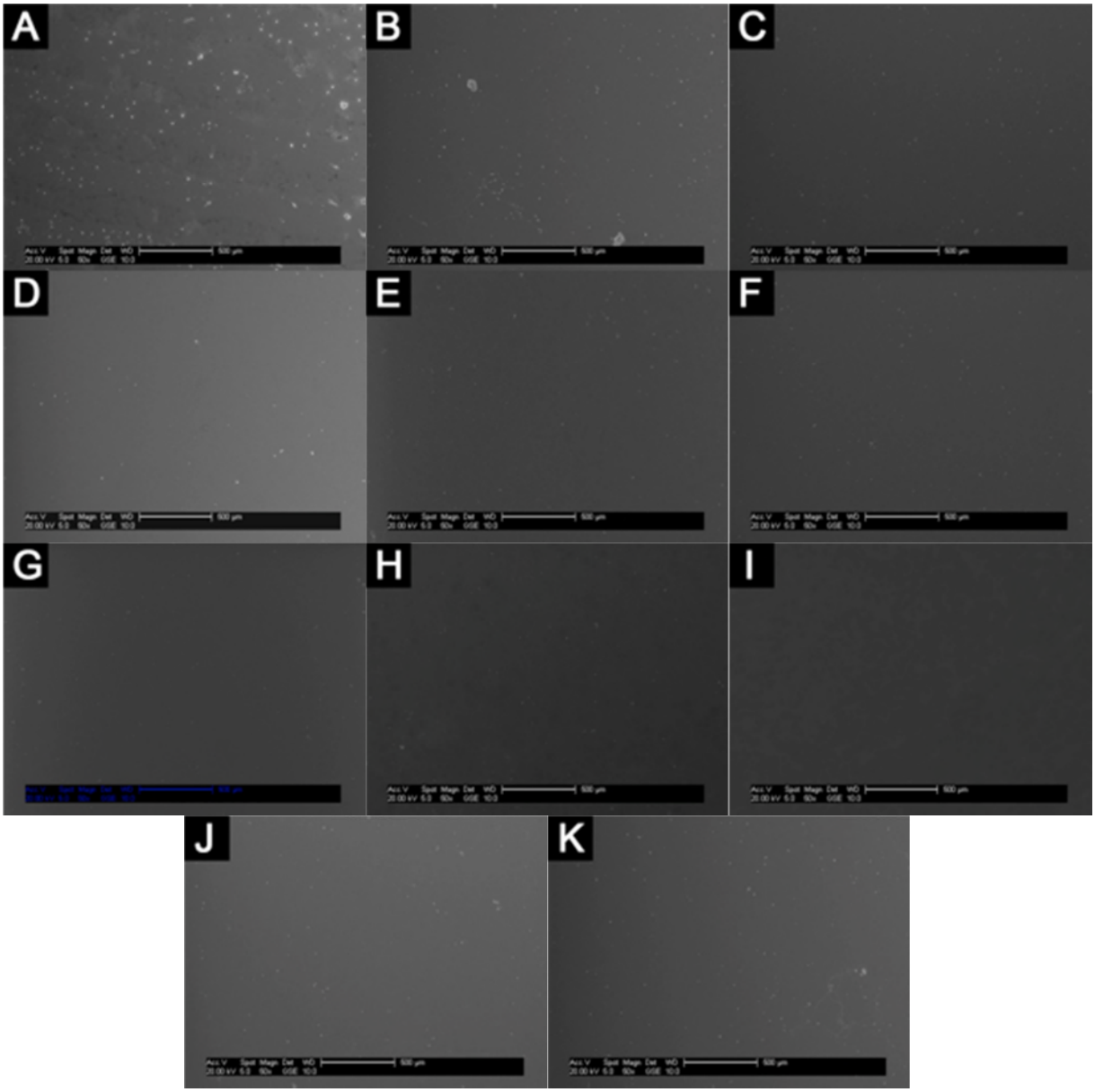

Figure 9-3 The microstructures of tested samples after 9 weeks of incubation with *Amphora sp.*: glass (A), PDMS (B), PDMS/SiO_2 20:1 (C), PDMS/TiO_2 20:1(D), PDMS/TiO_2 10:1 (E), PDMS/ZnO 20:1 (F), PDMS/ZnO 10:1 (G), PDMS/MWCNT 20:1 (H), PDMS/MWCNT 10:1 (I), PDMS/NBT 20:1 (J), PDMS/NBT 10:1 (K)

Appendix D

Table 9-1Comparison between the experimental and thermodynamic modeling results of cell attachment to the PDMS based coatings

Species	Order of cell attachment	
B. subtilis	**experimental attachment**	PDMS/MWCNT 20:1 < PDMS/TiO_2 10:1 < PDMS/TiO_2 20:1 < PDMS < PDMS/ZnO 20:1 < PDMS/MWCNT 10:1 < PDMS/ZnO 10:1 < PDMS/SiO_2 20:1
	W	PDMS/TiO_2 20:1 < PDMS < PDMS/TiO_2 10:1 < PDMS/ZnO 10:1 < PDMS/MWCNT 10:1 < PDMS/MWCNT 10:1 < PDMS/ZnO 20:1 < PDMS/SiO_2 20:1
Skeletonema sp.	**experimental attachment**	PDMS/TiO_2 10:1 < PDMS/ZnO 20:1 = PDMS/TiO_2 20:1 = PDMS < PDMS/NBT 10:1 < PDMS/SiO_2 20:1 < PDMS/MWCNT 20:1 < PDMS/ZnO 10:1 < PDMS/MWCNT 10:1 < PDMS/NBT 20:1
	W	PDMS < PDMS/TiO_2 20:1 < PDMS/TiO_2 10:1 < PDMS/NBT 20:1 < PDMS/NBT 10:1 < PDMS/MWCNT 20:1 < PDMS/ZnO 10:1< PDMS/SiO_2 20:1 < PDMS/MWCNT 10:1 < PDMS/ZnO 10:1
Amphora sp.	**experimental attachment**	PDMS/ZnO 20:1 < PDMS/TiO_2 10:1 < PDMS = PDMS/SiO_2 20:1 < PDMS/ZnO 10:1 < PDMS/MWCNT 20:1 < PDMS/NBT 10:1 = PDMS/TiO_2 20:1 < PDMS/NBT 20:1 < PDMS/MWCNT 10:1

	W	PDMS < PDMS/TiO_2 20:1 < PDMS/TiO_2 10:1 < PDMS/NBT 20:1 < PDMS/ZnO 10:1 < PDMS/NBT 10:1 < PDMS/ZnO 20:1 < PDMS/MWCNT 20:1 < PDMS/MWCNT 10:1 < PDMS/SiO_2 20:1
D. Salina	**experimental attachment**	PDMS/ZnO 20:1 = PDMS/MWCNT 20:1 < PDMS/NBT 20:1 < PDMS/MWCNT 10:1 < PDMS/TiO_2 10:1 < PDMS/NBT 10:1 = PDMS/ZnO 10:1 < PDMS < PDMS/TiO_2 20:1 < PDMS/SiO_2 20:1
	W	PDMS < PDMS/TiO_2 20:1 < PDMS/TiO_2 10:1 < PDMS/NBT 20:1 < PDMS/NBT 10:1 < PDMS/MWCNT 20:1 < PDMS/ZnO 10:1 < PDMS/SiO_2 20:1 < PDMS/MWCNT 10:1 < PDMS/ZnO 10:1